

The Islamic University of Gaza
Electrical Engineering Department



**Nonlinear Resonant Tunneling Diode
(RTD) Circuits for Microwave A/D
Conversion**

By

Ahmed R. S. AL-Farra

Supervisor

Prof. Dr. Hala J. El-Khozondar

**A Thesis Submitted in Partial Fulfillment of the
Requirements for the Degree of Master of Science in
Electrical Engineering**

May, 2012

Abstract

In this work, we design a nonlinear transmission line (NLTL), which is loaded with Resonant Tunneling Diode (RTD) to be suitable for microwave analog to digital converter (ADC). A resonant tunneling diode has a negative differential resistance that means when the voltage increases the current decreases. The equivalent circuit of monostable line is given. The simulation for the NLTL is performed by using OrCad program. Results show that a spike is produced and after a charging time constant, another switching occurs. Hence – similar to a relaxation oscillator - the spiking period is determined by the amplitude and frequency of the input current. The transmission line itself ensures the generation and propagation of identical spikes such as solitons formed after few diodes.

ملخص الرسالة

تعني هذه الرسالة بدراسة خطوط النقل غير الخطية (NLTL)، حيث أنها تتكون من خطوط نقل عادية والتي تمثل موصلين متوازيين يتم ربطهما بطريقة دورية مع احد الثنائيات المستخدمة لإغراض خاصة مثل ثنائي الرنين النفقي (RTD) و ثنائي شوتكي و الثنائي ذو السعة المتغيرة. في هذه الرسالة يتم التركيز على ثنائي الرنين النفقي لأنه يتمتع بخصائص عالية مثل السرعة في الأداء و قدرة ضائعة صغيرة. في الدراسات السابقة لهذا الموضوع اهتم الباحثين فقط بتوليد إشارات ذات زمن دوري قصير أو إعادة تشكيل موجة الدخل باستخدام كل من ثنائي شوتكي و الثنائي ذو السعة المتغيرة. في هذه الدراسة تم استخدام ثنائي الرنين النفقي لتوليد مثل تلك الإشارات و أيضا تمت الاستفادة من هذه الإشارات في تصميم خط نقل غير خطي ذو أهمية بالغة في علم الاتصالات ، هذه الدائرة هي محول عادي إلى رقمي (ADC) المستخدمة في أنظمة الاتصالات التي تعمل في حزمة ترددات الموجات الدقيقة (Microwave) و التي تصل إلى 0.1THz و الجميع يعرف مدى أهمية هذه الدائرة اليوم و خاصة أن علم الاتصالات بلغ اليوم من التطور ما بلغ. ممكن لهذا المحول أن يتم تصميمه ليعطي أي تشفير (Code) و تمت الدراسة على تصميم تشفير مهم لما يحمل من مميزات، هو التشفير الرمادي (Gray Code) لان هذا الكود يوجد به تغير واحد في الخانات التي يتكون منها أي كوديين متتاليين وهذا بدوره يقلل من نسبة الخطاء التي ممكن أن تنتج في عملية فك التشفير Decoding عند المستقبل.

اعتمد التصميم على التالي:

- 1- استخدام البرنامج الإلكتروني الشهير في تصميم و تحليل الدوائر الإلكترونية "اوركاد "
- 2- خصائص موجة الدخل (الجهد و التردد) ، حيث لوحظ عندما يتم تغيير خصائص موجة الدخل يتم تغيير عدد النبضات المتولدة.
- 3- طول خط النقل غير الخطي (عدد الخلايا المكونة لهذا الخط)، تم الوصول إلى الهدف المطلوب عندما كان الخط غير الخطي يتكون من ١٨ خلية.
- 4- خصائص ثنائي الرنين النفقي.
- 5- قيم عناصر الدائرة المكافئة لثنائي الرنين النفقي.



Dedicated to

For the soul of my father,
For my mother,
For my father in- law,
For my wife,
For my sweet kids Sami, Hala and Ghazal,
For my brothers, and
For my sisters

Acknowledgements

First and foremost, all praise is due to Allah, the Almighty, who gave me the opportunity, strength, and patience to carry out this work. I would like to give my sincere gratitude to my supervisor Associate Prof. Dr. Hala J. El-Khozondar for her continuous support, great guidance, endless help, good knowledge and perpetual inspiration she gave me.

Special thanks go to Assistant Prof. Dr. Hatem Elaydi and Associate Prof. Dr. Rifa J. El-Khozondar, thesis examiners, for their patient guidance and generous support for this research. I would like to give my thanks to the Electrical Engineering department teachers and fellow associates for their help and support during my course of study. Finally, words will not be enough to thank my family for their infinite support and patience.

Table of Contents

List of Figures	viii
List of Tables	xi
Abbreviations	xii
1- Introduction	1
1.1 Introduction	1
1.2 Motivation	2
1.3 Literature Review.....	2
1.4 Contribution.....	7
2- Electrical Transmission Lines.....	8
2.1 Types of electrical Transmission Lines.....	8
2.2 The Lumped Element Circuit Model For a Transmission Line.....	9
2.2.1 Wave Propagation on a Transmission Line.....	11
2.2.2 Lossless Transmission Line.....	14
2.3 Terminated Lossless Transmission Line	15
2.4 Special Cases of LosslessTerminated Line	18
2.4.1 Lossless Transmission Line with Matched Load.....	18
2.4.2 Short Circuited Lossless Transmission Line	19
2.4.3 Open Circuited Lossless Transmission Line	20
3- Spatial PurposeDiodes.....	21
3.1 Varactor diode	21
3.1.1 Introduction	21
3.1.2 Varactor Diode Operation	21
3.1.3 Symbol and Equivalent Circuit.....	23
3.1.4 Expression for Transition Capacitance	24
3.1.5 Applications.....	24
3.2 Schottky Diode	25
3.2.1 Introduction	25
3.2.2 Schottky Diodes Construction and Symbol.....	26
3.2.3 Characteristic of Schottky Diode	27
3.2.4 Applications.....	28
3.2.5 Comparison Between Schottky Diode and Conventional Diode.....	29
3.3 Resonant Tunneling Diode	30

3.3.1 Introduction	30
3.3.2 Physical Structure of RTD.....	32
3.3.3 Equivalent Circuit of RTD	33
3.3.4 RTD Current-Voltage Characteristics.....	33
3.3.5 Characteristic Model Equation	36
3.3.6 Advantage of RTD	37
3.3.7 Application of RTD.....	38
3.3.8 Comparison of RTD and Conventional Diode	39
4- Nonlinear Transmission Line and Soliton Waves	40
4.1 Nonlinear Transmission Line Concept.....	40
4.1.1 Nonlinear System.....	40
4.1.2 Nonlinear Transmission Line Models	40
4.1.3 Paractical Nonlinear Transmission Line(NLTL)	41
4.1.4 Structure of NLTL	42
4.1.5 NLTL Characteristics	44
4.1.5.1 Dispersion	44
4.1.5.2 Nonlinearity	44
4.1.5.3 Dissipation	44
4.1.6 Nonlinear Transmission Line Applications	44
4.2 Soliton Waves.....	45
4.2.1 Definition of Soliton Waves	45
4.2.2 Soliton Waves Applications	46
5- Analog to Digital Converter and Gray Code	47
5.1 Analog to Digital Converter	47
5.1.1 A/D Converter Constraints	48
5.1.2 Types of A/D Converter	48
5.1.3 What Makes a good A/D Converter?	48
5.1.4 A/D Converter Applications	49
5.2 The Gray Code.....	49
5.2.1 Why Use Gray Code?.....	50
5.2.2 Properties of Gray Code?	51
6- Microwave A/D Converter Design and Simulation.....	52
6.1 Nonlinearity of the RTD	53
6.2 RTD-NLTL for A/D Converter Design steps.....	56

6.2.1 Array of RTD Periodically loaded	56
6.2.2 Numerical analysis	56
6.3 Array of RTD// Inductor Periodically loaded.....	58
6.4 Modified RTD-NLTL	60
6.4.1 Basic properties and operating principle of the modified RTD-NLTL.....	60
6.4.2 Numerical analysis	61
6.4.2.1 Rectangular input signal	62
6.4.2.2 Sinusoidal input signal	64
6.5 Discussion.....	70
6.6 Proposed A/D Converter Metrics	71
6.6.1 Power Consumption	71
6.6.2 Conversion Rate and Speed.....	71
6.6.3 Resolution.....	72
6.6.4 Conversion Delay.....	73
6.6.5 Temperature effect	74
6.6.6 Cost	74
6.6.7 Size.....	74
6.6.8 Static and Dynamic Errors.....	75
7- Conclusion and Future Work.....	76
7.1 Conclusion.....	76
7.2 Future Work.....	76
Bibliography	77

List of Figures

Figure 2. 1	Types of transmission lines.....	8
Figure 2. 2	Uniform two-wire transmission line.....	9
Figure 2. 3	The equivalent circuit of a segment of two-wire transmission line.....	10
Figure 2. 4	The equivalent circuit of a segment of lossless transmission line.....	14
Figure 2. 5	A transmission line terminated in a load impedance z_L	15
Figure 2. 6	A transmission line reflection coefficient.....	17
Figure 2. 7	A transmission line terminated in a load and input impedances.....	17
Figure 2. 8	A transmission line terminated with matched load circuit.....	18
Figure 2. 9	A transmission line terminated with short load circuit.....	19
Figure 2. 10	A transmission line terminated with open load circuit.....	20
Figure 3. 1	The reverse biased varactor diode.....	22
Figure 3. 2	Varactor diode transition capacitance.....	22
Figure 3. 3	Varactor diode transition capacitance symbol and circuit.....	23
Figure 3. 4	Use of varactor diode in LC tuned circuit.....	24
Figure 3. 5	Schottky diode Symbol and Construction.....	26
Figure 3. 6	Basic internal construction of a Schottky diode.....	27
Figure 3. 7	Comparison of Characteristics.....	28
Figure 3. 8	Current-voltage characteristic of a commercial silicon tunnel diode.....	30
Figure 3. 9	Schematic diagram of double-barrier resonant tunneling diode.....	32
Figure 3. 10	RTD band diagram.....	32
Figure 3. 11	Equivalent circuit of RTD.....	33
Figure 3. 12	Si Esaki diode and its characteristic curve.....	34
Figure 3. 13	Schematic energy band diagram of RTD.....	36
Figure 3. 14	RTD current – voltage characteristics.....	37
Figure 4. 1	NLTL Models.....	41
Figure 4. 2	Linear transmission line with voltage dependent capacitor.....	42
Figure 4. 3	A metallic coplanar waveguide(CPW) on a dielectric substrate.....	42
Figure 4. 4	Schematic diagram of NLTL.....	42
Figure 4. 5	Equivalent circuit model of an NLTL.....	43
Figure 4. 6	Photo of an actual NLTL.....	43
Figure 4. 7	Close up view of a single element in the NLTL.....	43

Figure 4. 8	Plot of a solitary wave solution.....	46
Figure 5. 1	Basic Element of Communication System.....	47
Figure 6. 1	Schematic of the thesis purpose.....	52
Figure 6. 2	Nonlinearity for RTD.....	53
Figure 6. 3	Current-Voltage characteristic curve of RTD.....	54
Figure 6. 4	Current-Voltage characteristic curve of RTD created by Orcad.....	55
Figure 6. 5	Monolithic NLTL with Periodic Array of RTDs.....	56
Figure 6. 6	Equivalent circuit of one section of RTD-NLTL.....	57
Figure 6. 7	The output pulses element k=18 for input sinusoidal pulse.....	57
Figure 6. 8	Monolithic NLTL with Periodic Array of RTD//L.....	58
Figure 6. 9	Equivalent Circuit of One Section of RTD-NLTL.....	59
Figure 6. 10	The output pulse element k=18 for input sinusoidal pulse.....	59
Figure 6. 11	Sketch of an RTD-NLTL using a Coplanar Transmission Line.....	60
Figure 6. 12	Schematic Representation of the n th Section of RTD-NLTL.....	60
Figure 6. 13	Equivalent circuit of one section of RTD-NLTL.....	61
Figure 6.14	The output pulse at k=18 (green), k=19 (red), k=20 (blue) and k=21(yellow) for input rectangular pulse with amplitude 2.5V and pulse duration 40ps.....	62
Figure 6. 15	The output 9 pulses at element k=21 (blue) for input rectangular pulse with amplitude 1V and pulse duration 50ps (red).....	63
Figure 6. 16	The output 7 pulses at element k=21 (blue) for input rectangular pulse with amplitude 1V and pulse duration 40ps (red).....	63
Figure 6. 17	The output 8 pulses at element k=21 for input rectangular pulse with amplitude 5V and pulse duration 40ps.....	64
Figure 6. 18	The output 8 pulses per period at element k=18 for input sinusoidal pulse with amplitude 5V and frequency 10GHz.....	64
Figure 6. 19	The output 8 pulses per period at element k=18, 19, 20 and 21 for input sinusoidal pulse with amplitude 5V and frequency 10GHz.....	65
Figure 6. 20	The output train of pulses per period at element k=18 for input sinusoidal pulse with amplitude 5V and frequency 10GHz.....	65
Figure 6. 21	The output train of pulses per period at element k=18 for input sinusoidal pulse with amplitude 5V and frequency 10GHz.....	66
Figure 6. 22	The output 7 pulses at k=18 for input sinusoidal pulse with amplitude 2V and frequency 10GHz.....	67

Figure 6. 23 The output 4 pulses at k=18 for input sinusoidal pulse with amplitude 2V and frequency 20GHz. 67

Figure 6. 24 The output 2pulses at k=18 for input sinusoidal pulse with amplitude 2V and frequency 50GHz.....68

Figure 6. 25 The output 2 pulses at k=18 for input sinusoidal pulse with amplitude 5V and frequency 50GHz. 68

Figure 6. 26 The output 1 pulses at k=18 for input sinusoidal pulse with amplitude 5V and frequency 100GHz. 69

Figure 6. 27 Ultra-fast n-bit A/D converter.....70

Figure 6. 28 Zero delay between generated short pulses.....73

List of Tables

Table 3.1:	Comparison between Schottky diode and conventional diode.....	29
Table 3.2:	Comparison between RTD and Conventional Diode	39
Table 5.1:	Comparison between different types of analog to digital converter.....	48
Table 5.2:	Four bit Gray code	50
Table 6.1:	Comparison between power consumption of different types of ADC....	71
Table 6.2:	Comparison between speeds of different A/D converters.....	72
Table 6.3:	Comparison between different A/D converters costs	74
Table 6.4:	Comparison between the size of different A/D converters	75

Abbreviations

ADC	Analog-to-Digital Converters
RTD	Resonant tunneling diode
NLTL	Non linear transmission line
CPW	Coplanar waveguide
MMIC	Monolithic microwave integrated circuits
CMOS	Complementary Metal Oxide Semiconductor
KdV	Korteweg-de Vries
GaAs	Gallium Arsenide
MOSFET	Metal Oxide Semiconductor Field Effect Transistor
FDTD	Finite Difference Time Domain
FD	Finite Difference
KVL	Kirchhoff Voltage Law
KCL	Kirchhoff Current Law
PDE	Partial Differential Equation
TD	Tunneling diode
InP	International network Planning
AIAs	Aluminum Arsenide
NDR	Negative Differential Resistance
UWB	Ultra-Wideband
BCD	Binary Code Digit
MSB	Most Significant Bit
HFSS	High Frequency Structure Simulator

1- Introduction

1.1 Introduction

Currently, many researchers guide their attentions to study nonlinear transmission lines (NLTLs) for their importance in microwave engineering. NLTLs consists of coplanar waveguide (CPW) [1]. Among the very large number of guiding structures proposed and used in microwave applications, planar waveguides have proved an interest for monolithic microwave integrated circuits (MMICs). One significant advantage NLTLs have over other electrical pulse generating circuits is their integrability with other circuitry. The NLTL has been extensively studied over the past 40 years [2–4]. NLTLs are used for the development of solitons [5]. The concept of a solitary wave was introduced to science by John Scott Russell 170 years ago [6]. Solitons are a special class of pulse-shaped waves that propagate without changing their shape in nonlinear dispersive media [7–11]. NLTLs can easily be fabricated and integrated with resonant tunnelling diodes (RTDs) using InP technology [12–13], this line is called RTD-NLTL. Such RTD-NLTL can provide the basis of very interesting microwave signal generation and processing circuits such as an oscillator or an A/D converter. Moreover, recently there has been great progress in the development of high-speed devices in electronics and optoelectronics [14]. There has been a tremendous increase in interest in RTDs for various circuit applications since the pioneering work of Tsu and Esaki [15] who first proposed the resonant tunneling structures. RTDs are currently the widest bandwidth active semiconductor devices. RTDs have been shown to achieve a maximum frequency of up to 2.2 THz as opposed to 215 GHz in conventional Complementary Metal Oxide Semiconductor (CMOS) transistors[16]. RTDs have shown promising circuit characteristics in improving both analog and digital circuits, due to their high speed switching capability and versatile functionality. For example, several RTD-based circuits have been reported working at clock frequencies of GHz, including the basic logic gates [17], flip-flops [18], analog-to- digital convertor [19], amplifiers [20], oscillators [21], and pulse generators [22]. The use of subpicosecond electrical pulses is becoming increasingly important as a tool for broadband characterization of

ultrafast electronic circuits. In this thesis we concentrated on RTD-NLTL analog-to-digital converters (ADC's) , which are finding increased application in sampling scopes, digital receivers, and phased array radars [23–26].

1.2 Motivation

Nonlinear transmission lines(NLTL) for their importance in microwave engineering ranked first of the attention of scientists and researchers. Not long ago; issues such as generation a short pulses width and reshaping signals were the topics of the hour. Issues such as how to take advantage of these signals in modern communication systems barely be addressed.

A huge knowledge in wireless communication research, electromagnetic waves and electrical engineering would be achieved. It is well recognized that nonlinear transmission lines provides various advantages over the usual signal systems generation, especially when it is connected periodically with resonant tunneling diodes(RTDs). RTD-NLTL makes a type of stabilization possible and deal with higher frequencies up to terahertz that cannot be achieved with conventional one's such as Complementary Metal Oxide Semiconductor (CMOS)transistors. We can also implement a much more complex logic in communication actions making use of the recent advances in computer technology. Issues such as complexity, ease of implantation, economic cost, reliability play an important role in designing and selecting new sub-system. The RTD-NLTL which will be used in this thesis is efficient and powerful to get the best and optimization results.

1.3 Literature Review

In the last few years increasing interest has been given to study of nonlinear wave propagation along distributed or lumped wave variable capacitance transmission lines. Due to this purpose, Jageret *al.*[27] studied nonlinear wave propagation along periodic loaded transmission line. In his study a high frequency transmission line periodically loaded with varactor diodes was presented to study nonlinear wave propagation. The nonlinearity and dispersion characteristics are experimentally and theoretically analyzed. Experimental

results on shock wave formation and harmonic frequency generation are found to be in good agreement with theoretical predictions.

It has been demonstrated that by using fast photoconductive switches driven by short laser pulses, very short electrical pulses can be produced and measured, so Ketchen *et al.*[28] had studied generation of subpicosecond electrical pulses on coplanar transmission lines. In their study, they found electrical pulses shorter than 0.6ps were generated by photo conductively shorting a charged coplanar transmission line with 80fs laser pulses. After propagating 8mm on the line the electrical pulses broadened to only 2.6ps. They concluded their study as followed, they had generated electrical pulses shorter than 0.6 ps on a coplanar transmission line by using a new method of pulse generation, "the sliding contact." This method does not require any special lithographic features, allows pulse generation anywhere on the transmission line, and generates shorter pulses than the standard photoconductive gaps.

GaAs nonlinear transmission lines for picoseconds pulse generation and millimeter-wave sampling was studied by Rodwell *et al.*[29]. The GaAs nonlinear transmission lines (NLTL) is a monolithic millimeter-wave integrated circuit consisting of a high impedance transmission line loaded by reverse biased Schottky contacts. Through generation of shock waves on the NLTL, they had generated step function with 5V magnitude and less than 1.4ps fall time. Diode sampling bridges strobe by NLTL shock wave generators had attained bandwidth application in instruments for millimeter wave waveform and network measurements

Baker *et al.*[30] studied generation of kilovolt-sub nanosecond pulses using a nonlinear transmission line. They had introduced a nonlinear transmission line (NLTL) that was used to speed up the rise time of high voltage (> 1 kV) pulses. In their study, the theory of the NLTL was reviewed and practical implementations and limitations are discussed. They presented a technique by which nanosecond rise times can be changed into picoseconds rise times while maintaining the general shape of the pulse. This will increase the bandwidth of measuring systems by allowing shorter gating and faster turn-on times. Pulses

with rise times less than 5 ns and with amplitudes greater than 4 k V can be generated using power MOSFETS. The output of the power MOSFET pulse generator is then fed to a nonlinear transmission line (NLTL) and sharpened to the desired rise time. An NLTL was used to generate a 1.5 kV pulse with a rise time of 500 ps. The study was concluded with a discussion of generating pulses with amplitudes greater than 3.5 kV and rise times less than 200 ps.

Nonlinear transmission lines(NLTL's) integrated with sampling circuits have been used in a variety of millimeters wave and sub millimeters wave instruments, due to this purpose, Allen *et al.*[31] had studied DC-725GHz sampling circuits and subpicosecond nonlinear transmission lines using electrical coplanar wave guide. In this study they used nonlinear transmission lines fabricated with Schottky diodes on GaAs were used to electrically generate 3.7 V step functions that had a measured 10% - 90% fall time of 0.68ps. These NLTL's were integrated on wafer with sampling circuits that had measured 3dB bandwidth of 725GHz. The researchers observed that, the NLTL's varactor diodes at the output end of the line, the depletion edge was moving 145nm in 0.68ps, giving an average velocity of 2.1×10^7 cm/sec.

Nonlinear transmission lines (NLTL's) are studied for pulse steeping and compression, and for harmonic generation purpose . Giancarlo Bartolucci and other researchers [32] had studied diffusion capacitance effect on the response of monolithic nonlinear transmission lines. In their study, the effect of the diffusion capacitance upon the electrical performance of the Nonlinear transmission lines (NLTL's) was investigated. A comparison between the results obtained for the second harmonic generation by modeling the NLTL with and without the diffusion capacitance was presented.

Afshari *et al.* [33] studied nonlinear transmission lines for pulse shaping in silicon. They have introduced and analyzed pulse narrowing and edge sharpening passive nonlinear transmission lines, using accumulation – mode MOS varactors and the gradual scaling lines, showing simultaneous edge sharpening for both rising and falling edges in silicon. The experimental results show considerable improvement in the rise and fall times of the pulses. These

lines can have applications in ultra-wideband systems, broadband signal generations, and high speed serial communications.

The generation of short electrical pulses and millimeter wave oscillations on a resonant tunnel diode nonlinear transmission line has been studied in[34]. Where authors have shown by numerical simulation that stable short rectangular electrical pulse as pairs kink-antikink structures can be generated on a bistable RTD-NLTL from microwave sinusoidal input signal. This results from the compensation between amplification in the NDR- region and attenuation in the other parts of the current- voltage characteristics of the input wave. Also, for certain conditions, the variation in pulse length is a dynamic process along the line because the pulse can grow or shrink during the propagation. Moreover, RTD-NLTL can be used as millimeter wave oscillator.

Electrical soliton oscillator was studied by David S. Ricketts *et al.*[35]. In their study, Authors presented the first robust electrical soliton oscillator with full experimental demonstration. The oscillator is a one-port system that self-generates a periodic soliton pulse train from ambient noise. The soliton oscillator consists of an NLTL and a nonlinear amplifier utilizing an adaptive bias control. The NLTL is responsible for soliton formation. The amplifier is responsible for the initiation of startup, compensation of loss, and stabilization of oscillation in the steady state. The Soliton oscillator is a direct analog of the optical soliton mode-locked system such as a fiber ring laser.

The generation of electrical short pulses using Schottky line periodically loaded with electronic switches have been done by Narahara *et al.*[36]. Where, they proposed a method of generation of the electrical- short pulse with the modified Schottky line. By simply setting the voltage level of the input pulse to cross the threshold of the modified Schottky line, they got only the largest and the shortest solitons among the ones generated by the transmission on the modified Schottky line. Pulse propagation on the modified Schottky line is perturbatively treated so that they found that the soliton with larger amplitude is exponentially less attenuated. Moreover, they successfully demonstrated the short-pulse

generation using the proposed method through the numerical integration of the transmission equation of the modified Schottky line.

Essimbi *et al.*[37] have performed a study to generate an electrical short pulses using a Schottky transmission line periodically loaded with tunneling diodes. In their study, they proposed a method of generating electrical short pulses on a Schottky transmission line periodically loaded with resonant tunneling diodes as a key device. The behavior of the wave on the line was studied by computer experiment. As a result, the problem of a wide pulse breaking up into multiple pulses rather than a single pulse is solved. The results obtained from simulation for different area conditions show that the amplitude of the pulse decreases progressively during propagation, whereas in some cases the soliton amplitude is being amplified when travelling along the RTD-SNLTL.

El-Khozondar *et al.* studied transmission lines loaded with Schottky Diode [38]. In this study, she used a nonlinear relation between current and voltage for Schottky resonant tunneling diode and obtained a general form of equation similar to Van Der Pol equation for an oscillator. A Resonant tunneling diode (RTD) has a negative differential resistance that means when the voltage increases the current decreases. This property is very useful for oscillators manufacture. Also they studied some kinds of nonlinear transmission lines to show that it can be used in oscillators and show that it can reshape the sinusoidal signals to other shapes by using OrCad and Mathematica programs.

Because of emerging applications of the terahertz gap (100 GHz–10 THz) of the electromagnetic spectrum, there is growing interest in the development of signal sources operating at millimeter and sub-millimeter wavelengths. Essimbi *et al.*[39] was studied an Electrical short pulses generation using a resonant tunneling diode nonlinear transmission line. It was shown by computer experiments that a input rectangular input pulse as well as a sinusoidal input signal can be converted into a set of output spikes, suitable for ADC conversion at millimeter wave frequencies.

1.4 Contribution

This thesis presents methodologies for designing nonlinear transmission line which use a new equivalent circuit for resonant tunneling diodes, which is a high speed switch device. This design is useful in generation soliton waves, which are short width pulse signals. These signals are very important in microwave communication. The soliton waves are called spikes, which form is based on tuning RTD equivalent circuit components and the number of spikes is based on the characteristics of the input signal. As the amplitude and frequency of the input signal change the number of the output spikes is change. The best application which use this form of the output is an important electrical device which is an essential part of any communication system, it is an analog to digital converter(ADC). The approach presented in this thesis is design microwave 4-bits analog to digital converter with Gray code output, which consists of four monostable NLTLs , each one is design independent, then these outputs are combined with spatial method to achieve the desired goal.

This thesis contains seven chapters: The second chapter presents the transmission lines concept. The topic of chapter three is the resonant tunneling diodes and there operation. Chapter four presents nonlinear transmission lines. Chapter five introduce analog to digital converter and Gray code. The focus of chapter six is on the methodology, simulation and result. The conclusion and future works are followed in the last chapter.

2- Electrical Transmission Lines

2.1 Types of electrical transmission lines

Transmission line comprise of two or more parallel conductors used to connect a source to a load [40]. A typical engineering problem involves the transmission of a signal from a generator to a load. A transmission line is the part of the circuit that provides the direct link between source and load. Transmission lines can be realized in a number of ways. Figure 2.1 displays different examples of transmission lines. For simplicity, we use in most diagrams the parallel-wire line to represent circuit connections, but the theory applies to all types of transmission lines.

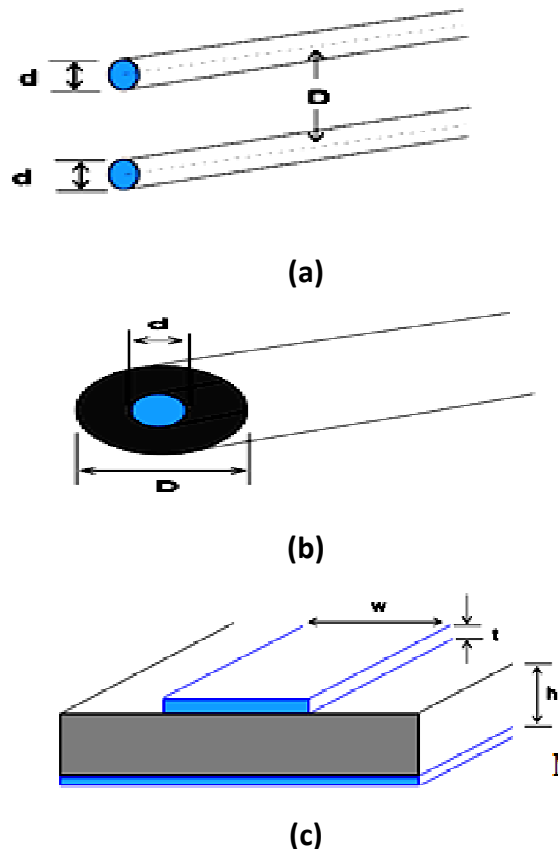


Figure 2.1: Types of transmission lines: (a) Two –wire line, (b) Coaxial cable
And (c) Microstrip[38]

2.2 The Lumped-Element Circuit Model For a Transmission Line

A lumped element in microwave circuits is defined as a passive component whose size across any dimension is much smaller than the operating wavelengths that there is no appreciable phase shift between the input and output terminals. Generally, keeping the maximum dimension less than $\lambda / 20$ is a good approximation where λ is the guide wavelength. Lumped elements for use at RF and microwave frequencies are designed on the basis of this consideration. RF and microwave circuits use three basic lumped-element building blocks; capacitors, inductors and resistors.

In many ways, transmission line theory bridges the gap between field analysis and basic circuit theory. Transmission lines are of significant importance in microwave network analysis. Transmission lines and waveguides offer an alternative way of transmitting signals in the form of guided wave propagation. Transmission lines are typically electrically large (several wavelengths) such that we cannot accurately describe the voltages and currents along the transmission line using a simple lumped-element equivalent circuit. We must use a distributed-element equivalent circuit which describes each short segment of the transmission line by a lumped element equivalent circuit.

Consider a simple uniform two-wire transmission line with its conductors parallel to the z -axis as shown in figure2.2. Uniform transmission line - conductors and insulating medium maintain the same cross-sectional geometry along the entire transmission line.

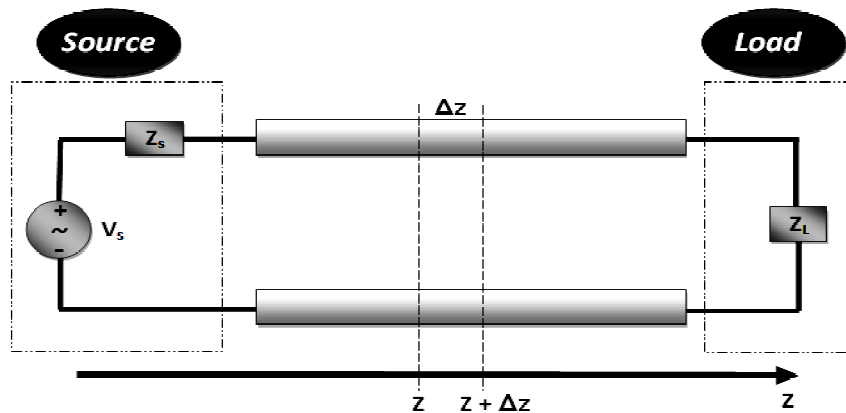


Figure2.2: Uniform two-wire transmission line

The equivalent circuit of a short segment Δz of the two-wire transmission line may be represented by simple lumped-element equivalent circuit as shown in figure 2.3.

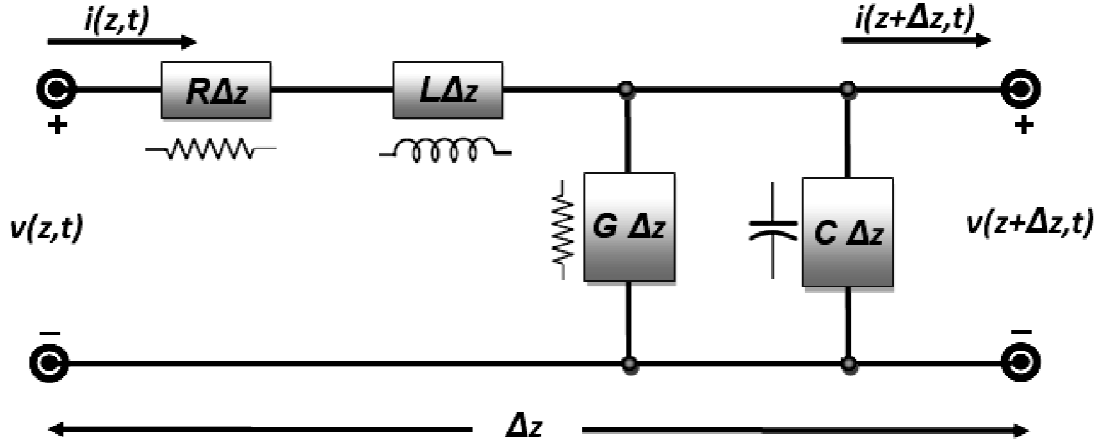


Figure 2.3: The equivalent circuit of a segment of two-wire transmission line [38]

Where R is a series resistance per unit length (Ω/m) of the transmission line conductors, L is a series inductance per unit length (H/m) of the transmission line conductors (internal plus external inductance), G is a shunt conductance per unit length (S/m) of the media between the transmission line conductors, and C is a shunt capacitance per unit length (F/m) of the transmission line conductors.

We may relate the values of voltage and current at z and $z+\Delta z$ by writing Kirchhoff voltage law (KVL) and Kirchhoff current law (KCL) equations for the equivalent circuit [40–41].

From the circuit of figure 2.3, Kirchhoff's voltage law can be applied to give

$$v(z, t) - R\Delta z i(z, t) - L\Delta z \frac{\partial i(z, t)}{\partial t} = v(z + \Delta z, t) \quad (2.1a)$$

and Kirchhoff's current law lead to

$$i(z, t) - G\Delta z v(z + \Delta z, t) - C\Delta z \frac{\partial v(z + \Delta z, t)}{\partial t} = i(z + \Delta z, t) \quad (2.1b)$$

Grouping the voltage and current terms and dividing by Δz gives

$$-Ri(z, t) - L \frac{\partial i(z, t)}{\partial t} = \frac{v(z + \Delta z, t) - v(z, t)}{\Delta z} \quad (2.2a)$$

$$-Gv(z + \Delta z, t) - C \frac{\partial v(z + \Delta z, t)}{\partial t} = \frac{i(z + \Delta z, t) - i(z, t)}{\Delta z} \quad (2.2b)$$

Taking the limit as $\Delta z \rightarrow 0$, the terms on the right hand side of the equations above become partial derivatives with respect to z which gives

$$\frac{\partial v(z, t)}{\partial z} = -Ri(z, t) - L \frac{\partial i(z, t)}{\partial t} \quad (2.3a)$$

$$\frac{\partial i(z, t)}{\partial z} = -Gv(z, t) - C \frac{\partial v(z, t)}{\partial t} \quad (2.3b)$$

Equations (2.3a) and (2.3b) are called time-domain transmission line equations (coupled PDE's). For time-harmonic signals, the instantaneous voltage and current may be defined in terms of phasors such that

$$v(z, t) = \text{Re}\{V(z)e^{j\omega t}\} \quad (2.4a)$$

$$i(z, t) = \text{Re}\{I(z)e^{j\omega t}\} \quad (2.4b)$$

The derivatives of the voltage and current with respect to time yield $j\omega$ times the respective phasor which gives

$$\frac{dV(z)}{dz} = -[R + j\omega L]I(z) \quad (2.5a)$$

$$\frac{dI(z)}{dz} = -[G + j\omega C]V(z) \quad (2.5b)$$

Equations (2.5a) and (2.5b) are called Frequency-domain (phasor) transmission line equations (coupled PDE's).

2.2.1 Wave Propagation on a Transmission Line

The derivatives of both sides of equations 2.5a and 2.5b with respect to z give us,

$$\frac{d^2V(z)}{dz^2} = -[R + j\omega L] \frac{dI(z)}{dz} \quad (2.6a)$$

$$\frac{d^2I(z)}{dz^2} = -[G + j\omega C] \frac{dV(z)}{dz} \quad (2.6b)$$

We then insert the first derivatives of the voltage and current found in the original phasor transmission line equations.

$$\frac{d^2V(z)}{dz^2} = [R + j\omega L][G + j\omega C]V(z) = \gamma^2V(z) \quad (2.7a)$$

$$\frac{d^2I(z)}{dz^2} = [G + j\omega C][R + j\omega L]I(z) = \gamma^2I(z) \quad (2.7b)$$

The voltage and current wave equations may be written as

$$\frac{d^2V(z)}{dz^2} - \gamma^2V(z) = 0 \quad (2.8a)$$

$$\frac{d^2I(z)}{dz^2} - \gamma^2I(z) = 0 \quad (2.8b)$$

Where γ is the complex propagation constant of the wave on the transmission line, which is a function of frequency and, given by

$$\gamma = \alpha + j\beta = \sqrt{(G + j\omega C)(R + j\omega L)} \quad (2.9)$$

Just as with unguided waves, the real part of the propagation constant (α) is the attenuation constant while the imaginary part (β) is the phase constant. The general equations for α and β in terms of transmission line parameters per-unit-length are

$$\alpha = \frac{1}{\sqrt{2}}\sqrt{RG - \omega^2LC + \sqrt{(R^2 + \omega^2L^2)(G^2 + \omega^2C^2)}} \quad (2.10)$$

$$\beta = \frac{1}{\sqrt{2}}\sqrt{-RG - \omega^2LC + \sqrt{(R^2 + \omega^2L^2)(G^2 + \omega^2C^2)}} \quad (2.11)$$

The general solutions to the voltage and current wave equations of (2.8) can be found as:

$$V(z) = V_0^+ e^{-\gamma z} + V_0^- e^{\gamma z} \quad (2.12a)$$

$$I(z) = I_0^+ e^{-\gamma z} + I_0^- e^{\gamma z} \quad (2.12b)$$

where the first term for +z direction and the second term for -z direction where V_0^+ , I_0^+ , V_0^- and I_0^- are wave amplitude along +z and -z directions.

The current equation may be written in terms of the voltage coefficients through the original phasor transmission line equations.

$$\begin{aligned} \frac{dV(z)}{dz} &= -[R + j\omega L]I(z) \\ -\gamma V_0^+ e^{-\gamma z} + \gamma V_0^- e^{\gamma z} &= -[R + j\omega L]I(z) \\ I(z) &= \frac{\gamma}{R + j\omega L} [V_0^+ e^{-\gamma z} - V_0^- e^{\gamma z}] = \frac{1}{Z_0} [V_0^+ e^{-\gamma z} - V_0^- e^{\gamma z}] \end{aligned}$$

The complex constant Z_0 is defined as the transmission line characteristic impedance and is given by[42]

$$Z_0 = \frac{R + j\omega L}{\gamma} = \frac{R + j\omega L}{\sqrt{(G + j\omega C)(R + j\omega L)}} = \sqrt{\frac{R + j\omega L}{G + j\omega C}} \quad (2.13)$$

The transmission line equations written in terms of voltage coefficients only are

$$V(z) = V_0^+ e^{-\gamma z} + V_0^- e^{\gamma z} \quad (2.14a)$$

$$I(z) = \frac{1}{Z_0} [V_0^+ e^{-\gamma z} - V_0^- e^{\gamma z}] \quad (2.14b)$$

The complex voltage coefficients may be written in terms of magnitude and phase as

$$V_0^+ = |V_0^+| e^{j\varphi^+} \quad (2.15a)$$

$$V_0^- = |V_0^-| e^{j\varphi^-} \quad (2.15b)$$

Where φ is the phase angle of the complex voltage V_0 .

The instantaneous voltage becomes

$$\begin{aligned} v(z, t) &= \text{Re}\{V(z)e^{j\omega t}\} \\ &= \text{Re}\{[V_0^+ e^{-\gamma z} + V_0^- e^{\gamma z}]e^{j\omega t}\} \\ &= \text{Re}\{[|V_0^+| e^{j\varphi^+} e^{-\alpha z} e^{-j\beta z} + |V_0^-| e^{j\varphi^-} e^{\alpha z} e^{j\beta z}]e^{j\omega t}\} \\ &= |V_0^+| e^{-\alpha z} \cos(\omega t - \beta z + \varphi^+) + |V_0^-| e^{\alpha z} \cos(\omega t + \beta z + \varphi^-) \end{aligned} \quad (2.16)$$

The wavelength and phase velocity of the waves on the transmission line may be found as follow.

$$v_p = \frac{\omega}{\beta} = \lambda f \quad (2.17)$$

$$\lambda = \frac{2\pi}{\beta} \quad (2.18)$$

2.2.2 Lossless Transmission Line

The line is said to be lossless if the conductance of the line is perfect, then its conductance is infinity ($\sigma_c = \infty$). If the transmission line loss is neglected ($R = G = 0$), the equivalent circuit reduces to the one as shown in figure2.4.

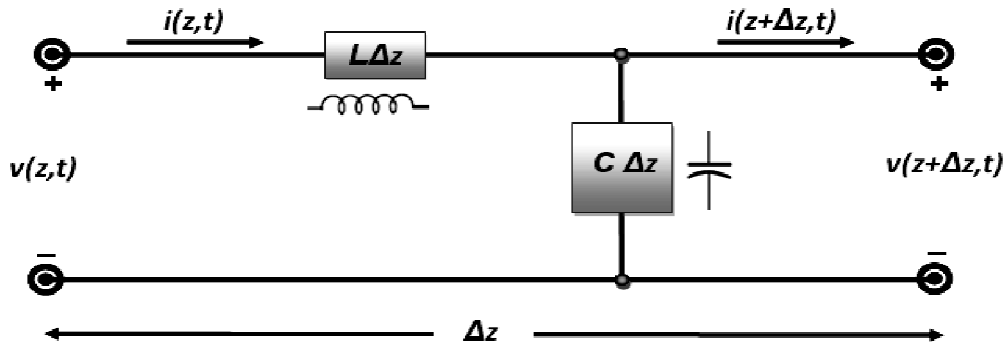


Figure2.4: The equivalent circuit of a segment of lossless two-wire transmission line[38]

Setting $R=G=0$ in equation (2.9), the propagation constant becomes,

$$\gamma = \alpha + j\beta = j\omega\sqrt{LC}$$

$$\beta = \omega\sqrt{LC} \quad (2.19a)$$

$$\alpha = 0 \quad (2.19b)$$

Given the purely imaginary propagation constant, the transmission line equations for the lossless line are:

$$V(z) = V_0^+ e^{-j\beta z} + V_0^- e^{j\beta z} \quad (2.20a)$$

$$I(z) = \frac{1}{z_0} [V_0^+ e^{-j\beta z} - V_0^- e^{j\beta z}] \quad (2.20b)$$

The characteristic impedance of the lossless transmission line is purely real and given by

$$Z_o = \sqrt{\frac{L}{C}} \quad (2.21)$$

The phase velocity and wavelength on the lossless line are

$$v_p = \frac{\omega}{\beta} = \frac{1}{\sqrt{LC}} \quad (2.22)$$

$$\lambda = \frac{2\pi}{\beta} = \frac{1}{f\sqrt{LC}} = \frac{v_p}{f} \quad (2.23)$$

2.3 Terminated Lossless Transmission Line

Figure 2.5 exhibits a lossless transmission line terminated in an arbitrary load impedance Z_L .



Figure 2.5: A transmission line terminated in a load impedance Z_L .

If we choose our reference point ($z = 0$) at the load termination, then the lossless transmission line equations evaluated at $z = 0$ give the load voltage and current.

$$V(z) = V_o^+ e^{-j\beta z} + V_o^- e^{j\beta z} \Big|_{z=0} = V(0) = V_o^+ + V_o^- \quad (2.24a)$$

$$I(z) = \frac{1}{Z_o} [V_o^+ e^{-j\beta z} - V_o^- e^{j\beta z}] \Big|_{z=0} = I(0) = \frac{V_o^+}{Z_o} - \frac{V_o^-}{Z_o} \quad (2.24a)$$

The ratio of voltage to current at $z = 0$ must equal the load impedance.

$$Z_L = Z_o \frac{V_o^+ + V_o^-}{V_o^+ - V_o^-}$$

Solving for V_0^- gives

$$V_0^- = \frac{Z_L - Z_0}{Z_L + Z_0} V_0^+ = \Gamma V_0^+$$

Where, Γ is the reflection coefficient which defines the ratio of the reflected wave to the incident wave. Figure 2.6 displays a transmission line reflection coefficient.

$$\Gamma = \frac{Z_L - Z_0}{Z_L + Z_0} \quad (2.25)$$

Note that the reflection coefficient is in general complex with $0 \leq |\Gamma| \leq 1$. If the reflection coefficient is zero ($Z_L = Z_0$), there is no reflected wave and the load is said to be matched to the transmission line. If $Z_L \neq Z_0$, the magnitude of the reflection coefficient is non-zero (there is a reflected wave). The presence of forward and reverse traveling waves on the transmission line produces standing waves. We may rewrite the transmission line equations in terms of the reflection coefficient as

$$V(z) = V_0^+ \left[e^{-j\beta z} + \frac{V_0^-}{V_0^+} e^{j\beta z} \right] = V_0^+ [e^{-j\beta z} + \Gamma e^{j\beta z}]$$

$$I(z) = \frac{V_0^+}{Z_0} \left[e^{-j\beta z} - \frac{V_0^-}{V_0^+} e^{j\beta z} \right] = \frac{V_0^+}{Z_0} [e^{-j\beta z} - \Gamma e^{j\beta z}]$$

or

$$V(z) = V_0^+ e^{-j\beta z} [1 + \Gamma e^{j2\beta z}] \quad (2.26a)$$

$$I(z) = \frac{V_0^+}{Z_0} e^{-j\beta z} [1 - \Gamma e^{j2\beta z}] \quad (2.26b)$$

The magnitude of the transmission line voltage may be written as

$$|V(z)| = |V_0^+| |1 + \Gamma e^{j2\beta z}| \quad (2.27)$$

The maximum and minimum voltage magnitudes are

$$|V(z)|_{max} = |V_0^+| [1 + |\Gamma|] \quad (2.27a)$$

$$|V(z)|_{min} = |V_0^+| [1 - |\Gamma|] \quad (2.27b)$$

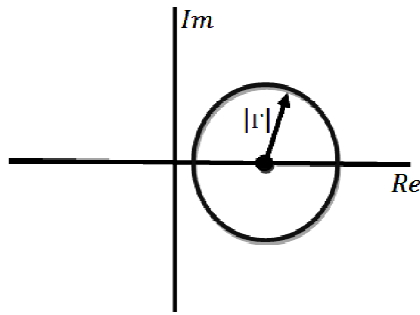


Figure2.6: A transmission line reflection coefficient

The ratio of maximum to minimum voltage magnitudes defines the standing wave ratio (s).

$$S = \frac{|V(z)|_{max}}{|V(z)|_{min}} = \frac{1+|\Gamma|}{1-|\Gamma|} \quad (2.28)$$

Note that the standing wave ratio is real with $1 \leq s \leq \infty$, where $s=1$ implies a matched load.

Figure 2.7 shows a lossless transmission line terminated in an arbitrary load impedance Z_L and its input impedance Z_{in} .

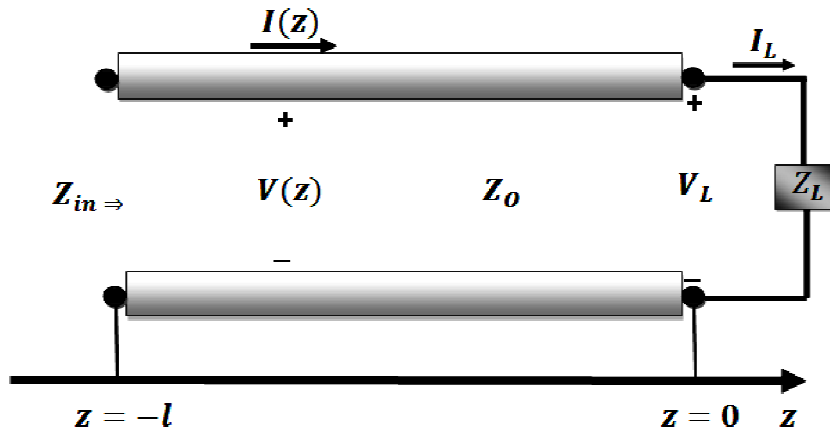


Figure2.7: A transmission line terminated in a load impedance Z_L and input impedance Z_{in} .

The impedance at any point on the transmission line is given by

$$Z(z) = \frac{V(z)}{I(z)} = \frac{V_0^+ [e^{-j\beta z} + \Gamma e^{j\beta z}]}{\frac{V_0^+}{Z_0} [e^{-j\beta z} - \Gamma e^{j\beta z}]}$$

$$\begin{aligned}
 &= Z_o \frac{e^{-j\beta z} + \Gamma e^{j\beta z}}{e^{-j\beta z} - \Gamma e^{j\beta z}} \\
 &= Z_o \frac{e^{-j\beta z} + \frac{Z_L - Z_o}{Z_L + Z_o} e^{j\beta z}}{e^{-j\beta z} - \frac{Z_L - Z_o}{Z_L + Z_o} e^{j\beta z}} \\
 &= Z_o \frac{(Z_L + Z_o)e^{-j\beta z} + (Z_L - Z_o)e^{j\beta z}}{(Z_L + Z_o)e^{-j\beta z} - (Z_L - Z_o)e^{j\beta z}} \\
 &= Z_o \frac{Z_L(2\cos(\beta z)) + Z_o(-j2\sin(\beta z))}{Z_o(2\cos(\beta z)) - Z_L(j2\sin(\beta z))} \\
 &= Z_o \frac{Z_L - Z_o j \tan(\beta z)}{Z_o - Z_L j \tan(\beta z)} \tag{2.29}
 \end{aligned}$$

The impedance at the input of a transmission line of length l terminated with an impedance Z_L is

$$Z_{in} = Z(-l) = Z_o \frac{Z_L + Z_o j \tan(\beta l)}{Z_o + Z_L j \tan(\beta l)} \tag{2.30}$$

2.4 Special Cases of Lossless Terminated Lines

2.4.1 Lossless Transmission Line with Matched Load ($Z_L = Z_o$)

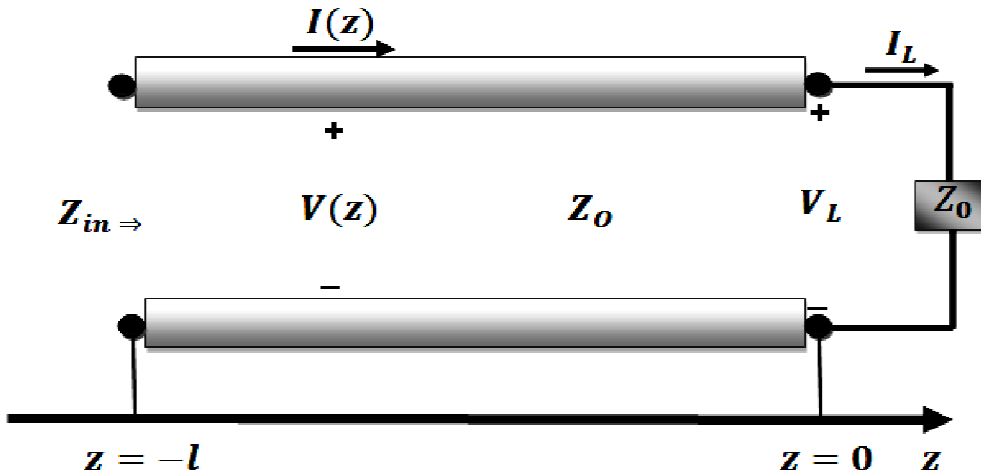


Figure 2.8: A transmission line terminated with matched load circuit.

Figure 2.8 shows a transmission line terminated with matched load circuit.

$$\Gamma = 0 \tag{2.31a}$$

$$S = 1 \quad (2.31b)$$

$$Z_{in} = Z_o \text{ (independent of line length)} \quad (2.31c)$$

$$V(z) = V_o^+ e^{-j\beta z} \quad |V(z)| = |V_o^+| \quad (2.31d)$$

$$I(z) = \frac{V_o^+}{Z_o} e^{-j\beta z} \quad |I(z)| = \frac{|V_o^+|}{Z_o} \quad (2.31e)$$

Note that the input impedance of the lossless transmission line terminated with a matched impedance is independent of the line length. Any mismatching the transmission line system will cause standing waves and make the input impedance dependence on the length of the line.

2.4.2 Short-Circuited Lossless Transmission Line ($Z_L = 0$)

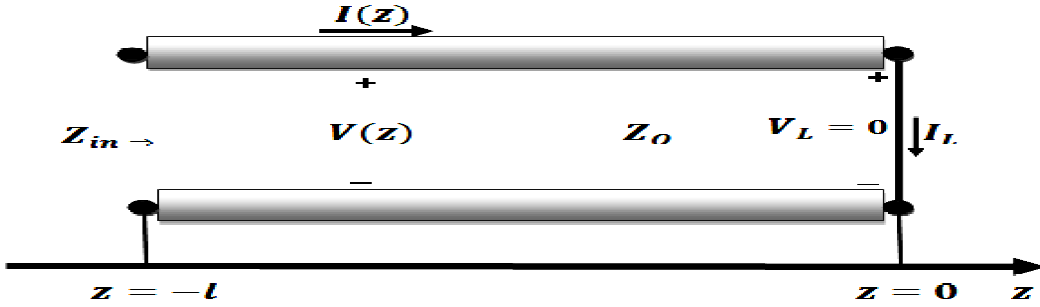


Figure 2.9: A transmission line terminated with short load circuit.

In figure 2.9, the transmission line terminated with short load circuit.

$$\Gamma = -1 \quad (2.32a)$$

$$S = \infty \quad (2.32b)$$

$$Z_{in} = jZ_o \tan(\beta z) \text{ (purely reactive, independent of line length)} \quad (2.32c)$$

$$V(z) = V_o^+ [e^{-j\beta z} - e^{j\beta z}] = -j2V_o^+ \sin\beta z \quad (2.32d)$$

$$I(z) = \frac{V_o^+}{Z_o} [e^{-j\beta z} + e^{j\beta z}] = 2 \frac{V_o^+}{Z_o} \cos\beta z \quad (2.32e)$$

The input impedance of a short-circuited lossless transmission line is purely reactive and can take on any value of capacitive or inductive reactance depending on the line length. The incident wave is totally reflected (with inversion) from the load setting up standing waves with $|V|_{min} = 0$ and $|V|_{max} = 2|V_o^+|$.

$$l = n \frac{\lambda}{2} \quad |Z_{in}| = 0, \quad n = 0, 1, 2, \dots \quad (2.32f)$$

$$l = (2n - 1) \frac{\lambda}{4} |Z_{in}| = \infty, \quad n = 0, 1, 2, \dots \quad (2.32j)$$

2.4.3 Open-Circuited Lossless Transmission Line ($Z_L = \infty$)

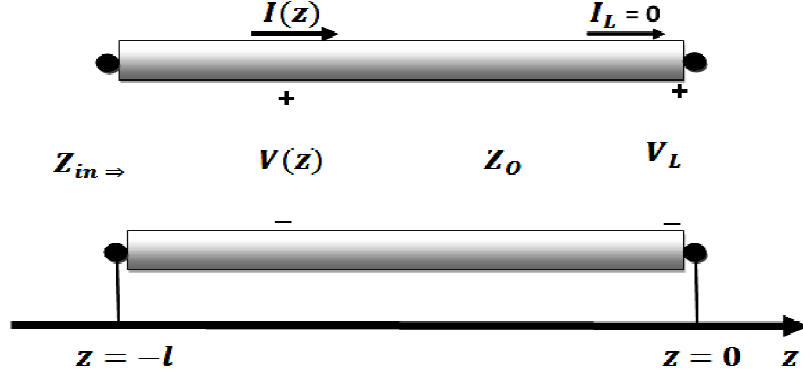


Figure 2.10: A transmission line terminated with open load circuit.

Figure 2.10 shows a transmission line terminated with open load circuit.

$$\Gamma = 1 \quad (2.33a)$$

$$S = \infty \quad (2.33b)$$

$$Z_{in} = -jZ_0 \tan(\beta z) \quad (\text{purely reactive, independent of line length}) \quad (2.33c)$$

$$V(z) = V_0^+ [e^{-j\beta z} + e^{j\beta z}] = 2V_0^+ \cos\beta z \quad (2.33d)$$

$$I(z) = \frac{V_0^+}{Z_0} [e^{-j\beta z} - e^{j\beta z}] = -2j \frac{V_0^+}{Z_0} \sin\beta z \quad (2.33e)$$

The input impedance of a short-circuited lossless transmission line is purely reactive and can take on any value of capacitive or inductive reactance depending on the line length. The incident wave is totally reflected (with inversion) from the load setting up standing waves with $|V|_{min} = 0$ and $|V|_{max} = 2|V_0^+|$.

$$l = n \frac{\lambda}{2} |Z_{in}| = 0, \quad n = 0, 1, 2, \dots \quad (2.33f)$$

$$l = (2n - 1) \frac{\lambda}{4} |Z_{in}| = \infty, \quad n = 1, 2, \dots \quad (2.33j)$$

3- Spatial purpose diodes

3.1 Varactor diode

3.1.1 Introduction

A varactor diode is a P-N junction diode that changes its capacitance, and its capacitance variation is very sensitive to reverse-biased voltage. It also known as Varicap Diode, VVC (Voltage Variable Capacitance), or tuning diode. Varactor diodes have been extensively used in microwave applications, which include band pass filter [43- 44], phase shifter [45], voltage-controlled oscillator [46- 47], mixer [48], nonlinear transmission line [49- 50], and frequency multiplier [51- 56]. The band pass filter and the phase shifter require a large capacitance change to obtain wide bandwidth performance. This is because these circuits generally use a varactor diode as an element of an LC resonant circuit and its resonance frequency is inversely proportional to the square root of capacitance value. In the voltage-controlled oscillator applications, the applied bias voltage determines oscillation frequency through capacitance variation. Therefore, the voltage-controlled oscillator requires proper capacitance- voltage characteristics for linear frequency tuning as well as a large capacitance change for a large bandwidth. On the other hand, highly nonlinear capacitance characteristics are important in such applications as mixer, nonlinear transmission line, and frequency multiplier because these circuits utilize harmonics generated through nonlinear impedance.

3.1.2 varactor diode operation

In a normal diode, the depletion region exists between p-region and n-region as shown in the figure 3.1a. The p-region and n-region act like the plates of capacitor while the depletion region acts like dielectric. Thus there exists a capacitance at p-n junction called transition capacitance, space charge capacitance, barrier capacitance or depletion region capacitance. It is denoted as C_T [57]. Mathematically it is given by the expression,

$$C_T = \frac{\epsilon A}{W} \quad (3.1)$$

Where ϵ is the permittivity of semiconductor, A is the area of cross section, and W is the width of depletion region.

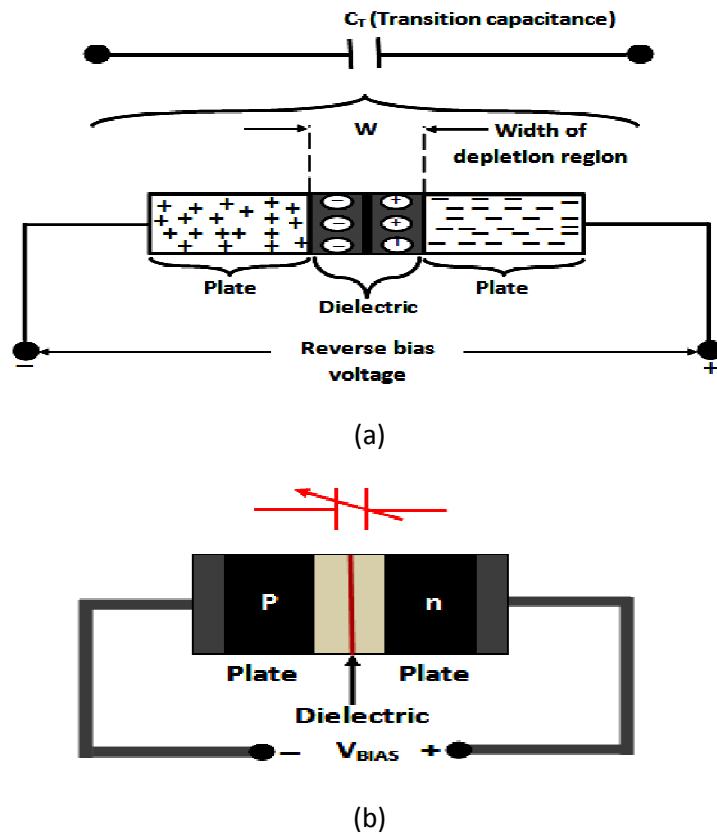


Figure 3.1: The reverse biased varactor diode: (a)depletion region and(b) a variable capacitor[57]

As the reverse biased applied to the diode increases, the width of the depletion region (W) increases. Thus the transition capacitance C_T decreases. In short, the capacitance can be controlled by the applied voltage. The variation of C_T with respect to the applied reverse bias voltage is shown in the figure 3.2.

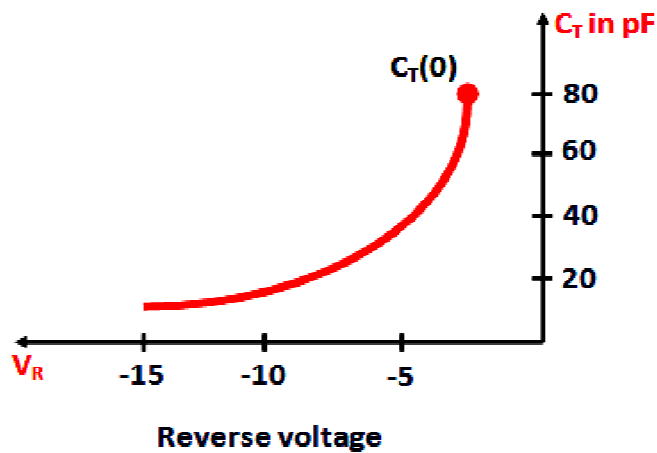


Figure3.2: Varactor diode transition capacitance[57]

The reverse voltage is negative. For a particular diode shown, C_T varies from 80pF to less than 5pF as V_R changes from 2V to 15V. In practice, the varactor diodes have positive temperature coefficient i.e. C_T value increases by small amount as the temperature increases.

3.1.3 Symbol and Equivalent Circuit

The figure 3.3a shows the symbol of varactor while the figure3.3b shows the first approximation for its equivalent circuit in the reverse bias region [57].

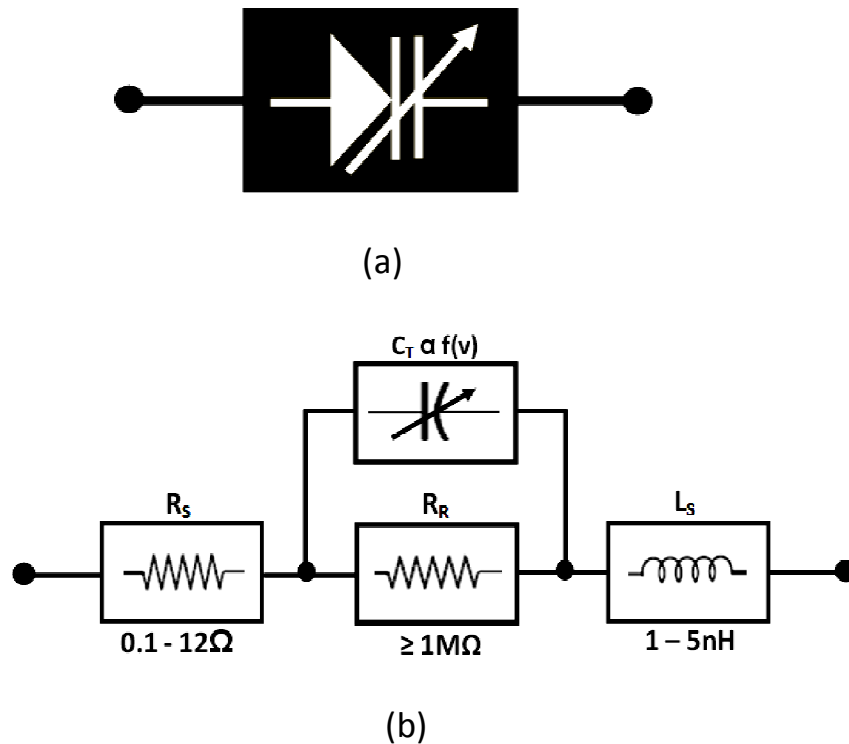


Figure3.3: Varactor diode transition capacitance, (a) symbol and (b) Equivalent circuit[57]

The R_R is the reverse resistance which is very large while R_s is the geometric resistance of diode which is very small. The inductance L_s indicates that there is a high frequency limit associated with the use of varactor diodes.

3.1.4 Expression for Transition Capacitance

For a varactor diode, the transition capacitance in terms of applied reverse bias voltage is given by [58],

$$C_T = \frac{K}{(V_j + V_R)^n} \quad (3.2)$$

Where K is a constant depends on semiconductor material and construction technique, V_j is the junction potential, V_R is magnitude of reverse bias voltage, and $n = \frac{1}{2}$ and $\frac{1}{3}$ for the alloy and diffused junctions respectively.

At the zero bias condition the capacitance is $C(0)$. In terms of $C(0)$, the transition capacitance is given by,

$$C_T = \frac{C(0)}{\left(1 + \left|\frac{V_R}{V_j}\right|\right)^n} \quad (3.3)$$

3.1.5 Applications

The main application of varactor diodes is LC tuned circuits. Figure 3.4 shows how varactor diode can be connected in a LC tuned circuits. The resonance frequency for a parallel LC tuned circuit is given by,

$$f_r = \frac{1}{2\pi\sqrt{LC}} \quad (3.4)$$

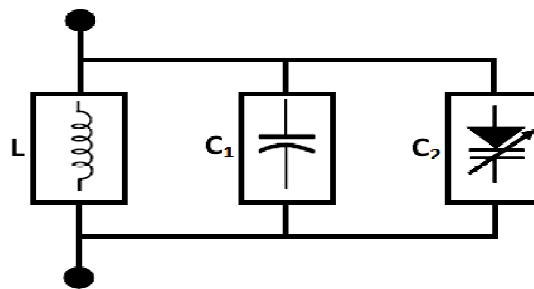


Figure3.4: Use of varactor diode in LC tuned circuit[58]

As varactor diode is connected in parallel, the resultant capacitance become $C_1 + C_2$. Hence the resonance frequency becomes,

$$f_r = \frac{1}{2\pi\sqrt{L(C_1 + C_2)}} \quad (3.5)$$

Where, C_2 is transition capacitance of varactor diode. The value of C_2 can be changed by controlling the voltage applied to the circuit. Hence circuit can be tuned by changing voltage applied at a resonance frequency, this is called electrical tuning.

The various other applications of varactor diodes are: tuned circuits, FM modulations, automatic frequency control devices, adjustable band pass filters, parametric amplifiers, and television receivers.

3.2 Schottky Diode

3.2.1 Introduction

The point contact diode is one of the earliest solid state semiconductor devices constructed. This type of diode is made when metal makes contact with a semiconductor surface. The point contact diode was later studied by Walter H. Schottky circa 1938 who formulated a theory as to why the diode worked; subsequently this device was named the Schottky diode to honor his contributions.

A Schottky diode is a junction of a lightly doped n-type semiconductor with a metal electrode. The junction of a doped semiconductor is usually n-type with a special metal electrode [59]. Schottky diodes acts as rectifiers and have been used for over 25 years in the power supply industry. The primary advantages of this diodes have very low forward voltage drop, where the value is typically 0.2 to 0.5 volt compare to the 0.6 to 0.8 found in silicon junction diode [59] (this lower voltage drop translates into higher system efficiency) and can produce fast switching speeds that approach zero time making them ideal for output stages of switching power supplies. This feature also stimulated their additional functioning in very super frequency (3- 30 GHz) applications for the communication links, generally referred to as microwave links [60-62]. This latter feature also including very low power involving signal and switching diode requirements of less than 100 picoseconds. These require small Schottky devices with low capacitance [63]. Schottky diode provides a high performance, cost-effective solution for today's circuit designs for retina application [64].

The Schottky barrier diode is a majority carrier device. This means that there is no diffusion capacitance associated with a forward-biased Schottky diode. The elimination of the diffusion capacitance makes the Schottky diode a higher frequency device. Also, when switching a Schottky diode from forward to reverse bias, there is no minority carrier stored charge to remove. Since there is no minority carrier storage time, so that the Schottky diode can be used in fast-switching application [65].

3.2.2 Schottky diodes construction and symbol.

The diodes which are specially manufactured to solve this problem of fast switching are called Schottky diodes. Its construction is different than the conventional p-n junction diode. It consist of a metal to semiconductor junction as shown in figure3.5b. These diodes are also called Schottky barrier diodes, surface barrier diodes or hot carrier diodes. The symbol for the Schottky diode is shown in figure3.5a.

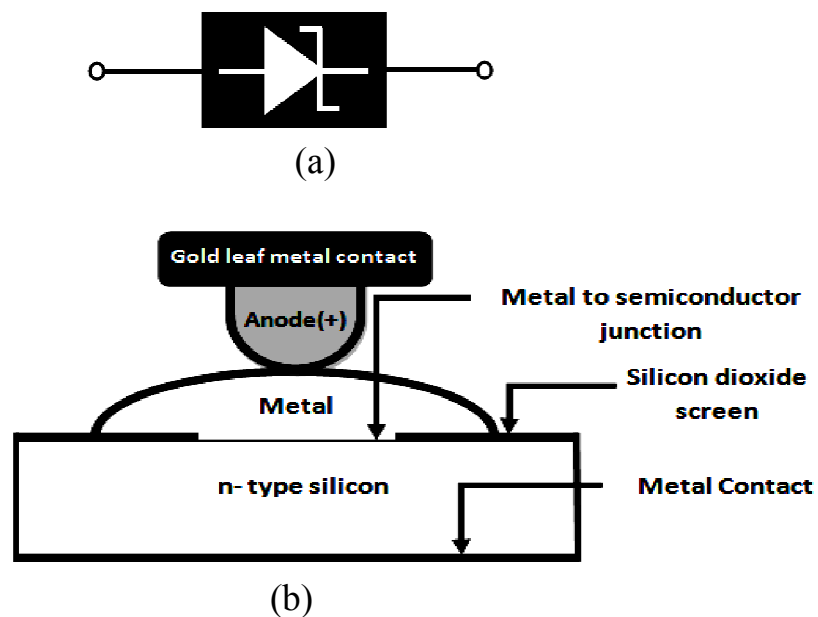


Figure3.5: Schottky diode, (a) Symbol and (b) Construction [58]

Schottky diodes are used primarily in high frequency and fast switching. They are also known as hot carrier diodes. A Schottky diode is formed by joining a doped semiconductor region (usually n-type) with a metal such as gold, silver or

platinum. Rather than a pn junction, there is a metal to semiconductor junction, as shown in figure3.6. The forward voltage drop is typically around 0.3 V [57].

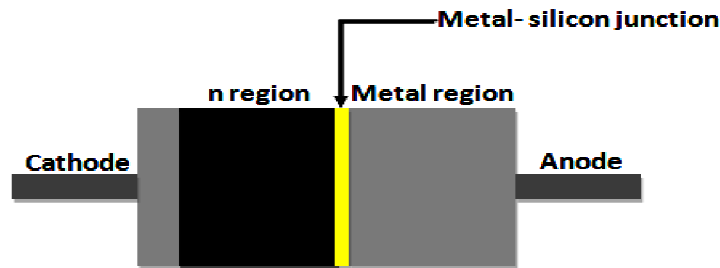


Figure3.6: Basic internal construction of a Schottky diode[57]

The Schottky diode operates only with majority carriers. There are no minority carriers and thus no reverse leakage current as in other types of diodes. The metal region is heavily occupied with conduction band electrons, and the n-type semiconductor region is lightly doped. When forward biased, the higher energy electrons in the n region are injected into the metal region where they give up their excess energy very rapidly. Since there are no minority carriers, as in a conventional rectifier diode, there is a very rapid response to a change in bias. The Schottky is a fast switching diode, and most of its applications make use of this property. It can be used in high frequency application and in many digital circuits to decrease switching times[58].

3.2.3 Characteristic of Schottky diode

Due to the minority carrier free region, Schottky diode cannot store the charge. Hence due to lack of charge storage, it can switch off very fast than a conventional diode. It can be easily switched off for the frequencies above 300MHz. The barrier at the junction for a Schottky diode is less than that of normal p-n junction diode, in both forward and reverse bias region. The barrier potential and breakdown voltage in forward and reverse bias region respectively are less than p-n junction diode. The barrier potential of Schottky diode is 0.25 V as compared to 0.7 V for normal diode. The figure3.7 shows the comparison of characteristics of Schottky diode and a conventional p-n junction diode[58].

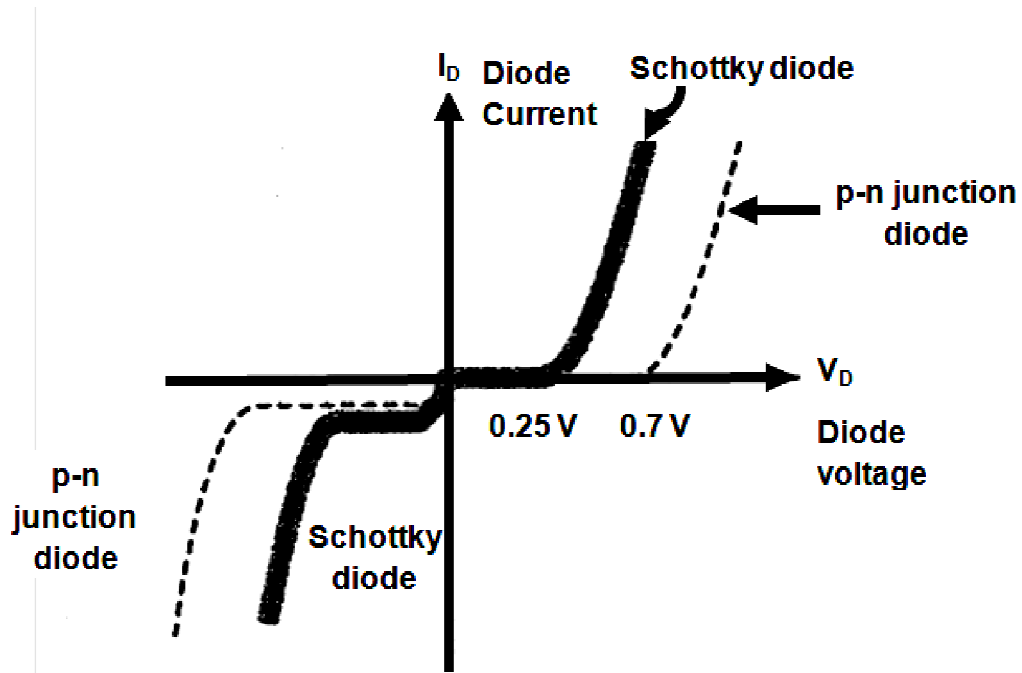


Figure3.7 : Comparison of characteristics[58]

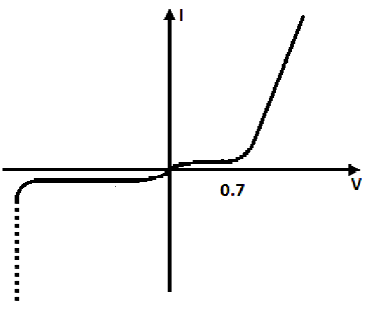
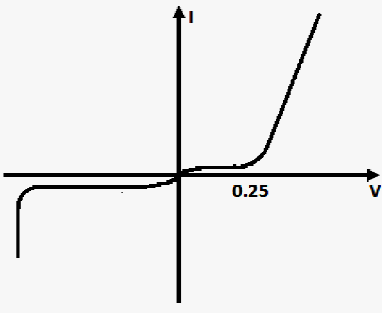
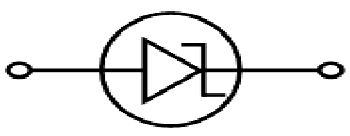
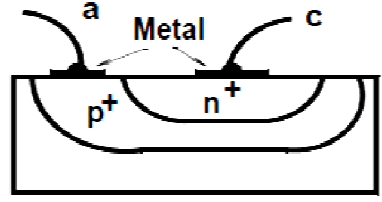
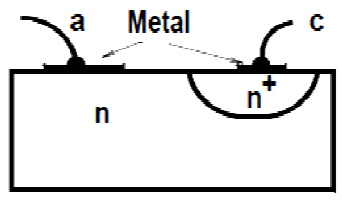
3.2.4 Applications

Due to fast switching characteristics, the Schottky diodes are very useful for high frequency applications such as digital computers, high speed TTL, radar system, mixers, detectors in communication equipments and analog to digital converters[66].

3.2.5 Comparison between Schottky diode and conventional diode

The comparison between Schottky diode and conventional diode is given in table 3.1

Table 3.1: Comparison between Schottky diode and conventional diode

Parameter	p-n junction diode	Schottky diode
Junction	Semiconductor to semiconductor	Semiconductor to metal
Carriers	Minority and majority	Only majority
Reverse recovery time	More	less
Barrier potential	More about 0.7 V	Less about 0.25 V
Breakdown voltage	More	less
Switching speed	less	high
PIV rating	More	less
Frequency range	Up to 10 MHz	Very high more than 300 MHz
Characteristics		
symbol		
Application	Mainly rectifiers and low frequency devices	High frequency devices digital computers, radar systems, Schottky TTL logics, mixers etc.
Structure		

3.3 Resonant Tunneling Diode

3.3.1 Introduction

There are many reasons why resonant tunneling diodes (RTDs) are of interest to the semiconductor community. First, they can be used to test and modify models of semiconductor behavior that take into account quantum effects, such as the envelope approximation based on using effective masses of carriers. Further, the simple vertical transport structure is the basis for more complicated, multilayer devices using quantum interface effects to create new inter-sub-band structure and devices (e.g. photo detectors). Finally, RTDs have a number of interesting device applications of their own. For example, they are among the limited electronic devices that can reach towards terahertz frequencies, offering possibilities for signal generation, switching, analog-to-digital conversion and detection. RTDs maintain their position as the fastest large signal semiconductor switching device with slow rates as fast as 300 mV/ps [66].

The resonant tunnel diode, also known as the Esaki diode, was first discovered by Leo Esaki in 1957 [67] when exploring internal field emission in heavily-doped reverse biased germanium p-n junctions. He observed the distinctive N-shaped current-voltage (I-V) characteristic of this same junction when biased in the forward bias direction similar to the I-V characteristic of the Si tunnel diode shown in Figure 3.8.

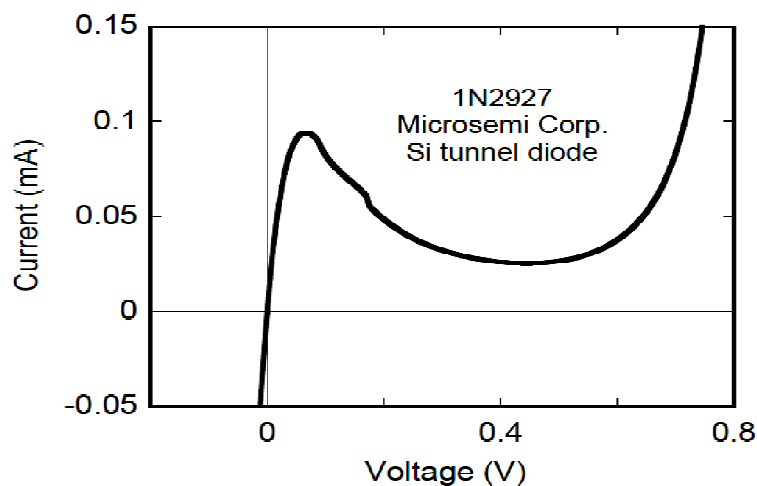


Figure 3.8: Current-voltage characteristic of a commercial silicon tunnel diode [66]

Following Esaki's discovery, tunnel diodes have received interest because of their remarkable multivalve I-V characteristic and inherent high switching speeds. They have been used in circuits such as amplifiers [68], oscillators [69], pulse generators [70], and analog-to-digital converters (ADCs) [71]. More recently it has been shown that incorporating tunnel diodes (Esaki diodes or resonant tunneling diodes (RTDs)) with transistors can improve circuit performance [72], by increasing the speed of signal processing circuitry or decreasing power consumption at the same speed. A variety of these hybrid III – V transistor/RTD circuits have been demonstrated, e.g., ADCs [73] and oscillators [74]. A new tunnel diode differential comparator has been proposed [75] which lowers power dissipation by a factor of two relative to a transistor-only comparator while also increasing speed. In prior work, silicon tunnel diodes have achieved an oscillation frequency as high as 48 GHz [76]. A transmission line pulse generator has been previously demonstrated using InP-based RTDs [77]. Tunneling diodes (TDs) have been widely studied for their importance in achieving very high speed in wide-band devices and circuits that are beyond conventional transistor technology. A particularly useful form of a tunneling diode is the Resonant Tunneling Diode (RTD) has been shown to achieve a maximum frequency of up to 2.2 THz as opposed to 215 GHz in conventional Complementary Metal Oxide Semiconductor (CMOS) transistors. [78] The very high switching speeds provided by RTDs have allowed for a variety of applications in wide-band secure communications systems and high-resolution radar and imaging systems for low visibility environments.

Tunneling diodes provide the same functionality as a CMOS transistor where under a specific external bias voltage range, the device will conduct a current thereby switching the device "on". However, instead of the current going through a channel between the drain and source as in CMOS transistors, the current goes through the depletion region by tunneling in normal tunneling diodes and through quasi-bound states within a double barrier structure in RTDs.

3.3.2 Physical Structure of RTD

Resonant tunneling diodes are commonly formed from heterostructures consisting of layers of GaAs and AlAs as shown in figure 3.9. For example, the sequence from GaAs substrate of GaAs/AlAs/ GaAs/AlAs/ GaAs presents a structure where free electrons in GaAs layers can exist at energies below the bottom of the AlAs conduction band. Hence, the AlAs layers act as barriers to electron transport [79].

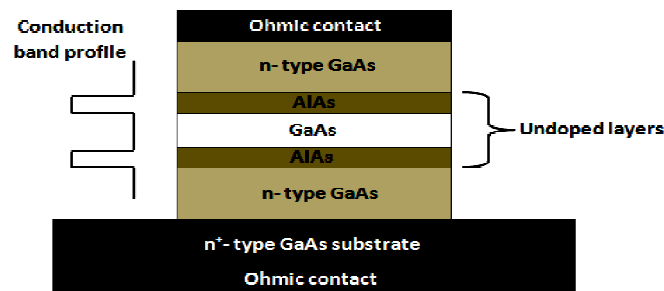


Figure 3.9: Schematic diagram of double-barrier resonant tunneling diode [79]

The energy band diagram of the heterojunction is observed in figure 3.10. There are five physical parameters that can be varied in an RTD: 1) the barrier height, 2) the well depth, 3) the symmetry of the structure, 4) the quantum well width, 5) the barrier width.

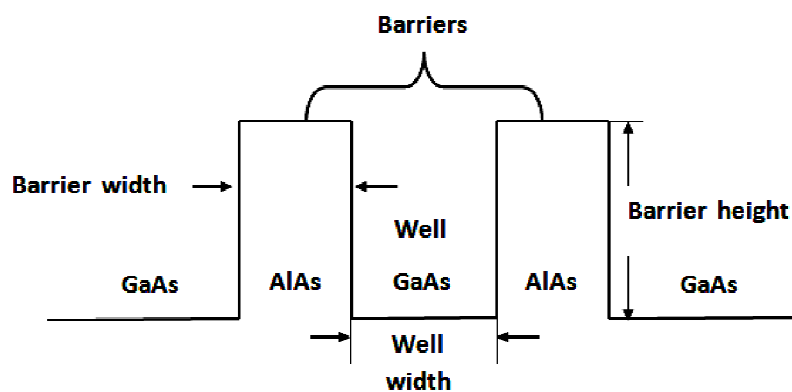


Figure 3.10: RTD band diagram [79]

3.3.3 Equivalent Circuit of RTD

The equivalent circuit of the double barrier resonant tunneling diode used for analysis is shown in figure3.11. The intrinsic RTD consist of three parallel branches: a variable capacitance(C_n), variable resistance and inductance in series with conductance.

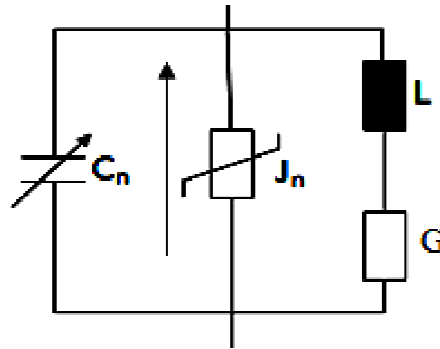


Figure3.11: Equivalent circuit of RTD

3.3.4 RTD Current-Voltage Characteristics

A semiconductor has a forbidden region where there are no states available for its electrons. This region called the band gap. The states below this gap (which comprise the valence band) are almost all filled. The states above it (the conduction band) are almost empty. The number of empty states in valence band, or electrons in the conduction band, can be controlled by adding either acceptor impurities or donor impurities to the semiconductor crystal. Each acceptor impurity takes one electron out of the valence band, and each donor gives one electron to the conduction band. In this way p-type (empty states in valence band) and n-type (electrons in conduction band) regions can be built into a crystal. The surface where two of these regions touch each other is called a p-n junction. Figure 12 and 13 represent the conduction and valence bands in the vicinity of a junction at different values of applied bias. One can see that as the bias is increased the bands which overlap each other at zero bias become uncrossed. Since tunneling is represented by a horizontal transition on this picture, the current decreases as the bands become uncrossed.

The origin of the Esaki current can be qualitatively understood by considering the change in the characteristics of a conventional p-n junction diode as one

goes to higher and higher concentrations of free carriers in the semiconductor crystal. As one increases the density of the charge carriers, the reverse breakdown voltage decreases. When a large forward voltage is applied, the diode goes out of the reverse breakdown condition, and the current falls to a small level. The reverse breakdown current that flows with forward bias is the Esaki current.

The nonlinear I-V characteristic of an Esaki tunnel diode figure 3.12 originates from electron transport across a degenerately doped $p^+ - n^-$ junction figure 3.12. Heavy doping (typically $> 10^{19}/\text{cm}^3$) in these junctions creates high electric fields, exceeding two million volts per centimeter, across a depletion layer of several nanometers. Across this thin depletion layer, electrons can quantum-mechanically tunnel. The tunneling phenomenon is responsible for a high conductance near zero bias. A negative differential resistance (NDR) arises in the tunnel diode in a small range of biases typically between approximately 100 and 300 mV.

The current-voltage characteristic of an Esaki diode can be qualitatively explained using the band diagram and I-V characteristic as shown schematically in figure 3.13. When reverse bias is applied, figure 3.13a, current flows by electron tunneling from occupied states on the p-side valence band into unoccupied states in the n-side conduction band. In equilibrium, with no applied bias, figure 3.13b, the net tunneling current is zero. When a forward bias is applied, current flows by electron tunneling from occupied states in the n-side conduction band into unoccupied states in the p-side valence band.

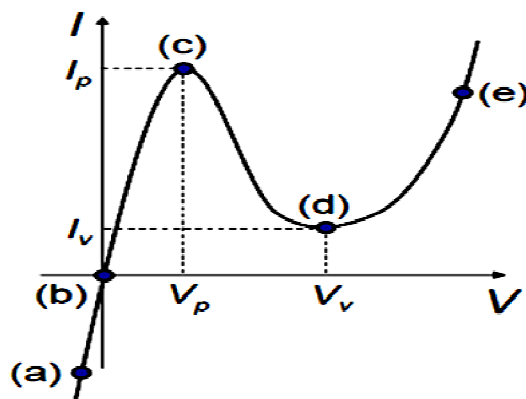
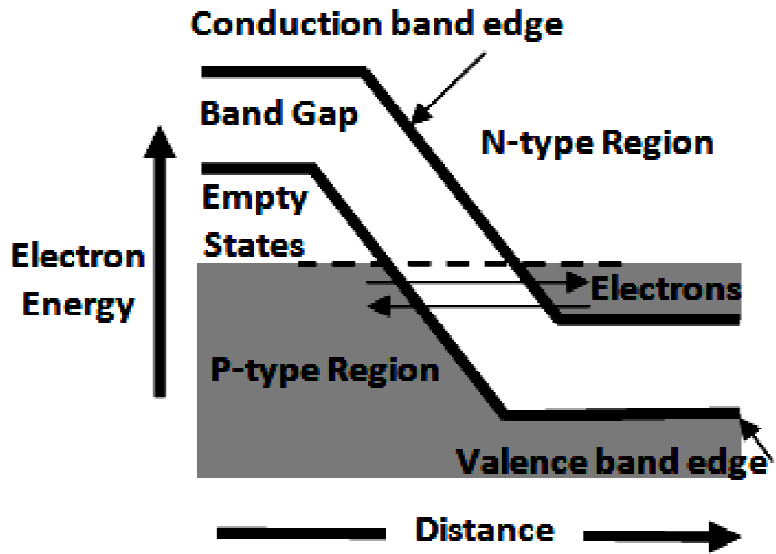
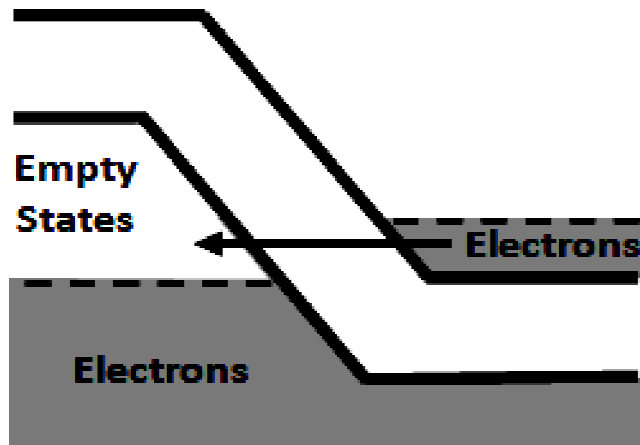


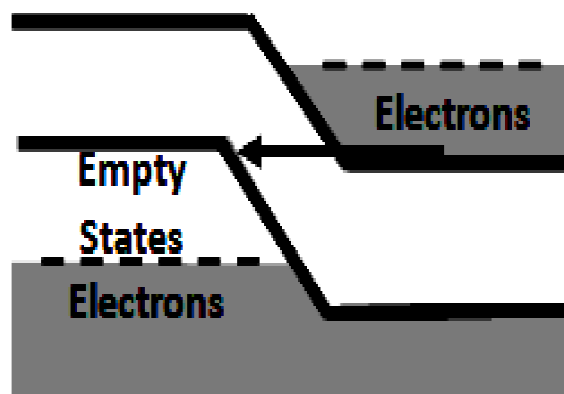
Figure 3.12: Si Esaki diode characteristic curve[49]



(a)



(b)



(c)

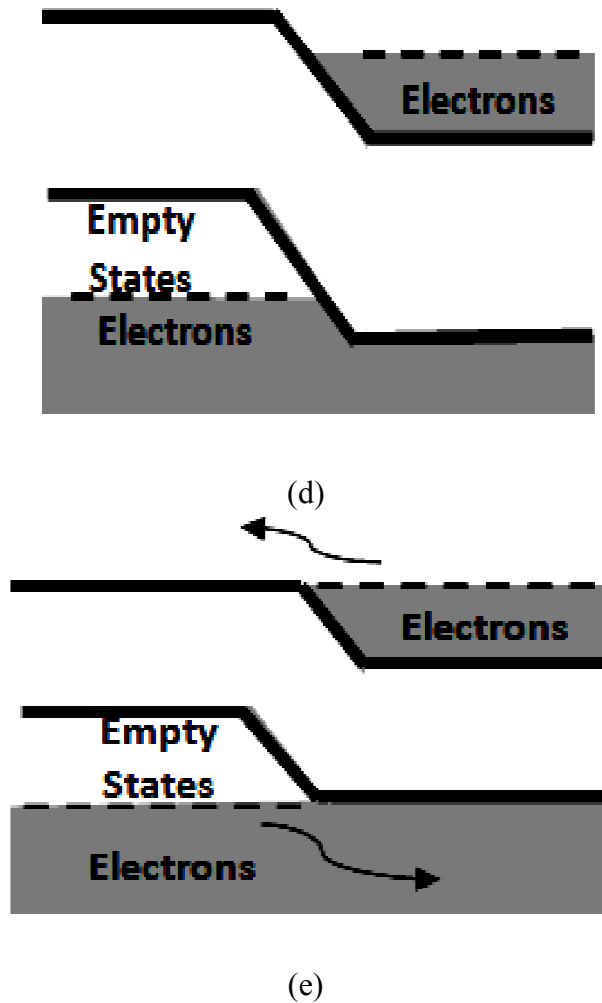


Figure 3.13: Schematic energy band diagram of RTD[49]

Maximum alignment between electrons on the n side and holes on the p side gives rise to a peak current I_p at a voltage V_p as labeled in figure 3.13c. When the conduction band minimum on the n side is raised above the valence band maximum on the p side, the valley current I_v results at a voltage V_v figure 3.13d. With further increase in the voltage, the current increases due to tunneling through defect states in the depletion layer and thermionic emission over the diode internal barrier, figure 3.13e.

3.3.5 Characteristic Model Equation

The N shape can be modeled by current–voltage relationship approximated by

$$J(V) = BV(V - U_1)(V - U_2), \quad (3.6)$$

Where U_1, U_2 are constants, and B is a factor which is determined by the slope at $V = 0$. A sketch of the above relation is depicted in figure3.14, where S_1 and

S_2 represented the positive and negative area for the $J(V)$ characteristic. An external bias current is assumed such that the $J(V)$ relation exhibits a bistable behavior of the RTD.

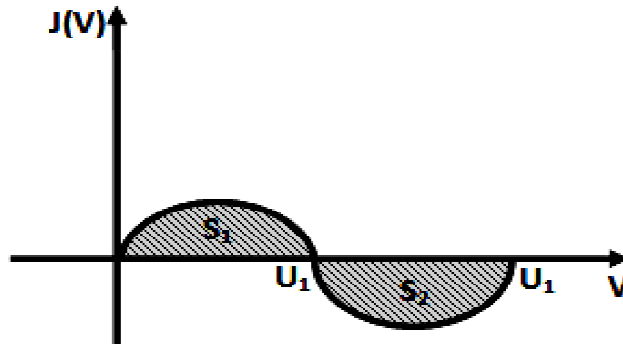


Figure 3.14: RTD current – voltage characteristics[33]

3.3.6 Advantage of RTD

The advantages of a tunnel diode are[80]:

- 1- Environmental immunity i.e. the peak point (V_p , I_p) is not a sensitive function of temperature.
- 2- Low cost.
- 3- Simplicity i.e. a tunnel diode can be used along a d.c. supply and few passive elements to obtain various application circuits.
- 4- Low noise.
- 5- High speed i.e. the tunneling takes place at speed of light hence the switching times of the order of a nanosecond are easily obtained and switching times as low as 50 psec also can be obtained.
- 6- Low power consumption.

3.3.7 Application of RTD

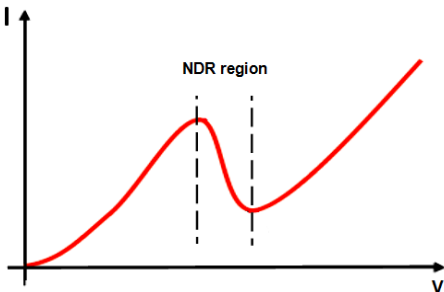
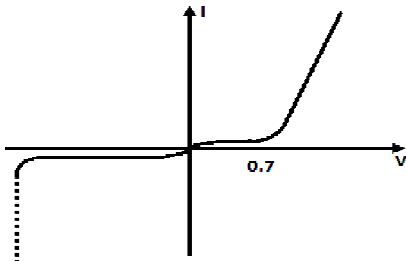
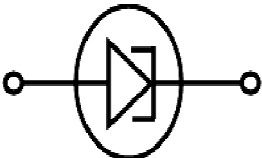
The various other applications of RTD are[81]:

- 1- As a high speed switch.
- 2- In pulse and digital circuits.
- 3- In negative resistance and high frequency (microwave) oscillator.
- 1- In switching networks.
- 2- In timing and computer logic circuitry.
- 3- Design of pulse generator and amplifiers.

3.3.8 Comparison between RTD and Conventional Diode

The comparison of resonant tunneling diode and conventional p-n diode is given in table 3.2[81]:

Table 3.2: Comparison between RTD & semiconductor diode

Sr. No.	Resonant Tunneling Diode(RTD)	Conventional p-n junction diode
1	Impurity concentration is high about 1 part in 10^3 atoms	Impurity concentration is low about 1 part in 10^8 atoms
2	Depletion region width is about 5 microns, which is 1/100th the of typical p-n junction diode.	The width of depletion region is high compared to the RTD
3	The carrier velocities are very high at low forward bias, hence can punch through the depletion region.	The carrier velocities are low at low forward bias, hence cannot penetrate the depletion region.
4	The V-I characteristics shows the negative resistance region.	The V-I characteristics does not show the negative resistance region.
5		
6	The materials used for construction are germanium or gallium arsenide.	The silicon is most popularly used.
7	<p style="text-align: center;">The symbol is,</p> 	<p style="text-align: center;">The symbol is,</p> 
8	The switching time is very low of order of nano to picoseconds.	The switching time is high.
9	Used for high frequency oscillation, high speed application such as computers, pulse and digital circuits and switching networks.	Used for rectifiers and other general purpose application.

4- Nonlinear Transmission Line and Soliton Waves

4.1 Nonlinear Transmission Line Concept

4.1.1 Nonlinear System

Definition in mathematics, a nonlinear system is a system which is not linear, that is, a system which does not satisfy the superposition principle, or whose output is not directly proportional to its input. Less technically, a nonlinear system is any problem where the variable(s) to be solved for cannot be written as a linear combination of independent components[82].

Most of real life problems involve nonlinear systems, the nonlinear systems are very hard to solve explicitly but qualitative and numerical techniques may help to give some information on the behavior of the solutions . In the nonlinear system when the input is a wave of certain frequency then the output is a group of other frequencies .

4.1.2 Nonlinear Transmission Line Models

The model of an NLTL is similar to a standard distributed transmission line model as we mentioned in chapter 2 except either the inductors or capacitors are nonlinear [83], as shown in figure 4.1. In practice, the implementation in figure 4.1b is selected, as nonlinear capacitors are more readily available in standard processes than nonlinear inductors. Nonlinear capacitors can be implemented using varactor or Schottky diodes [83-84]. Discrete NLTLs are implemented using discrete inductors and varactors [85- 86], and distributed NLTLs are implemented by periodically loading a microstrip [87] or coplanar waveguide (CPW) [84 - 88] transmission line with diodes. NLTLs accept a periodic input signal and compress it into a series of rectified pulses.

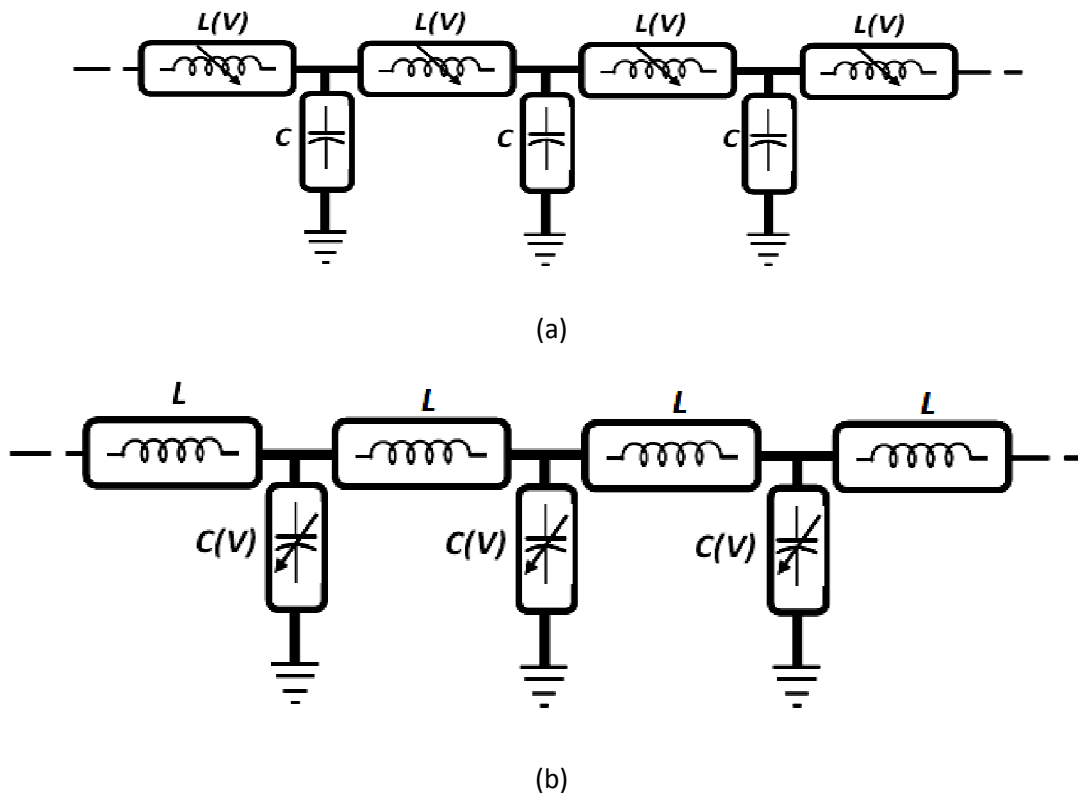


Figure 4.1: NLTL Models, (a) discrete inductors and (b) varactors

4.1.3 Practical Nonlinear Transmission line(NLTL)

The NLTL can be constructed from a linear transmission line (two conductors running in parallel) by periodically loading it with voltage-dependent capacitors (varactors) such as reversed-biased *pn* junction diodes, Schottky diodes, or metal-oxide- semiconductor (MOS) capacitors as shown in figure 4.2. Alternatively, the NLTL can be obtained by forming an artificial *LC* transmission line with varactors and discrete inductors as illustrated in figure 4.1a and 4.1b respectively. The NLTL is a nonlinear dispersive medium. The nonlinearity originates from the varactors, whose capacitance changes with the applied voltage. The dispersion arises from the structural periodicity, i.e., periodic lumped loading of varactors. A common feature of any periodic structure like the NLTL is the existence of a cutoff frequency, beyond which no Fourier component can propagate, and below which different Fourier components travel at different speeds (i.e. dispersion).

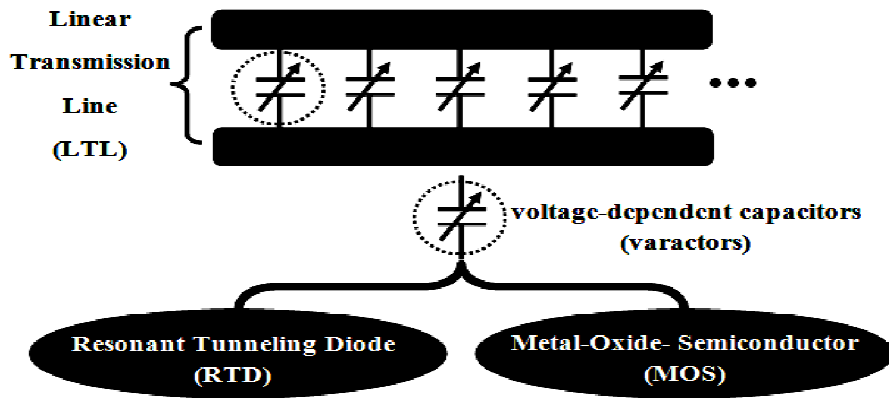


Figure 4.2: Linear transmission line with voltage dependent capacitor

4.1.4 Structure of NLTL

NLTLs consisting of coplanar waveguide (CPW) [83] (figure 4.3) periodically loaded with reverse biased Schottky diodes provide nonlinearity due to the voltage dependent capacitance, dispersion due to the periodicity, and dissipation due to the finite conductivity of the CPW conductor and series resistance of the diodes. A schematic diagram of the circuit is shown in figure 4.4. An approximate equivalent circuit consisting of series inductors and shunt capacitors (figure 4.1b) is much easier to analyze than the transmission line circuit.

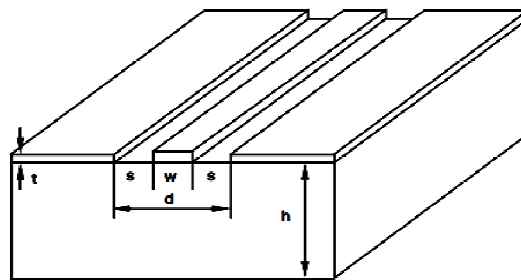


Figure 4.3: A metallic coplanar waveguide(CPW) on a dielectric substrate[83]

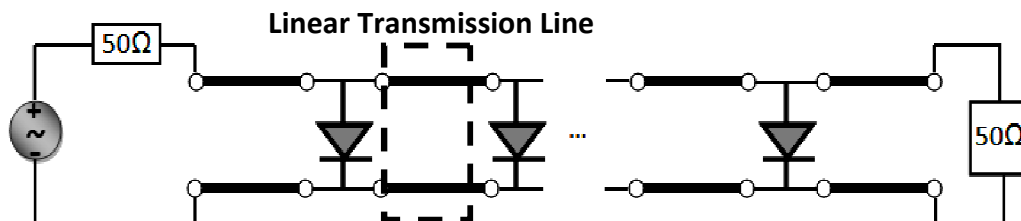


Figure 4.4: Schematic diagram of NLTL[83]

A nonlinear transmission line (NLTL) is defined as a lumped transmission line containing a series inductor and a shunt Schottky varactor in each section [89]. The advantage of RTD diodes is that they can be used for signal generation and detection at frequencies well above transistor bandwidth. An equivalent circuit model of one section of an NLTL is shown in figure 4.5, followed by photos of an actual NLTL circuit figure 4.6 and a close up view of a single element in NLTL figure 4.7.[83]

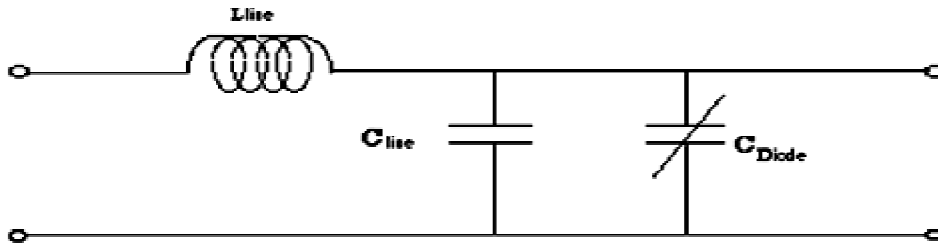


Figure 4.5: Equivalent circuit model of an NLTL[83]

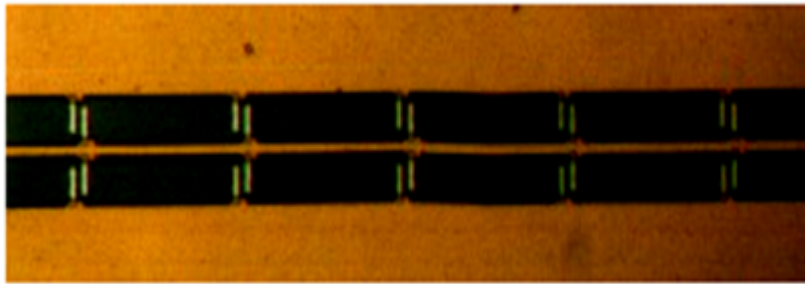


Figure 4.6: Photo of an actual NLTL [83]

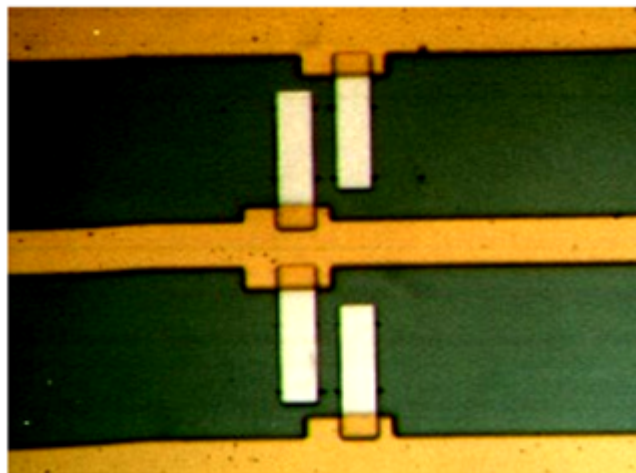


Figure 4.7: Close up view of a single element in the NLTL[83]

4.1.5 NLTL Characteristics

The NLTL has three fundamental and quantifiable characteristics just as any non ideal transmission line. These are nonlinearity, dispersion, and dissipation[38].

4.1.5.1 Dispersion

Dispersion is a variation in phase velocity with frequency. At low frequencies, loss is dominated by coplanar waveguide (CPW) resistivity. At high frequencies, loss is dominated by diode series resistance.

4.1.5.2 Nonlinearity

Diodes present two sources of nonlinearity: conductive and reactive. The conductive nonlinearity is evident in the $I(V)$ (current and voltage) curves and the reactive nonlinearity is evident in the $C(V)$ (capacitance and voltage) curves .

4.1.5.3 Dissipation

There are two main sources of dissipation in an NLTL. These are diode series resistance and metallic losses. Diode losses arise from the nonzero contact and bulk resistances of the structure while metallic losses arise from the geometry and finite conductivity of the CPW. Another source of loss is radiation, where some portion of the propagating energy is coupled into the substrate; but this loss mechanism is much less significant in an NLTL than the other two.

4.1.6 Nonlinear transmission line Applications

- 1- NLTLs are used for the development of solitons , which are employed in high-speed electronic circuits such as an electrical shock generator [90].
- 2- NLTLs can be used as broadband delay lines at low signal levels by varying the bias voltage and hence the propagation velocity, which varies as the inverse square root of the $C(V)$ curve.
- 3- NLTLs can be employed to generate free propagating broadband pulses of electromagnetic radiation, which can then be utilized in millimeter-wave reflectometry applications.
- 4- The NLTL is also being considered for use as the pulse compressor in both ultra wideband and collision avoidance radar systems. A full collision avoidance radar system proof-of-principle implementation is currently being

developed at 24 GHz, with the intent to eventually build a system at 94 GHz[91].

- 5- Nonlinear transmission lines (NLTLs) find applications in a variety of high speed, wide bandwidth systems including picoseconds resolution sampling circuits, laser and switching diode drivers, test waveform generators, and mm-wave sources [92].

4.2 Soliton Waves

The concept of a solitary wave was introduced to science by John Scott Russell 170 years ago [93]. In 1834 he observed a wave which was formed when a rapidly drawn boat came to a sudden stop in narrow channel. According to his diary, this wave continued “at great velocity, assuming the form of a large solitary elevation, a well-defined heap of water that continued its course along the channel apparently without change of form or diminution of speed.” These solitary waves, now called *solitons*, have become important subjects of research in diverse fields of physics and engineering. There is a considerable body of work on solitons in applied mathematics [94 -95], applied physics especially in optics [96 -99] and a few works in electronics [100- 102]. The ability of solitons to propagate with small dispersion can be used as effective means to transmit data, modulated as short pulses over long distances; one example of this is the ultra wideband impulse radio that has recently gained popularity [103]. Since the 1970s, various investigators have discovered the existence of solitons in nonlinear transmission lines (NLTLs), through both mathematical models and physical experiments (see for example Refs. [104- 108]).

4.2.1 Definition of Soliton Wave

A soliton is a solitary wave which asymptotically preserves its shape and velocity after a nonlinear interaction with other solitary waves or even an arbitrary localized disturbance. In mathematics and physics, a soliton is a self-reinforcing solitary wave(a wave packet or pulse) that maintains its shape while it travels at constant speed. Solitons are caused by a cancellation of nonlinear and dispersive effects in the medium. "Dispersive effects" refer to dispersion relations between the frequency and the speed of the waves. Solitons arise as the

solutions of a widespread class of weakly nonlinear dispersive partial differential equations describing physical systems. The soliton phenomenon was first described by John Scott Russell (1808-1882) who observed a solitary wave in the Union Canal in Scotland. He reproduced the phenomenon in a wave tank and named it the "Wave of Translation". In 1895 Diederik Korteweg and Gustav de Vries provided what is now known as the Kdv equation ($u_t - 6uu_x + u_{xxx} = 0$), including solitary wave and periodic conical wave solutions. A solitary wave is a non-singular and localized wave which propagates without change of its properties (shape, velocity etc.). Solitary wave type solution is Shown in figure 4.8.

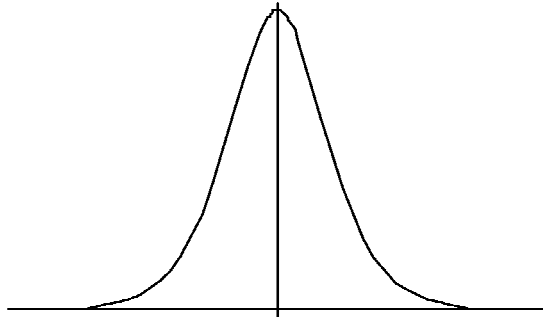


Figure 4.8: Plot of a solitary wave solution[105]

4.2.2 Soliton Waves applications

- 1- Soliton pulses can be used as the digital information carrying 'bits' in optical fibers.
- 2- Solitary waves are very useful to study the fluid dynamical problems and in plasma studies.
- 3- Josephson junction, solitons are used to study the propagation of magnetic flux through the junction.
- 4- Solitary waves arises in the study of nonlinear dynamics of DNA
- 5- Optical fibers and telecommunications
- 6- Electrical transmission lines
- 7- Statistical mechanics
- 8- Stratified fluids
- 9- Water waves in channels, shallow water and the ocean
- 10- Quantum field theory

5- Analog-to-Digital Converter & Gray Code

5.1 Analog-to-Digital Converter

An analog-to-digital converter (abbreviated ADC, A/D or A to D) is a device that converts a continuous quantity to a discrete digital number. Some examples of continuous time signals are speech, medical imaging, sonar, radar, electronic warfare, instrumentation, consumer electronics, and telecommunications. The reverse operation is performed by a digital-to-analog converter (DAC). Typically, an ADC is an electronic device that converts an input analog voltage (or current) to a digital number proportional to the magnitude of the voltage or current. However, some non-electronic or only partially electronic devices, such as rotary encoders, can also be considered ADCs. The digital output may use different coding schemes. Typically the digital output will be a two's complement binary number that is proportional to the input, but there are other possibilities. An encoder, for example, might output a Gray code. Two purposes of ADC, these are (1) to enable computer analysis of the signal, and, (2) to enable digital transmission of the signal. Figure 5.1 illustrates the basic element of electrical transmission system. High-speed analog-to-digital converters (ADCs) are the key building blocks in many applications including high-data-rate serial links [109]–[111], ultra-wideband (UWB) systems [112], the read channels of magnetic and optical data storage devices [113], high-speed instrumentation [114, 115], wideband radar and optical communications [116].

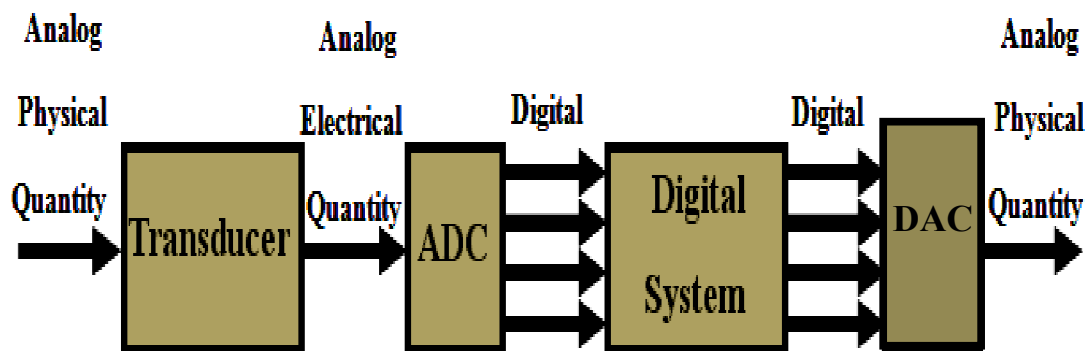


Figure 5.1: Basic element of communication system [116]

5.1.1 A/D Converter Constraints

- 1- Resolution
- 2- Speed
- 3- Cost

As with any engineering system these constraints are dependent on each other. Trade-offs must be made.

5.1.2 Types of A/D Converters

1. Dual slope integrating converters
2. Successive-approximation converters
3. Flash (Parallel) converters
4. Voltage to frequency converters
5. Ramp converters

5.1.3 What Makes a good A/D Converter?

1. High resolution
2. High speed
3. Low cost

Generally, in order to improve one of these aspects, you must degrade one or more of the others.

Table5.1 illustrate a comparison between different types of analog to digital converter

Table5.1:Comparison between different types of analog to digital converter

	Analog to Digital Converter				
	Dual Slope Integrating	Successive-Approximation	Flash (Parallel)	Voltage to Frequency	Ramp Converters
Resolution	High	Medium	Poor	Poor	Medium
Speed	Poor	Medium	Extremely High	Medium	High
Cost	Low	Medium	High	Medium	Medium

5.1.4 A/D Converter Applications

- 1- Video data digitizing
- 2- Radar
- 3- Barcode scanners
- 4- Digital instrumentation
- 5- Transient signal analysis
- 6- Modulators
- 7- Medical imaging

5.2 The Gray Code

What we now call “Gray code” was invented by Frank Gray. It was described in a patent that was awarded in 1953; however, the work was performed much earlier, the patent being applied for in 1947. Gray was a researcher at Bell Telephone Laboratories; during the 1930s and 1940s he was awarded numerous patents for work related to television.

The term “Gray code” is sometimes used to refer to any single-distance code, that is, one in which adjacent code words (perhaps representing integers differing by 1) differ by 1 in one digit position only. Gray introduced what we would now call the canonical binary single-distance code, though he mentioned that other binary single-distance codes could be obtained by permuting the columns and rotating the rows of the code table. The codes of Gray, and natural extensions to bases other than binary, are only a very small subset of all single-distance codes.

The Gray code is an unweighted code; that is, there are no specific weights assigned to bit position. The important feature of the Gray code is that it exhibits only a single bit change from one code number to the next. This property is important in many application, such as shaft position encoder, where error susceptibility increases with the number of bit changes between adjacent numbers in a sequence. The Gray code is not an arithmetic code.

Table 5.2 is a listing of four bit Gray code number for numbers from 0 through 15. Like the binary numbers, the Gray code can have any number of bits. Notice the single bit change between successive code numbers. For instance, in going

from decimal 3 to decimal 4, the Gray code changes from 0010 to 0110, while the binary code change from 0011 to 0100, a change of three bits. The only one bit change is in the third bit from the right in Gray code; the others remain the same. Binary numbers are shown for reference.

Table5.2: Four- bit Gray code

Gray Code				Decimal	Binary			
2 ³	2 ²	2 ¹	2 ⁰		2 ³	2 ²	2 ¹	2 ⁰
0	0	0	0	0	0	0	0	0
0	0	0	1	1	0	0	0	1
0	0	1	1	2	0	0	1	0
0	0	1	0	3	0	0	1	1
0	1	1	0	4	0	1	0	0
0	1	1	1	5	0	1	0	1
0	1	0	1	6	0	1	1	0
0	1	0	0	7	0	1	1	1
1	1	0	0	8	1	0	0	0
1	1	0	1	9	1	0	0	1
1	1	1	1	10	1	0	1	0
1	1	1	0	11	1	0	1	1
1	0	1	0	12	1	1	0	0
1	0	1	1	13	1	1	0	1
1	0	0	1	14	1	1	1	0
1	0	0	0	15	1	1	1	1

5.2.1 Why Use Gray Code?

Gray Code is the most popular Absolute encoder output type because its use prevents certain data errors which can occur with Natural Binary during state changes. For example, in a highly capacitive circuit (or sluggish system response), a Natural Binary state change from 0011 to 0100 could cause the counter/PLC to see 0111. This sort of error is not possible with Gray Code, so the data is more reliable.

5.2.2 Properties of Gray code

- 1- Adjacent words in the Gray code sequence differ in one bit position only.
- 2- The Gray code is cyclic.
- 3- Not arithmetic
- 4- Not weighted (e.g. $2^22^12^0$)
- 5- Limits the amount of error that can occur when several bits change between numbers
- 6- No limit to number of converted bits

6-Microwave A/D Conversion Design and Simulation

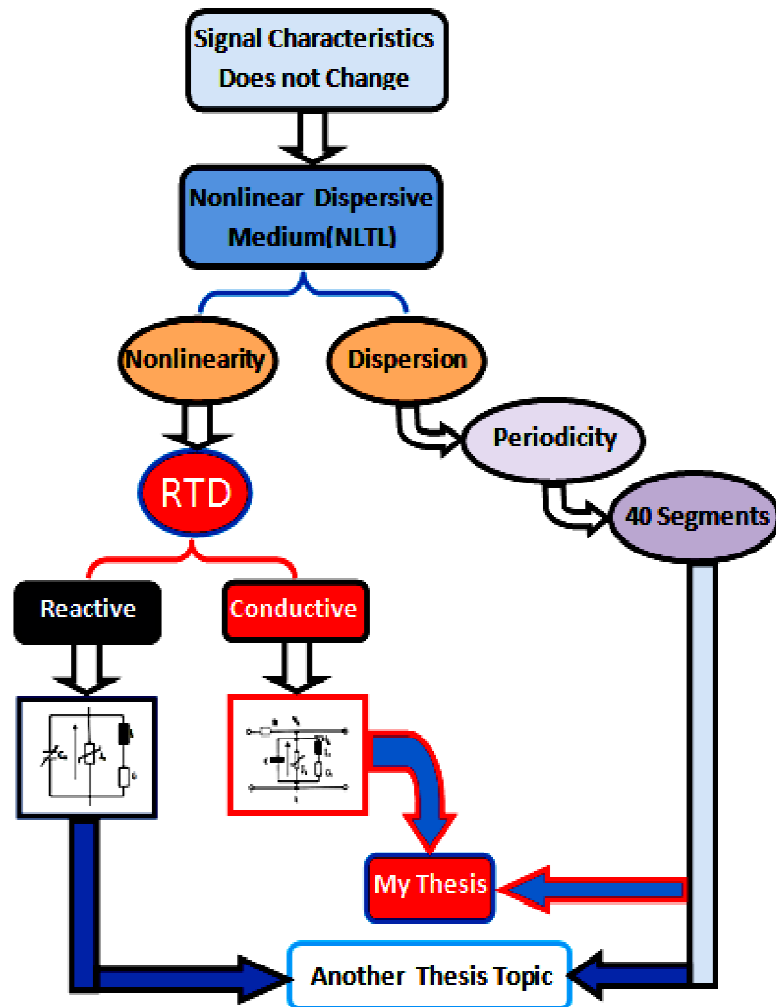
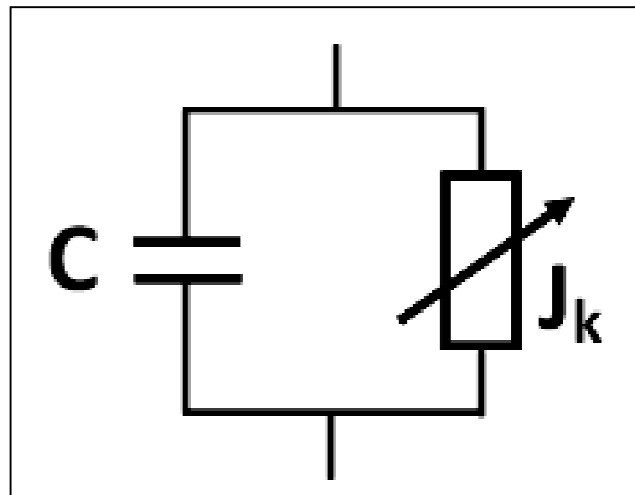


Figure 6.1 : Schematic of the thesis purpose

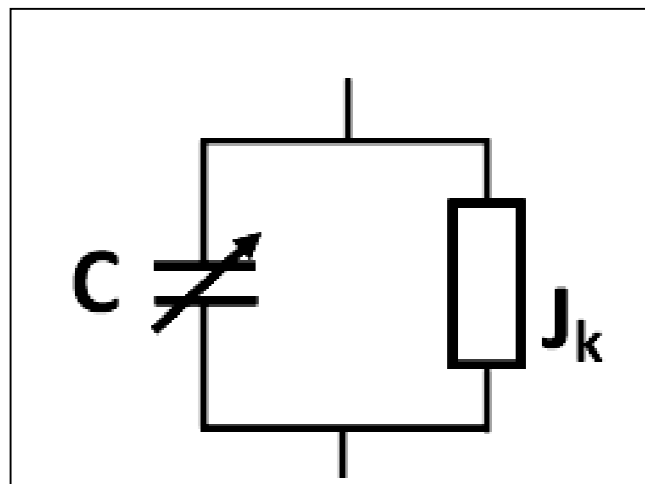
The purpose of this work is to design A/D converter. Schematic 6.1 summaries the Process of assigning the problem and how to satisfy its purpose. The basic idea behind the design of A/D converter is to get a signal with constant properties. This can be satisfy in nonlinear dispersive medium, this medium has two main properties which are nonlinearity and dispersion. The nonlinearity methodology of this thesis is depend on RTD, there are two types of nonlinearity reactive and conductive , we are concentrated on the second one. Dispersion is depend on periodicity which mean that, the electronic circuit must consists of more than one segments, in this work we use 40 segments .

6.1 Nonlinearity of the RTD

Recently, a huge amount of work has been dedicated to the study of resonant tunnelling diodes (RTDs) which can provide gain and directly be used as the key component for oscillator circuits approaching the THz frequency range. This high speed device has led to a variety of analog and digital applications. Diodes present two sources of nonlinearity; conductive and reactive. The conductive nonlinearity is evident in the $I(V)$ (current and voltage) curves, which is represented by RTD model equation. The reactive nonlinearity is evident in the $C(V)$ (capacitance and voltage) curves represented by variable capacitance. Figure 6.2 illustrates the conductive and reactive nonlinearity for RTD.



(a)



(b)

Figure 6.2: (a) Conductive Nonlinearity and (b) Reactive Nonlinearity for RTD.

The focus of this work is on conductive nonlinearity, where the characteristic equation is the key element in RTD equivalent circuit.

To get to the desired goal first we must be successful in the process of representation RTD equivalent circuit in the Orcad program . The current – voltage relation for RTD is shown in figure 6.3 is modelled by

$$J_k (V)=BV_k (V_k -U_1)(V_k -U_2) \tag{6.1}$$

Where J_k is an external bias current and $U_1, U_2 >0$ have been supposed, and B is an amplitude factor determined by the slope at $V=0$ and V_k is the voltage of node k .

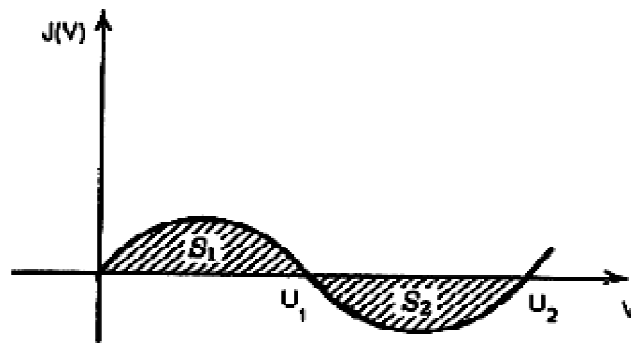
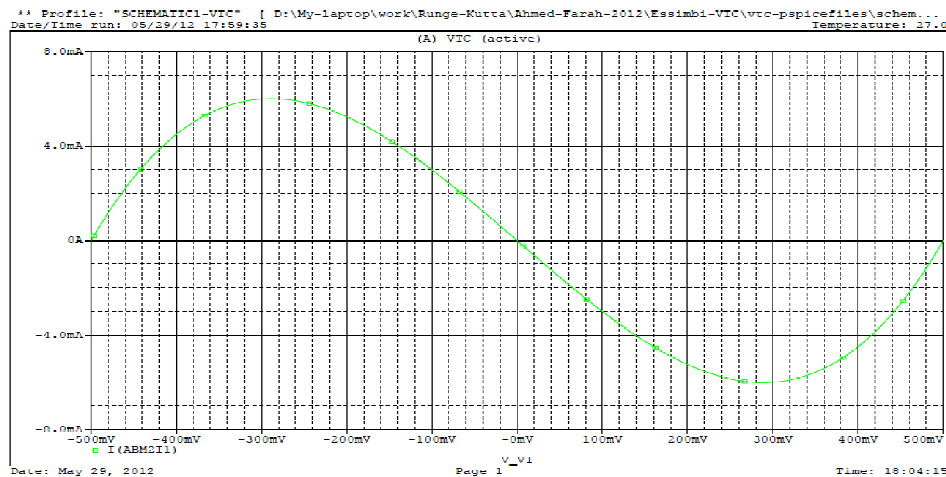
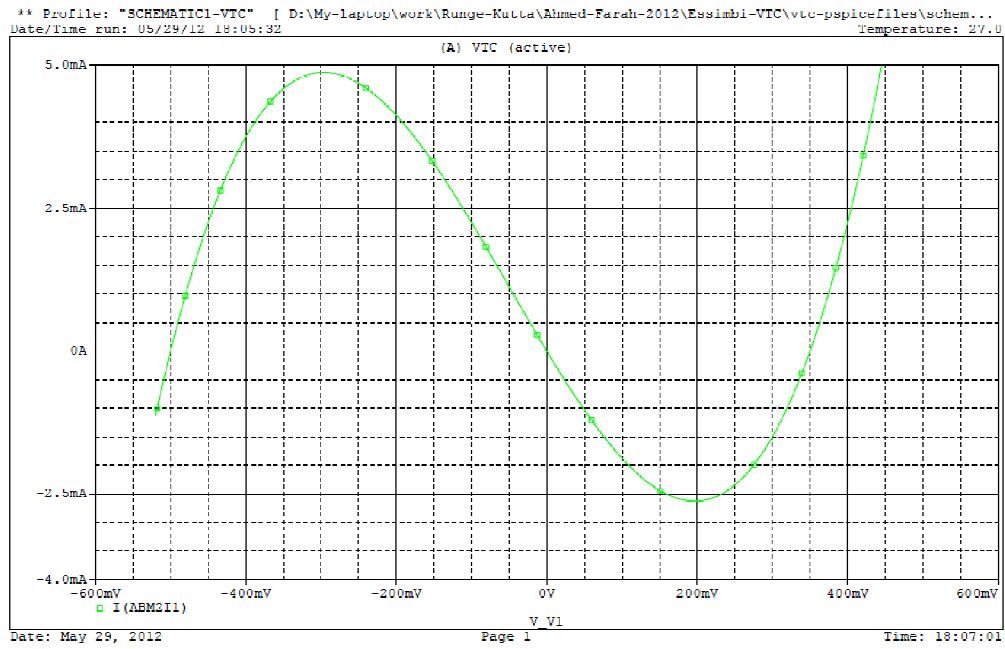


Figure 6.3: Current-Voltage characteristic curve of RTD[33]

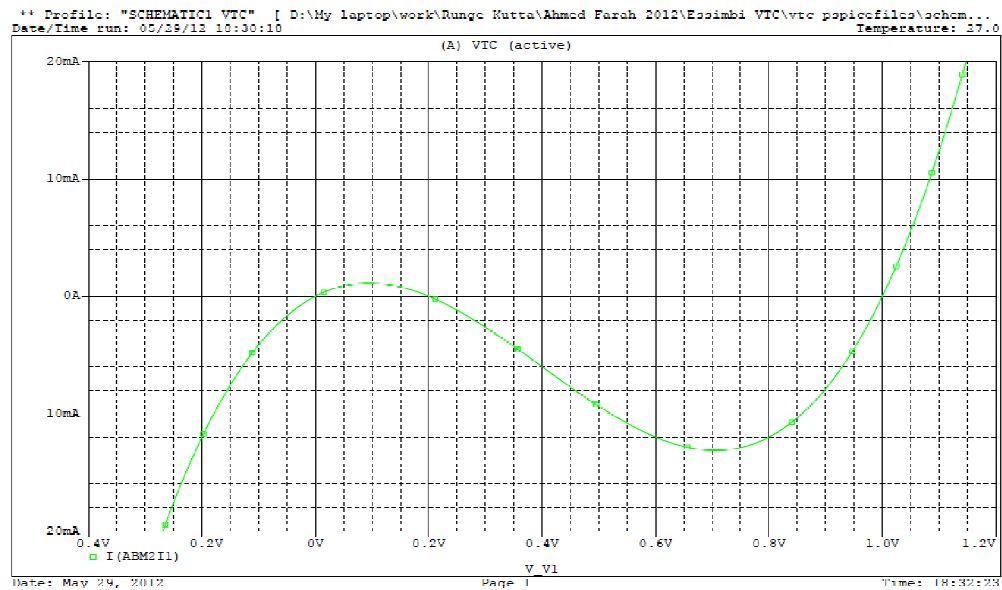
The nonlinear current–voltage characteristic curve created by Orcad is illustrated in figure 6.4.



(a)



(b)



(c)

Figure 6.4: Current-Voltage characteristic curve of RTD created by Orcad

(a) $S_1 = S_2$ with $B = 1\text{AV}^{-3}$, $U_1 = -0.5\text{V}$, and $U_2 = 0.5\text{V}$

(b) $S_1 > S_2$ with $B = 1\text{AV}^{-3}$, $U_1 = -0.5\text{V}$, and $U_2 = 0.35\text{V}$

(c) $S_1 < S_2$ with $B = 1\text{AV}^{-3}$, $U_1 = 0.2$, and $U_2 = 1\text{V}$

6.2 RTD-NLTL for A/D Converter Design steps

6.2.1 Array of RTD Periodically loaded

The first step to reach our goal is to load pure RTD equivalent circuit periodically with CPW as illustrated in figure 6.5. The equivalent circuit of one section of this RTD-NLTL is shown in figure 6.6.

6.2.2 Numerical analysis

we have used a computer OrCad program to study the RTD-NLTL. The proposed RTD-NLTL is composed of $N = 40$ identical segments, resistively attached to linear resistor having the value, $R = 0.5\Omega$. The electrical parameters of each segment are $B = 1\text{AV}^{-3}$ and $C = 0.01 \text{ pF}$. sinusoidal input signal with amplitude equal 5V and frequency equal to 10GHz is launched into the network and the characteristic of the RTD case $S_1/S_2 < 1$ to study freely propagating waves. Propagation of the output wave behavior is illustrated in figure 6.7. This figure look like square wave, so the function of this line is to reshape signal input waveform. This shape doesn't serve our desired goal, so a modification in this circuit must be met .

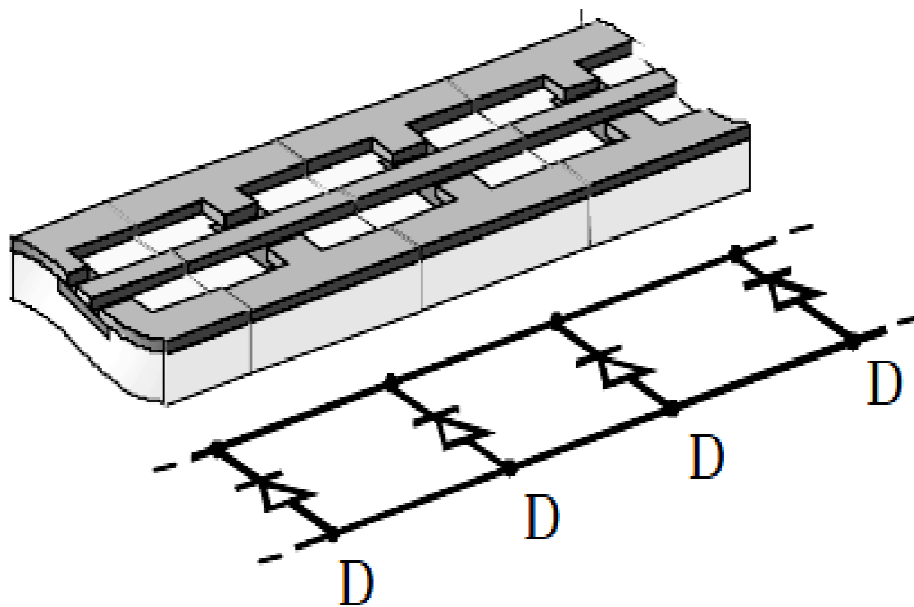


Figure 6.5: Monolithic NLTL with periodic array of RTDs

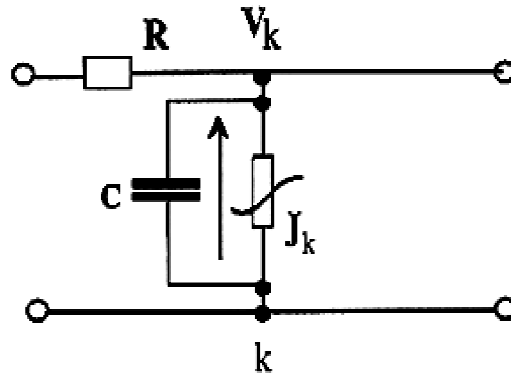
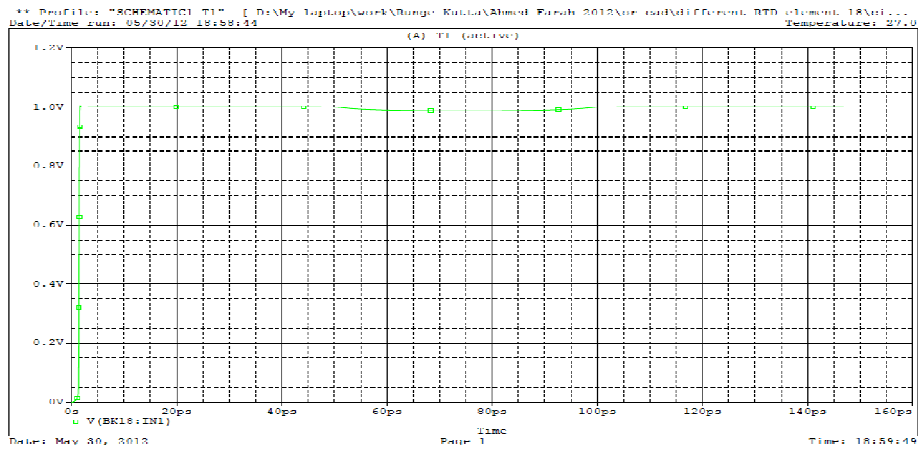
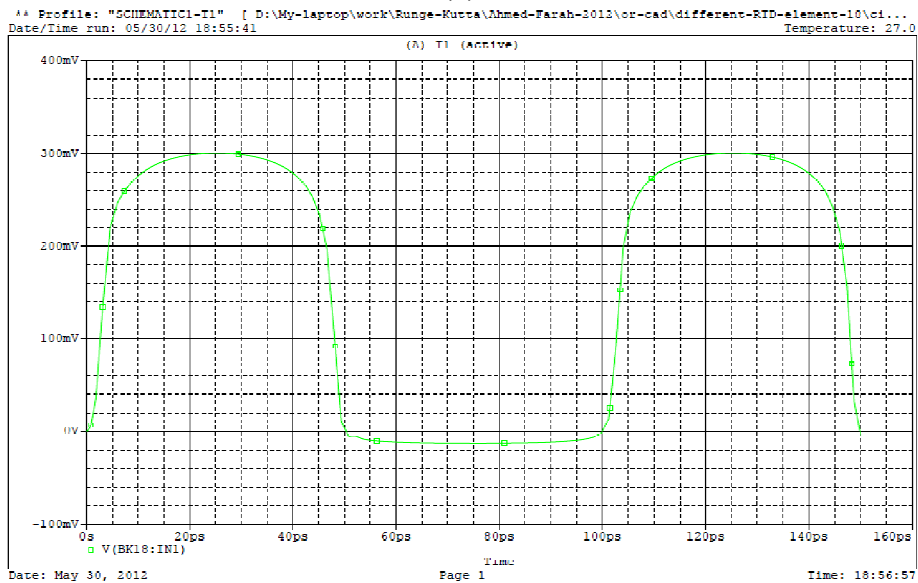


Figure 6.6: Equivalent circuit of one section of RTD-NLTL



(a)



(b)

Figure 6.7: The output pulses element $k=18$ for input sinusoidal pulse with amplitude 5V and frequency 10GHz.

(a) Large scale and (b) Small scal.

6.3 Array of RTD// Inductor Periodically loaded

The second step to reach our desired goal is to load RTD equivalent circuit periodically with CPW as illustrated in figure 6.8. The equivalent circuit of one section of this RTD//L-NLTL is shown in figure 6.9.

we have used a computer OrCad program to study the RTD//L-NLTL. The proposed RTD-NLTL is composed of $N = 40$ identical segments, resistively attached to linear resistor having the value, $R = 0.5\Omega$. The electrical parameters of each segment are $B = 1AV-3$, $C = 0.01$ Pf and $L1 = 10$ pH. sinusoidal input signal with amplitude equal 5V and frequency equal 10GHz is launched into the network and the characteristic of the RTD case $S1/S2 < 1$ to study freely propagating waves. Propagation of the output wave behaviour is illustrated in figure 6.10. This figure look like a pulse, so the function of this line is a pulse generator. This output Means that we are approaching the desired goal, so a little modification in this circuit must be met .

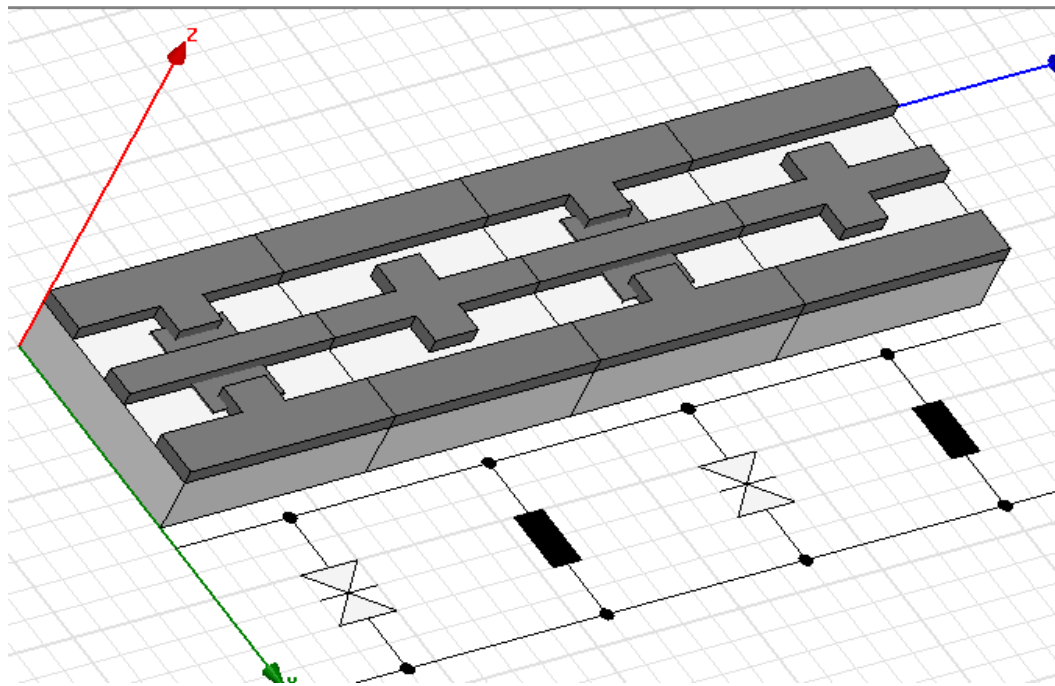


Figure 6.8: Monolithic NLTL with periodic array of RTD//L

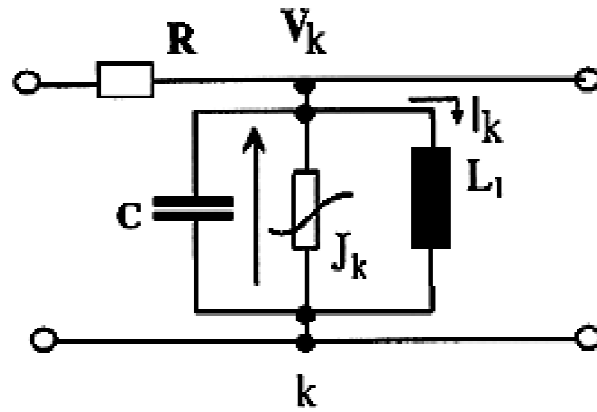


Figure 6.9: Equivalent circuit of one section of RTD-NLTL

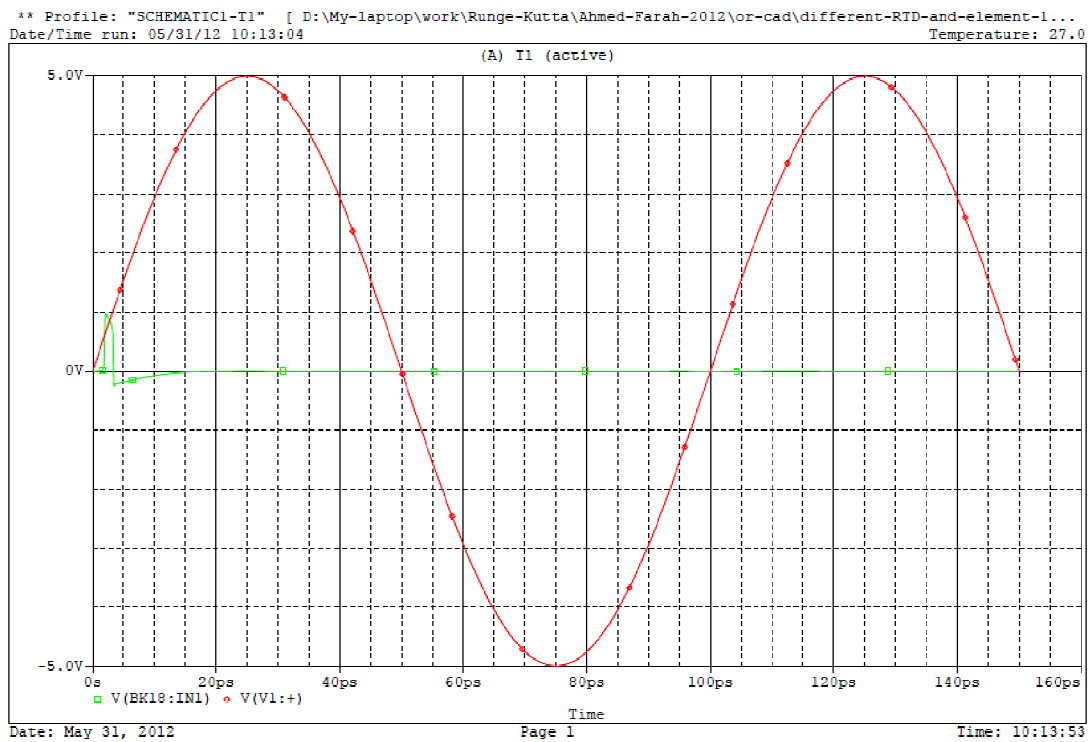


Figure 6.10: The output pulse element $k=18$ for input sinusoidal pulse with amplitude 5V and frequency 10GHz

6.4 Modified RTD-NLTL

6.4.1 Basic properties and operating principle of the modified RTD-NLTL

A schematic sketch of the proposed RTD-NLTL is displayed in figure 6.11. The RTD-NLTL is a coplanar transmission line periodically loaded with RTDs as seen in figure 6.11. Figure 6.12 represents the proposed NLTL which consists of 40 units of a repeated identified linear segments to study the behavior of NLTL. K.V.L and K.C.L are applied to single unit and generalized to the whole unit of the RTD-NLTL. Figure 6.13 shows the equivalent circuit of the one unit of the RTD-NLTL. Each section encompasses a T-shape piece corresponding to the transmission line. It consists of a series resistance R , and parallel circuit consists of the active RTD, $J(V_k)$ in parallel with a series inductance-conductance (L_1, G_1) circuit and parallel to the capacitance.

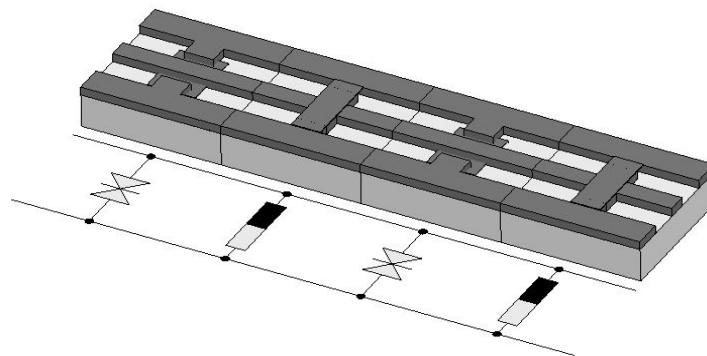


Figure 6.11: Sketch of an RTD-NLTL using a coplanar transmission line.

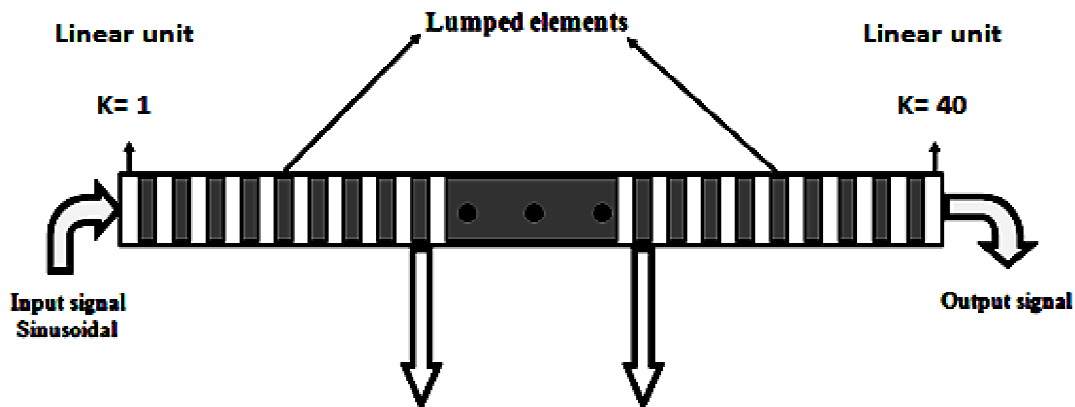


Figure 6. 12: Schematic representation of the n^{th} section of RTD-NLTL

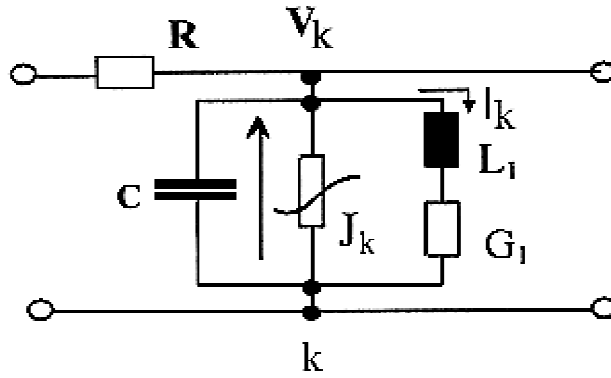


Figure 6.13: Equivalent circuit of one section of RTD-NLTL

A set of equations that describes the voltage along the line is given by applying Kirchoff's voltage law, the voltage across the inductance L_1 is

$$L_1 \frac{dI_k}{dt} = V_k - \frac{I_k}{G_1} \quad (6.2)$$

and using Kirchoff's current law, the current passing through C is

$$C \frac{dV_k}{dt} = \frac{1}{R} (V_{k-1} - 2V_k + V_{k+1}) - J_k - I_k \quad (6.3)$$

Where V_k , I_k are the voltages at element k and the resulting current through the series inductance-conductance (L_1 , G_1) circuit respectively.

6.4.2 Numerical analysis

we have used a computer OrCad program to study the RTD-NLTL. The modified RTD-NLTL is composed of $N = 40$ identical segments, resistively attached to linear resistor having the value, $R = 0.5\Omega$. The electrical parameters of each segment are $B = 1AV^{-3}$, $C = 0.01$ pF, $L_1 = 10$ pH, $R_1 = 1/G_1 = 5 \Omega$. Initial rectangular pulses as well as a sinusoidal input signal are launched into the network to study freely propagating waves. Furthermore, we considered the following : $S_1 > S_2$, $S_1 < S_2$, and $S_1 = S_2$.

6.4.2.1 Rectangular input signal

Case 1: $S_1/S_2 > 1$

The values of $U_1=0.35V$ and $U_2 = 0.5V$ are chosen such that $S_1/S_2 > 1$. Figure 6.14 shows the numerical results for an initial input square signal with amplitude of magnitude equal to 2.5 V and pulse duration of value equal to 40ps. The output is taken for elements from $k=18$ to $k=21$. It is clear that the output is one signal with amplitude vanishing along the line. This means that the effect of $J(V)$ is dissipative.

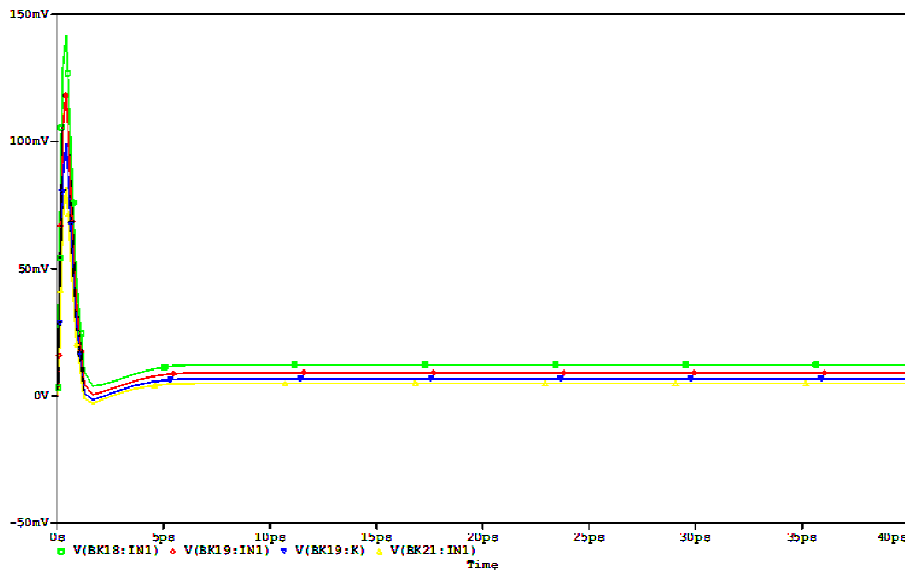


Figure 6.14: The output pulse at $k=18$ (green), $k=19$ (red), $k=20$ (blue) and $k=21$ (yellow) for input rectangular pulse with amplitude 2.5 V and pulse duration 40ps.

Case 2: $S_1/S_2 < 1$

We have taken an input rectangular signal with amplitude 1V and pulse duration 50ps for $U_1=0.2$ and $U_2=1$ which implies that $S_1/S_2 < 1$. Figure 6.15 demonstrates the numerical results at element $k=21$. The red line indicates for the input signal and the blue line indicates for the output signal. It is clear that the output of the RTD-NLTL contains 9 pulses. Following, the value of the amplitude of initial rectangular pulse stayed constant (1V) and the value of its pulse duration is changed to 40ps. Numerical results at element $k=21$ are exhibited in figure 6.16. The input signal is represented by red lines and the

output is represented by blue lines. It is shown that the RTD-NLTL produce output signal consists of 7 pulses. Next, for the same frequency of the rectangular input signal (40ps), we changed the amplitude value to 5 V. We observed from Figure 6.17 the appearance of 8 pulses generated at element $k=21$. The blue line refers to the output pulses and the red line refers to the input rectangular pulse. We notice that the number of pulses depends on the characteristic parameters of the input signal; the number of pulses is altered in a characteristic way. This implies that for the case $(S1/S2) < 1$, the system acts as a source of energy so that losses are rewarded by magnification along the network.

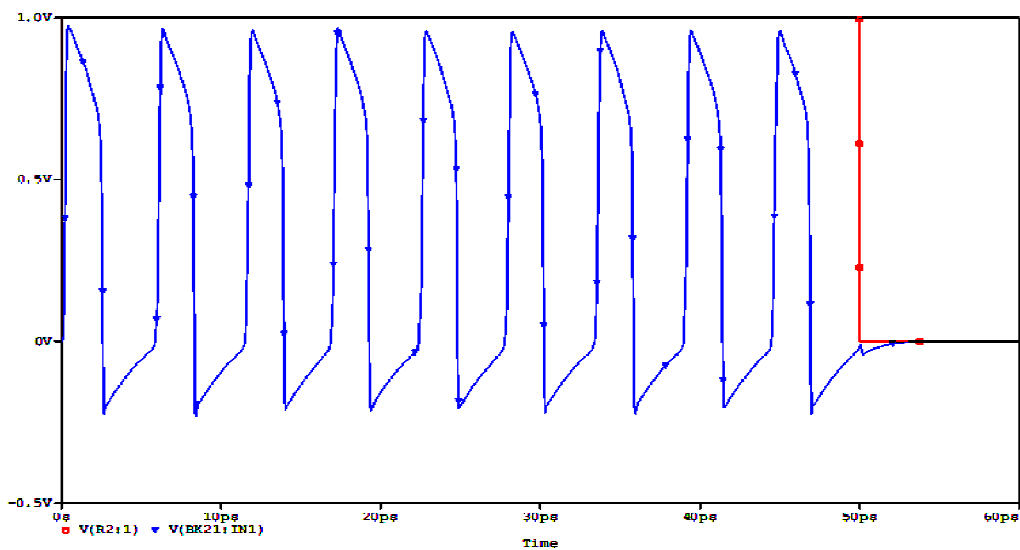


Figure 6.15: The output 9 pulses at element $k=21$ (blue) for input rectangular pulse with amplitude 1V and pulse duration 50ps (red).

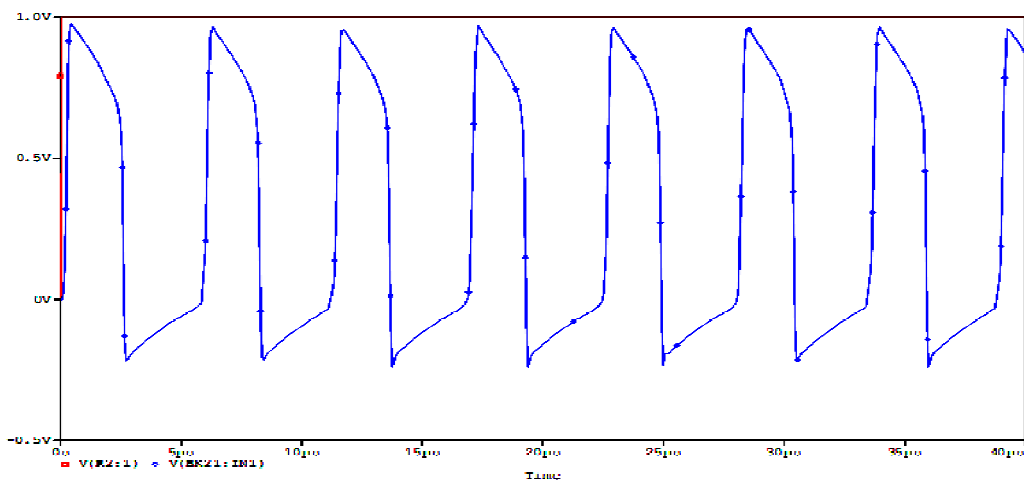


Figure 6.16: The output 7 pulses at element $k=21$ (blue) for input rectangular pulse with amplitude 1V and pulse duration 40ps (red).

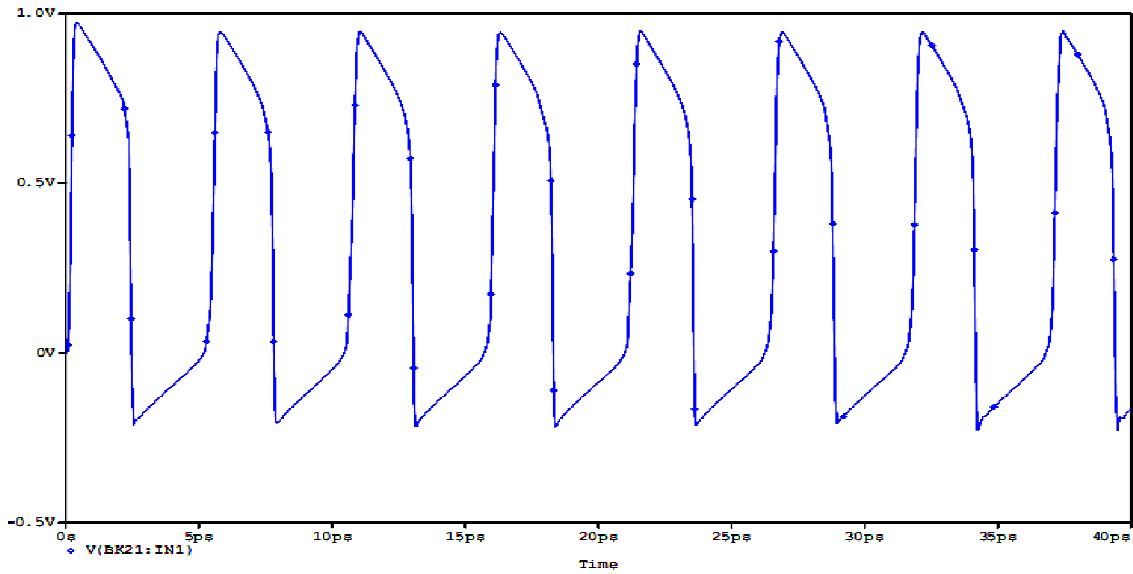


Figure 6.17: The output 8 pulses at element k=21 for input rectangular pulse with amplitude 5V and pulse duration 40ps.

6.4.2.2 Sinusoidal input signal Case 1: $S1/S2 < 1$

In this case, we apply sinusoidal signal at the input of the RTD-NLTL with frequency of 10GHz and amplitude of 5V. The output at element k=18 (green line) is illustrated in figure 6.18. The input signal is represented by red line. We see a group of 8 pulses per period appearing only in the positive part of the input signal. The output is taken at element k=18,19, 20 and 21 at the same time, we observe that the same number of identical pulses in the positive part of the input signal as illustrate in figure 6.19.

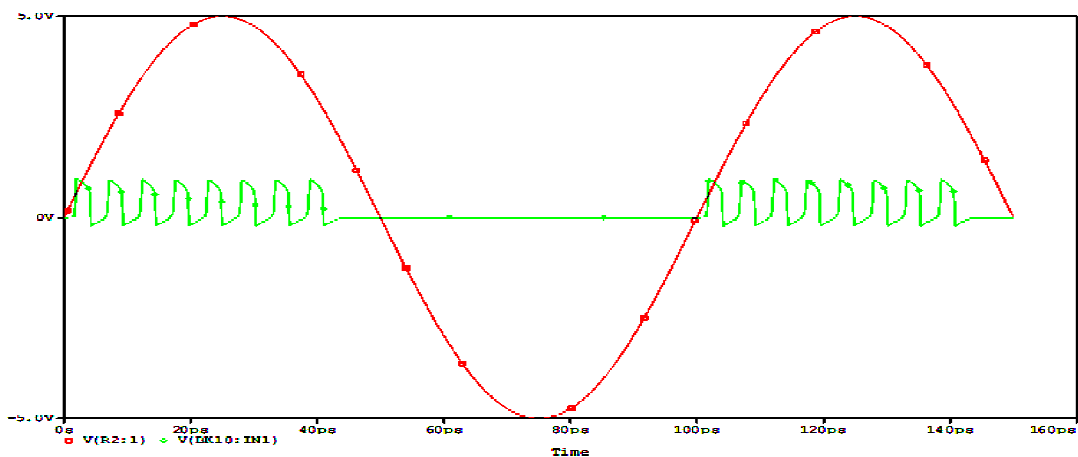


Figure 6.18: The output 8 pulses per period at element k=18 for input sinusoidal pulse with amplitude 5V and frequency 10GHz.

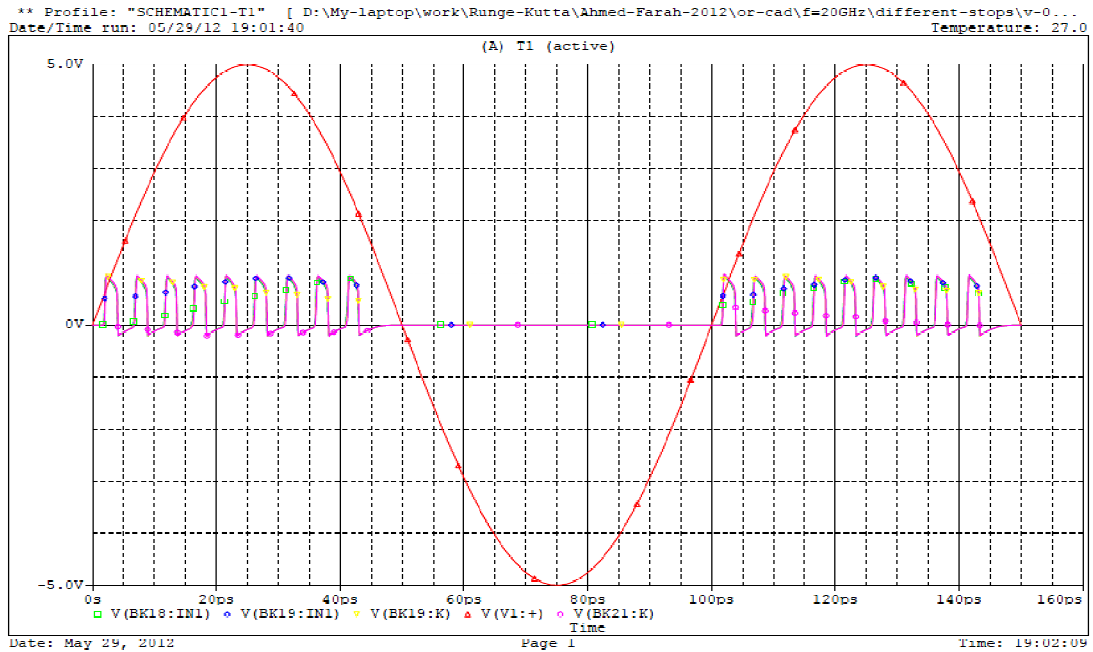


Figure 6.19: The output 8 pulses per period at element k=18, 19, 20 and 21 for input sinusoidal pulse with amplitude 5V and frequency 10GHz.

Case 2: $S1/S2 = 1$

In this case, we apply sinusoidal signal at the input of the RTD-NLTL with frequency of 10GHz and amplitude of 5V. The output at element k=18 (green line) is illustrated in figure 6.20. The input signal is represented by red line. We see a train pulses per period appearing in the positive and negative part of the input signal.

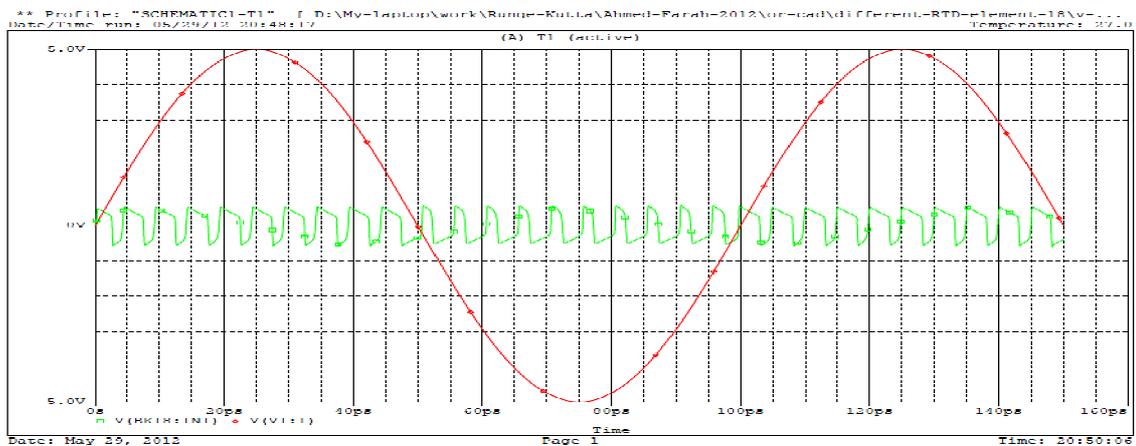


Figure 6.20: The output train of pulses per period at element k=18 for input sinusoidal pulse with amplitude 5V and frequency 10GHz.

Case 3: $S1/S2 > 1$

In this case, we apply sinusoidal signal at the input of the RTD-NLTL with frequency of 10GHz and amplitude of 5V. The output at element $k=18$ (green line) is illustrated in figure 6.21. We see a pulse per period appearing in the positive part of the input signal. This pulse has a very small amplitude

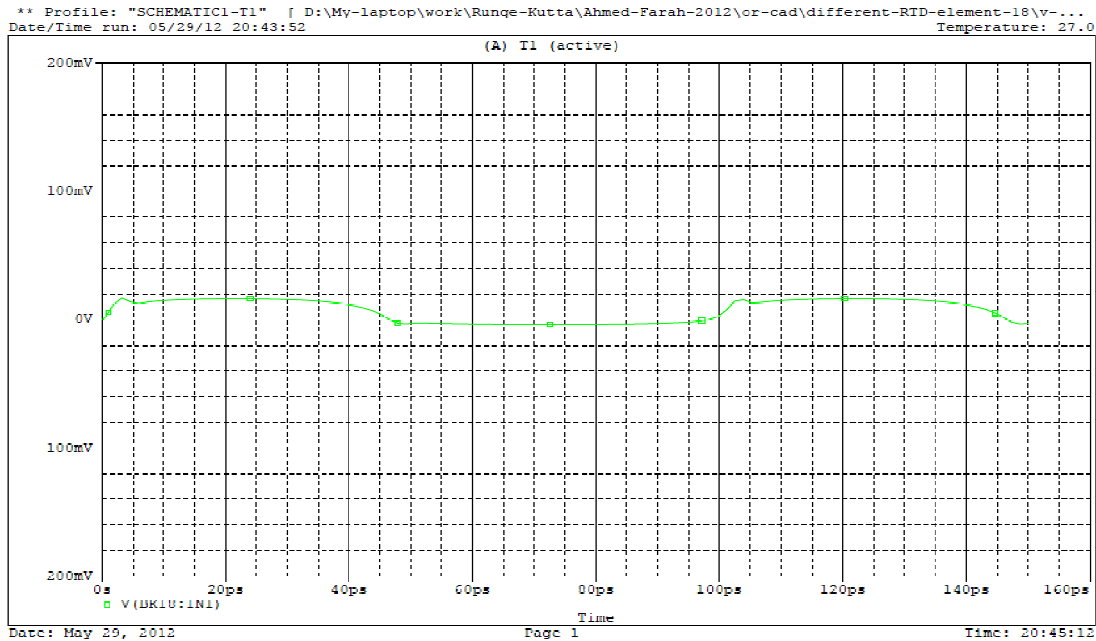


Figure 6.21: The output train of pulses per period at element $k=18$ for input sinusoidal pulse with amplitude 5V and frequency 10GHz.

Additionally, the duration of the input sinusoidal signal remained constant 10 GHz and the amplitude of the sinusoidal wave is changed to 2V. The output at element $k=18$ is shown in figure 6.22. We notice from figure 6.22 that we can get a set of 7 pulses appearing in the positive part of the input signal.

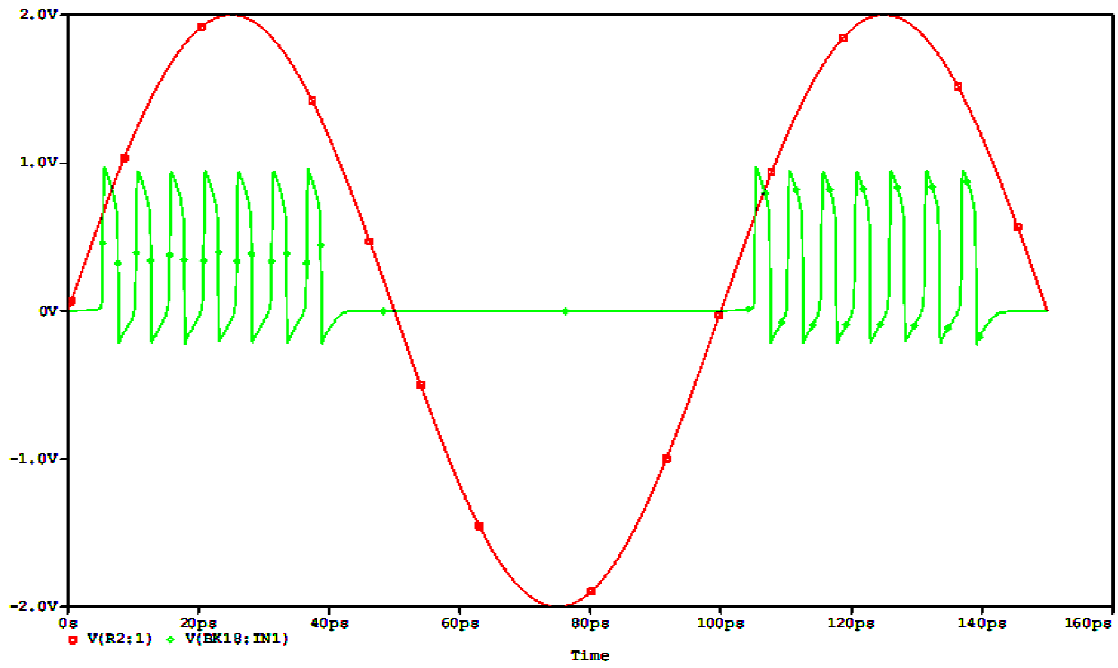


Figure 6.22: The output 7 pulses at $k=18$ for input sinusoidal pulse with amplitude 2V and frequency 10GHz.

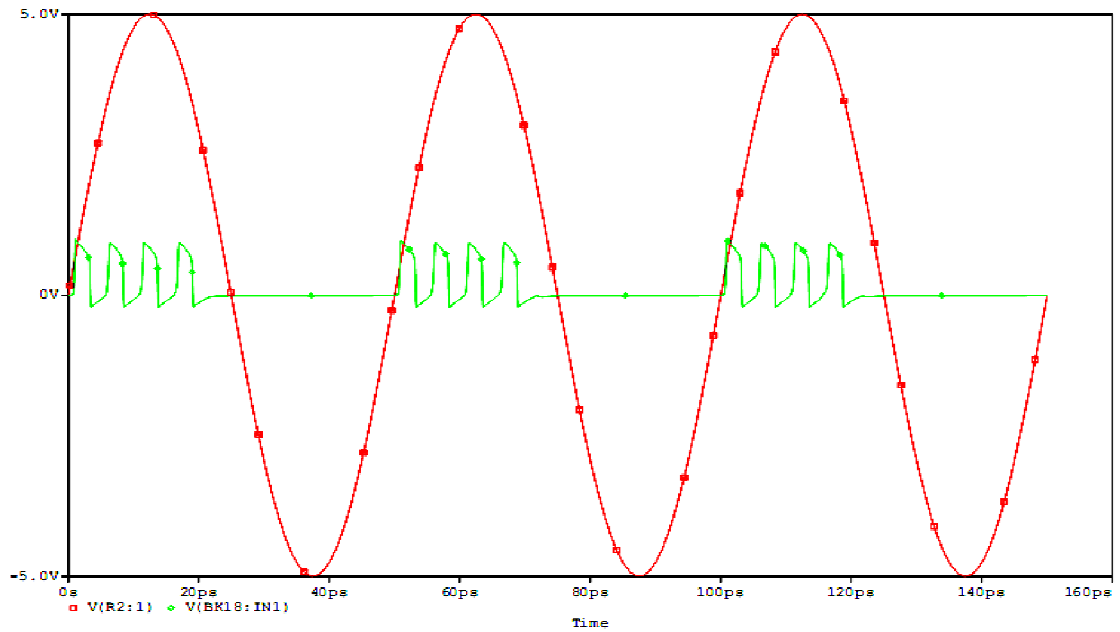


Figure 6.23: The output 4 pulses at $k=18$ for input sinusoidal pulse with amplitude 5V and frequency 20GHz

Further, for the same amplitude 2V, we set the frequency to 20GHz. Figure 6.23 exhibits that the output at k=18 is a set of 4 pulses in the positive part of the input signal.

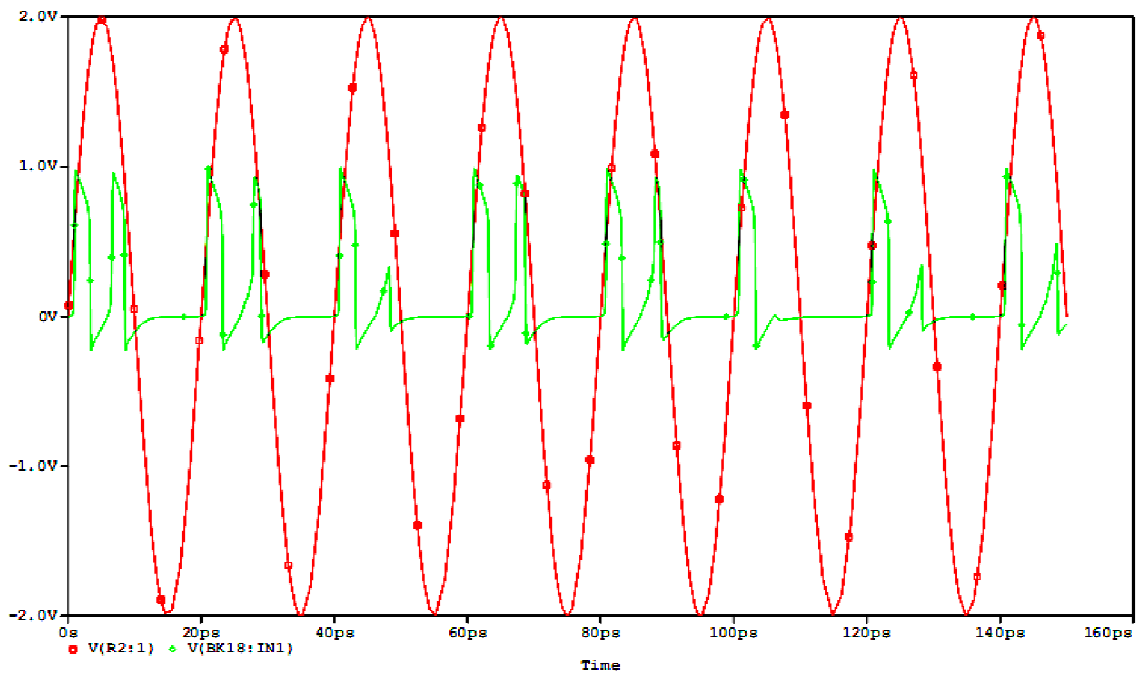


Figure 6.24: The output 2 pulses at k=18 for input sinusoidal pulse with amplitude 2V and frequency 50GHz

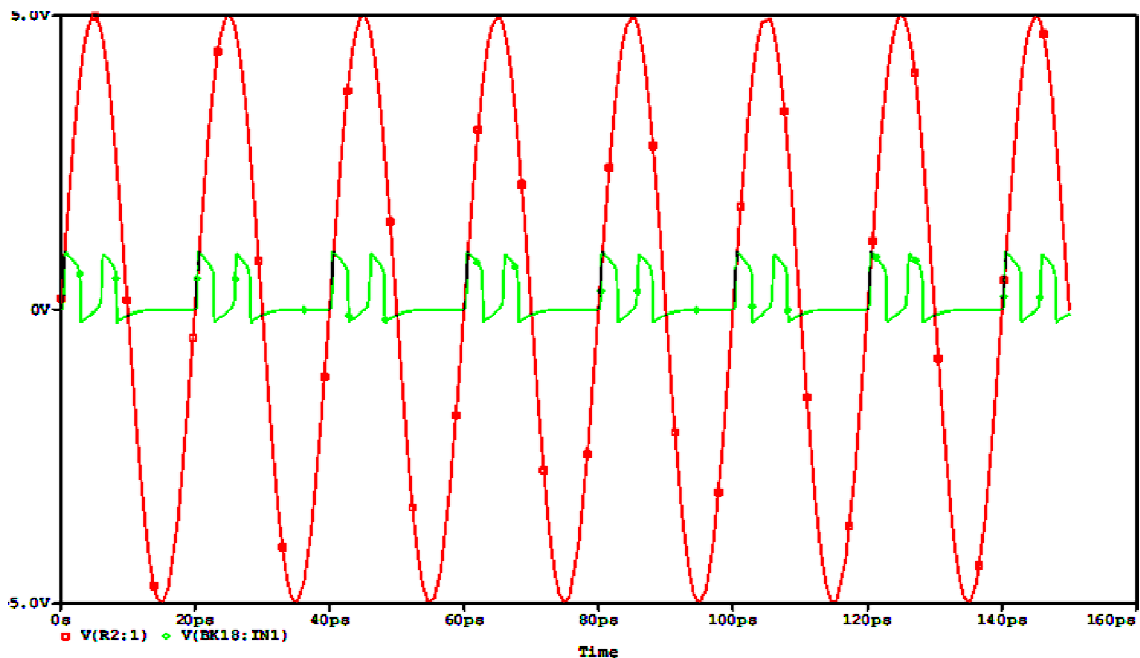


Figure 6.25: The output 2 pulses at k=18 for input sinusoidal pulse with amplitude 5V and frequency 50GHz.

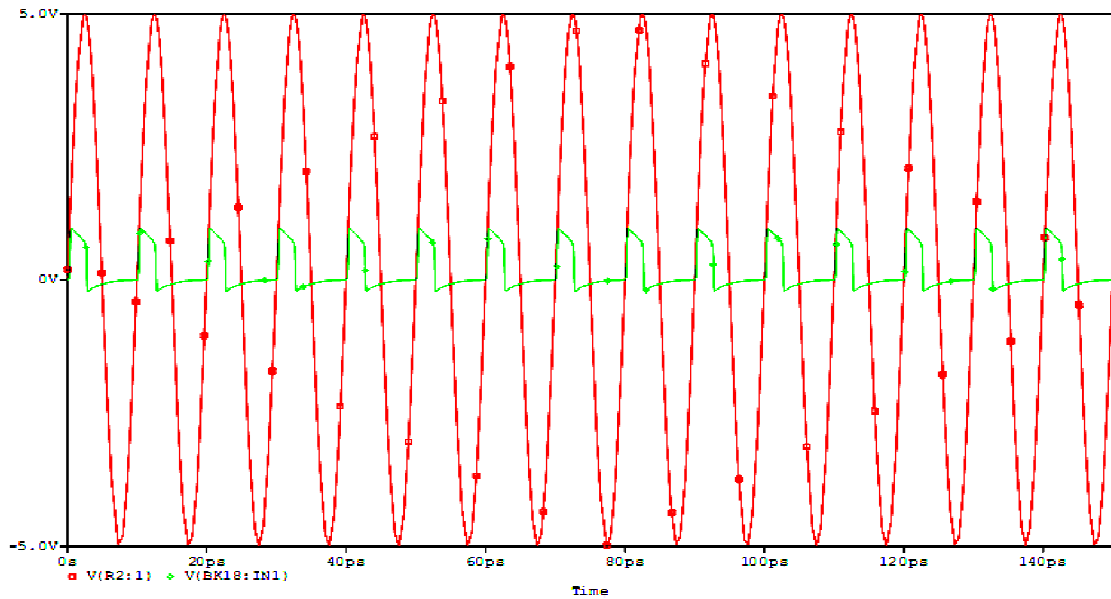


Figure 6.26: The output 1 pulses at $k=18$ for input sinusoidal pulse with amplitude 5V and frequency 100GHz.

Figure 6.24 demonstrates the output at element $k=18$ for input sinusoidal signal with amplitude 2V and frequency 50GHz. The output is a collection of 2 pulses in the positive part of the input signal. However, the collection of the 2 pulses does not have a fixed pulse shape. Next, for the same frequency 50 GHz, we changed the value of the amplitude to 5V. The numerical results at element $k=18$ are shown in figure 6.25. Figure 6.26 demonstrates the output at element $k=18$ for input sinusoidal signal with amplitude 5V and frequency 100GHz. We see from figure 6.25 that we can get a cluster of 2 pulses which maintain their shape as they propagate along the NLTL. Thus, it is obvious that the number of the pulses changes as the characteristics of the input signal is changed. The final designed circuit of the ultra fast 4-bit analog to digital converter is illustrated in figure 6.27, it shows that n -bit ultra fast ADC requires n - monostable NLTL .

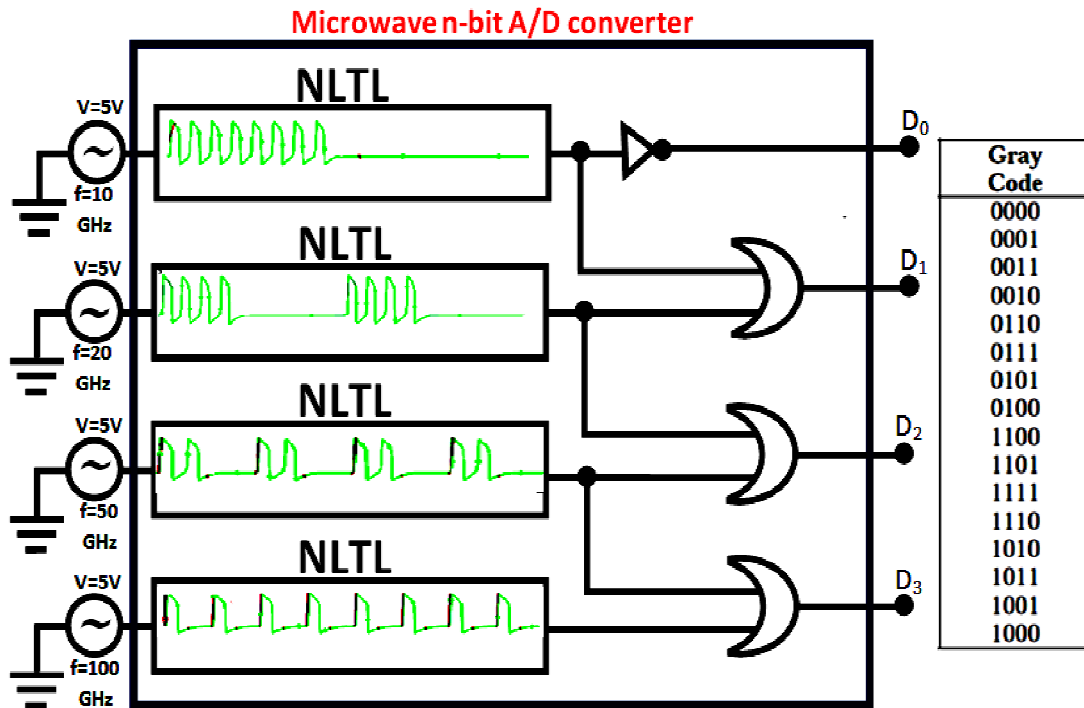


Figure 6.27: Ultra-fast 4-bit A/D converter

6.5 Discussion

we examined the effect of changing frequency of the input signal on the output spikes number and position. From the previous circuit analysis, we deduct that the circuit source is roughly the following. An input current source charges the capacitance C up to a threshold value given by J (V) of the RTD. Therefore, a switching up occurs which will be inverted due to the LG time constant. As a result, a spike is produced and after RC time constant another switching occurs. Hence the spiking period is determined by the amplitude of the input current. When the input frequency or the input amplitude is changed, the number, phase, and position of the spikes are altered in a characteristic way.

6.6 Proposed A/D Converter Metrics

6.6.1 Power Consumption

The lower power consumption is required when an engineer goes to design any electronic device. The measured values agree with the expected power consumption for this design. The total of power consumption is considerably lower than other published ADC architectures. Table 6.1 shows a comparison between power consumption of different types of ADC.

Table 6.1 : Comparison between power consumption of different types of ADC

Type	Power Dissipation
Dual Slope	Low
Flash	High
Successive approx	Low
Sigma-Delta	Low
My Design	Very low

6.6.2 Conversion Rate and Speed

The amount of time that is required from the beginning of one conversion to the time the converted value is available to read from the A/D converter. It is usually stated in microseconds. The specified conversion rate is often an ideal condition. Conversion time should take into consideration settling to a stable condition to allow conversion to the stated accuracy. Data sheets will often state “throughput”, which is the inverse of conversion rate. For example, an A/D converter that has a conversion rate of $8\mu\text{s}$ will have an ideal throughput of 125 KHz ($10^6 \div 8$). Throughput is an important consideration when trying to sample a continuous waveform that must be reproduced.

In this prototype the conversion rate is 2.5ps, that mean this A/D converter is ultra high speed. Table 6.2 shows a comparison between speeds of different A/D converters.

Table 6.2 : Comparison between speeds of different A/D converters

Type	Speed(relative)
Dual Slope	Slow
Flash	Very fast
Successive approx	Medium fast
Sigma-Delta	low
My Design	Ultra fast

6.6.3 Resolution

The resolution of the converter indicates the number of discrete values it can produce over the range of analog values. The values are usually stored electronically in binary form, so the resolution is usually expressed in bits. In consequence, the number of discrete values available, or "levels", is a power of two. For example, an ADC with a resolution of 4-bits can encode an analog input to one in 256 different levels, since $2^4 = 16$. The values can represent the ranges from 0 to 15 . Resolution can also be defined electrically, and expressed in volts. The minimum change in voltage required to guarantee a change in the output code level is called the least significant bit (LSB) voltage. The resolution Q of the ADC is equal to the LSB voltage. The voltage resolution of an ADC is equal to its overall voltage measurement range divided by the number of discrete values:

$$Q = \frac{E_{FSR}}{2^M}, \tag{6.4}$$

Where M is the ADC's resolution in bits and EFSR is the full scale voltage range (also called 'span'). EFSR is given by

$$E_{FSR} = V_{RefHi} - V_{RefLow} , \quad (6.5)$$

Where V_{RefHi} and V_{RefLow} are the upper and lower extremes, respectively, of the voltages that can be coded. Normally, the number of voltage intervals is given by

$$N = 2^M - 1, \quad (6.6)$$

Where M is the ADC's resolution in bits.

Prototype resolution calculation

- Input signal $x(t) = A\sin(t)$, $A = 5V$
- Full scale measurement range = 0 to 5 volts
- ADC resolution is 4 bits: $2^4 - 1 = 16 - 1 = 15$ quantization levels (codes)
- ADC voltage resolution, $Q = (5V - 0V) / 15 = 5V / 15 = 0.33V$

6.6.4 Conversion Delay

Because the NLTL is nonlinear dispersive medium, so the generated short pulses are propagated with an identical period along the line, even if we are change the frequency of the input signals. Figure 6.28 illustrates the delay between generated pulses. Dependant on figure 6.28 we can get optimum case for conversion delay between output codes. Conversion delay = zero second, which manes; that the generated pulses have identical period.

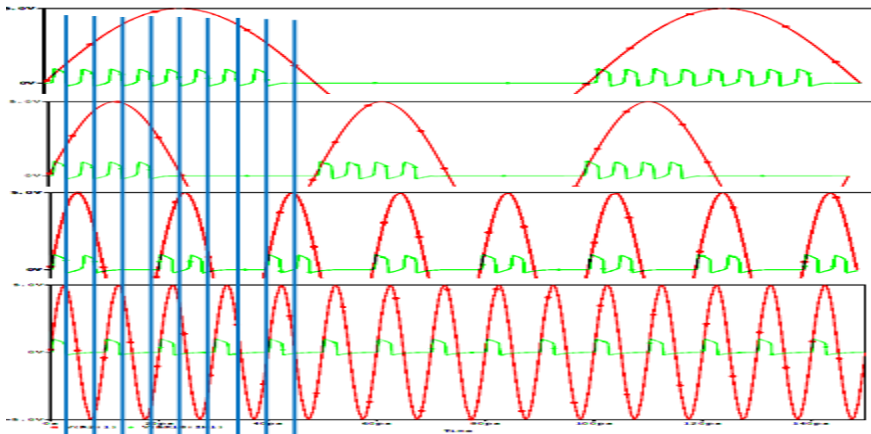


Figure 6.28: Zero delay between generated short pulses

6.6.5 Temperature effect

RDT has temperature operating rang -260 to 850°C (-436 to 1582°F) this means that the prototype is valid to operate in different environmental.

6.6.6 Cost

Cost factor is one of the most important factors that must take into account when designing any electronic device. The cost of RTD is the lowest semiconductor device, our prototype doesn't use any comparator , amplifiers and switches, so the designed system achieve optimal cost. Table 6.3 represents different devices costs.

Table 6.3: Comparison between different A/D converters costs

Type	Cost(Relative)
Dual Slope	Med.
Flash	High
Successive approx	Low
Sigma-Delta	low
My Design	low

6.6.7 Size

A Monolithic Microwave Integrated Circuit, or MMIC (sometimes pronounced "mimic"), is a type of integrated circuit (IC) device that operates at microwave frequencies (300 MHz to 300 GHz). It takes advantage of their provides up to 1 watt of power in microwave frequency band. The primary advantage of MMIC technology is its lower fabrication cost compared with other one's like III-V technologies, such as Indium Phosphide (InP). MMICs are dimensionally small (from around 1 mm² to 10 mm²) and can be mass produced, which has allowed the proliferation of high frequency devices such as cellular phones. The size in

my design case of a monolithic integration, an area of $200\mu\text{m} \times 500\mu\text{m}$. Table 6.4 shows comparison between the size different designs.

Table 6.4: Comparison between the size of different A/D converters

Type	Area
Dual Slope	Low
Flash	High
Successive approx	Low
Sigma-Delta	Depend on resolution
My Design	Very low

6.6.8 Static and dynamic errors

The Statics and dynamics errors associated with an ideal N-bit ADC are those related to the sampling and quantization processes, since our designed ADC operation doesn't depend on these processes Statics and dynamics errors are zero. These errors include the following:

- Integral nonlinearity (INL) errors
- Differential nonlinearity (DNL) errors
- Offset, gain, and linearity errors
- Signal-to-noise ratio (SNR).
- Signal-to-noise-and-distortion ratio

7- Conclusion and Future Work

7.1 Conclusion

In conclusion a novel monostable RTD-NLTL in MMIC technology was proposed which can generate characteristic pulse pattern for a given input signal. That was the position and number of spikes at the output depended on the input signal amplitude and frequency. we used OrCad program to analyze the proposed RTD-NLTL for millimeter-wave sources. we got collections of pulses at the output frequencies up to 0.1 THz. These NLTL can be used to realize an ultra-fast n-bit A/D converter with Gray code output for example. Thus we proposed common n-channel (for n bits) coplanar signal divider to provide input amplitudes by power of 2. Hence each channel delivers a spike train to the output array establishing a Gray code.

7.2 Future Work

- Theoretically, manufacturing the RTD-NLTL that has been reached in this thesis by using High Frequency Structure Simulator(HFSS) program.
- This thesis recommends applying other type of inputs like ramp signals.
- A good research problem in mind is to design different Analog-to-digital converter approaches. RTD –NLTL approach may be replaced by either Schottky Diode-NLTL model or Varactor Capacity Diode- NLTL and compared with RTD –NLTL.
- Take advantage of the signals generated that can be extended to cover other types of practical application like Voltage to frequency converter.
- In the proposed design, we were able to generate pulses at the output frequencies up to 0.1 THz. It can be extended to higher frequency by introducing any improvement on the designed circuit.

Bibliography

- [1] M. Remoissenet, "Waves Called Solitons," ch. 3: Solitons in Nonlinear Transmission Lines, pp. 37–64, 1999.
- [2] M. J. Rodwell et al., "Active and nonlinear wave propagation devices in ultrafast electronics and optoelectronics," Proc. IEEE, vol. 82, no. 7, pp. 1037–1059, 1994.
- [3] J. R. Alday, "Narrow pulse generation by nonlinear transmission lines," Proc. IEEE, vol. 22, no. 6, p. 739, 1964.
- [4] D. W. van derWeide, "Delta-doped Schottky diode nonlinear transmission lines for 480-fs, 3.5-V transients," Appl. Phys. Lett., vol. 65, no. 7, pp. 881–883, 1994.
- [5] R. Hirota and K. Suzuki, "Studies on lattice solitons by using electrical networks," J. Phys. Soc. Jpn., Vol. 28, 1366-1367, 1970.
- [6] J. S. Russell, "Report on waves," in Rep. 14th Meeting of the British Association for the Advancement of Science, pp. 311–90, 1844.
- [7] A. C. Scott, F. Y. F. Chu, and D. W. McLaughlin, "The soliton: A new concept in applied science," Proc. IEEE, vol. 61, no. 10, pp. 1443–1483, 1973.
- [8] N. J. Zabusky and M. D. Kruskal, "Interactions of solitons in a collisionless plasma and the recurrence of initial states," Phys. Rev. Lett., vol. 15, no. 6, pp. 240–243, 1965.
- [9] P. G. Drazin and R. S. Johnson, Solitons: An Introduction. Cambridge, U.K.: Cambridge Univ. Press, 1989.
- [10] A. T. Filippov, The Versatile Soliton. Boston, MA: Birkhauser, 2000.

- [11] M. Remoissenet, *Waves Called Solitons: Concepts and Experiments*. New York: Springer-Verlag, 1999.
- [12] M. Reddy, S. C. Martin, A. C. Molnar, R. E. Muller, R. P. Smith, P. H. Siegel, M. J. Mondry, M. J. Rodwell, H. Kroemer and S. J. Allen , "Monolithic Schottky-collector resonant tunnel diode oscillator arrays to 650 GHz ," IEEE Trans. Sonics Ultrason., vol. 18, no. 5, pp. 218 - 221, May 1997.
- [13] I. Jaeger, D. Kalinowski, A. Stöhr, J. Stiens, R. Vounckx and D.," Millimetre wave signal generation using resonant tunneling diodes NLTL-resonators "Microwave and Optical Technology Letters, vol. 49, No. 12,pp. 2907-2909, Dec. 2007.
- [14] M.J.W. Rodwell, S.T. Allen, R.Y. Yu, M.G. Case, U. Bhattacharya, M. Reddy, E.C. Carman, M. Kamegawa, Y. Konishi, J. Pusk, R. Pullela," Active and nonlinear wave propagation devices in ultrafast electronics and optoelectronics " Proc. IEEE., Vol. 82, No. 7, pp. 1037 – 1059, Jul. 1994.
- [15] L.L Chang, L. Tsu and T. Esaki, "Resonant tunnelling in semiconductor double barriers ," Applied Physics Letters, vol. 24, no. 12, pp. 593-595, June, 1974.
- [16] M. Reddy,"Schottky-collector Resonant TunnelDiodes for Sub-Millimeter WaveApplications,"http://www.ece.ucsb.edu/Faculty/rodwell/Downloads/theses/madhu_the_sis.pdf, 1997.
- [17] W. Williamson, S. B. Enquist, D. H. Chow, H. L. Dunlap, S. Subramaniam, P. Lei, G. H. Bernstein, and B. K. Gilbert, "12 GHz clocked operation of ultralow power interband resonant tunneling diode pipelined logic gates,"IEEE J. Solid-State Circuits, vol. 32, no. 2, pp. 222-231, Feb. 1997.
- [18] H. Matsuzaki, T. Itoh, and M. Yamamoto, "A novel high-speed flip-flop circuit usingRTDs and HEMTs,"in Proc. Great Lake Symp. VLSI, pp. 154 -157, Mar. 1999.

- [19] T. P. E. Broekaert, B. Brar, J. P. A. van der Wagt, A. C. Seabaugh, F. J. Morris, T. S. Moise, E. A. Beam, and G. A. Frazier, "A monolithic 4-bit 2-Gsps resonant tunneling analog-to-digital converter," *IEEE J. Solid-State Circuits*, vol. 33, no. 9, pp. 1342 - 1349, Sept. 1998.
- [20] R. F. Trambaruo, "Esaki diode amplifiers at 7, 11 and 26 kMc/s," *Proc. I. R. E.*, vol. 48, pp. 20-22, 1960.
- [21] C. A. Burrus, "Millimeter wave Esaki diode oscillators," *Proc. I. R. E.*, vol. 48, pp. 20-24, 1960.
- [22] G. B. Smith, "Tunnel diode generates rectangular pulses," *Electronics*, vol. 33, pp. 124-128, 1960.
- [23] K. Poulton, K. L. Knudsen, J. Kerley, J. Kang, J. Tani, E. Cornish, and M. VanGrouw, "An 8 GSa/s 8-bit ADC system," in *Proc. Symp. VLSI Circ. Tech. Dig.*, pp. 23–24, 1997.
- [24] P. Xiao, K. Jenkins, M. Soyuer, H. Ainspan, J. Burghartz, H. Shin, M. Dolan, and D. Hareme, "A 4 b 8 GSample/s A/D converter in SiGe bipolar technology," in *IEEE Int. Solid-State Circ. Conf. Tech. Dig.*, pp. 124–125, 1997.
- [25] K. R. Nary, R. Nubling, S. Beccue, W. T. Colleran, J. Penney, and K.-C. Wang, "An 8-bit 2 Gigasample per second analog to digital converter," in *GaAs IC Symp. Tech. Dig.*, pp. 303–306, 1995.
- [26] F. Oehler, J. Sauerer, R. Hagelauer, D. Seitzer, U. Nowotny, B. Raynor, and J. Schneider, "A 3.6 Gigasample/s 5 bit analog to digital converter using 0.3 film AlGaAs-HEMT technology," in *GaAs IC Symp. Tech. Dig.*, pp. 163–166, 1993.
- [27] D. Jager and F. Tegude, "nonlinear wave propagation along periodic loaded transmission line," *J. Appl. Phys.* Vol. 15, No. 12, pp. 393-397, Nov. 1978.

- [28] M. Ketchen, D. Grischkowsky, T. Chen, C. Chi, N. Duling, III, N. Halas, J. Halbout, J. Kash, and G. Li, "generation of subpicosecond electrical pulses on coplanar transmission lines," J. Appl. Phys. Lett. Vol. 48, No. 12, pp. 393-397, March 1986.
- [29] M. Rodwell, M. Kamegawa, R. Yu, M. Case, E. Carman, and K. Giboney, "GaAs Nonlinear Transmission Lines for Picosecond Pulse Generation and Millimeter-Wave Sampling" , IEEE TRANSACTIONS ON MICROWAVE THEORY AND TECHNIQUES, Vol. 39, No. 7, pp. 1194-1204, JULY 1991.
- [30] R. Baker, D. Hodder, B. Johnson, P. Subedi and D. Williams, "Generation of kilovolt-subnanosecond pulses using a nonlinear transmission line" , Meas. Sci. Technol. Vol. 4, No. 12, pp. 893-895, May 1993.
- [31] U. Bhattacharya, S. Allen, and M. Rodwell, "DC-725 GHz Sampling Circuits Subpicosecond Nonlinear Transmission Lines Using Elevated Coplanar Waveguide" , IEEE MICROWAVE AND GUIDED WAVE LETTERS. Vol. 5, No. 2, pp. 50-52, Feb. 1995.
- [32] S. Ibuk, M. Ohnishi, T. Yamada, K. Yasuoka, and S. Ishii, "VOLTAGE AMPLIFICATION EFFECT OF NONLINEAR TRANSMISSION LINES FOR FAST HIGH VOLTAGE PULSE GENERATION," J. Appl. Phys. Vol. 64, No. 12, pp. 1548-1553, 1997.
- [33] E. Afshari and A. Hajimiri, "Nonlinear Transmission Lines for Pulse Shaping in Silicon", IEEE JOURNAL OF SOLID-STATE CIRCUITS, Vol. 40, No. 3, PP. 744-752, March 2005.
- [34] B.Z. Essimbi and D. Jager, "Generation of electrical short pulses using a Schottky transmission line periodically loaded with tunnelling diodes", Current Applied Physics, Vol. 5, No. 6, PP. 567-571, Sep. 2005.

- [35] D. Ricketts, X. Li and D. Ham, "Electrical Soliton Oscillator" , IEEE TRANSACTIONS ON MICROWAVE THEORY AND TECHNIQUES. Vol. 54, No. 1, pp. 373-382, Jan. 2006.
- [36] K. Narahara, T. Otsuji and E. Sano, "Generation of electrical short pulse using Schottky line periodically loaded with electronic switches", J. Appl. Phys., Vol. 100, No. 2, PP. 24511-24515, July 2006.
- [37] B. Z. Essimbi and D. Jager, "Generation of electrical short pulses using Schottky transmission line periodically loaded with tunneling diodes" , Physica Scripta, Vol. 81, No. 3, pp. 1-4, Feb. 2010.
- [38] H.J. El-Khozondar and I. M. Abo Ireban, "Transmission Lines and Schottky Diode," Master thesis, Univ. of Islamic, Physics Dept., Gaza , 2010.
- [39] B.Z. Essimbi and D. Jager, "Electrical short pulses generation using a resonant tunneling diode nonlinear transmission line", Phys. Scr., Vol. 85, No. 1, PP. 1-5, Feb. 2012.
- [40] N. O. Matthew, elements of electromanetics. ch. 11, USA: Oxford university, 2001.
- [41] H. William, J. A. Buck, Engineering Electromagnetics. ch. 13, 6rded. USA: McGraw-Hill , 2000.
- [42] T. R. Kuphaldt, Lessons In Electric Circuits, 6rd ed. Volume II – AC, 2007.
- [43] D. Ricketts, X. Li, N. Sun, K. Woo and D. Ham, "On the Self-Generation of Electrical Soliton Pulses" , IEEE JOURNAL OF SOLID-STATE CIRCUITS. Vol. 42, No. 8, pp. 1657-1668, Aug. 2007.
- [44] U. Karacaoglu and I. D. Robertson, "High selectivity varactor-tuned MMIC bandpass filter using lossless active resonators," in IEEE Microwave Millimeter- Wave Monolithic Circuits Symp., 1994, pp. 237-240.

- [45] S. R. Chandler, I. C. Hunter, and J. G. Gardiner, "Active varactor tunable bandpass filter," *IEEE Microwave Guided Wave Lett.*, vol. 3, no. 3, pp. 70-71, Mar. 1993.
- [46] D. M. Krafcsik, S. A. Imhoff, D. E. Dawson, and A. L. Conti, "A dual-varactor analog phase shifter operating at 6-18 GHz," *IEEE Trans. Microwave Theory Tech.*, vol. 36, no. 12, pp. 1938-1941, Dec. 1988.
- [47] B. N. Scott and G. E. Brehm, "Monolithic voltage controlled oscillator for X- and Ku-bands," *IEEE Trans. Microwave Theory Tech.*, vol. MTT-30, no. 12, pp. 2172-2177, Dec. 1982.
- [48] E. Reese, Jr. and J. M. Bcall, "Optimized X and Ku band GaAs MMIC varactor tuned FET oscillators," in *IEEE MTT-Sym.*, 1988, pp. 487-490.
- [49] J. N. Poelken and R. S. Robertson, "A comparison of planar doped barrier diode performance versus Schottky diode performance in a single balanced, MIC mixer with low LO drive," *IEEE Trans. Microwave Theory Tech.*, vol. 43, no. 6, pp. 1241-1246, June 1995.
- [50] M. J. W. Rodwell, M. Kamegawa, R. Yu, M. Case, E. Carman, and K. S. Giboney, "GaAs nonlinear transmission lines for picosecond pulse generation and millimeter-wave sampling," *IEEE Trans. Microwave Theory Tech.*, vol. MTT-39, no. 7, pp. 1194-1204, July 1991.
- [51] D. W. van der Weide, "Delimited Schottky diode nonlinear transmission lines for 480 fs, 3.5 V transients," *Appl. Phys. Lett.*, vol. 65, no. 7, pp. 881-883, Aug. 1994.
- [52] M. A. Frerking and J. R. East, "Novel heterojunction varactors," *Proc. IEEE*, vol. 80, no. 11, pp. 1853-1860, Nov. 1992.

- [53] W. C. B. Peatman, T. W. Crowe, and M. Shur, "A novel Schottky/2-DEG diode for millimeter- and submillimeter-wave multiplier applications," *IEEE Electron. Dev. Lett.*, vol. 13, no. 1, pp. 11-13, Jan. 1992.
- [54] R. J. Hwu, "A mm-wave high power monolithic back-to-back varactor diode frequency tripler," *Microwave J.*, pp. 240-253, May 1993.
- [55] A. Rydberg, H. Gronqvist, and E. L. Kollberg, "Millimeter- and submillimeter-wave multiplier using quantum-barrier-varactor (QBV) diodes," *IEEE Electron. Dev. Lett.*, vol. 11, no. 9, pp. 373-375, Sept. 1990.
- [56] S. M. Nilson, H. Gronqvist, H. Hjelmgren, A. Rydberg, and E. L. Kolberg, "Single barrier varactors for submillimeter wave power generation," *IEEE Trans. Microwave Theory Tech.*, vol. 41, no. 4, pp. 572-580, Apr. 1993.
- [57] A. V. Raisamen, "Frequency multipliers for millimeter and submillimeter wavelengths," *Proc. IEEE*, vol. 80, no. 11, pp. 1842-1852, Nov. 1992.
- [58] U. A. Bakshi and A. P. Godes, *Analog and Digital Electronics*. India: Shaniwar path, 2009.
- [59] T. L. Floyd, *Electronic devices*. 7th ed. Newyork: prentice Hall, 2005.
- [60] Y. H. Suh, K. Chang. (2002). A High-Efficiency Dual-Frequency Rectenna for 2.45 and 5.8-GHz Wireless Power Transmission. *IEEE Transactions on Microwave Theory and Techniques*.50: 1784-1789.
- [61] N. Parimon, S. S. M. Yusof, A. M. Hashim. (2008). Modeling and Characterization of Schottky Diode on AlGaAs/GaAs HEMT Structure for Rectenna Device. Second Asia International Conference on Modelling&Simulation, Kuala Lumpur, Malaysia.

- [62] F. Mustafa, N. I. Rusli, A. M. Hashim. (2008). Design and Characterization of Planar Antennas on the Semi-Insulated GaAs for Rectenna Devices. Second Asia International Conference on Modelling & Simulation.
- [63] F. Mustafa, N. Parimon, A. M. Hashim, S. F. A. Rahman, A. R. A. Rahman and M. N. Osman. (2010). Design, Fabrication and Characterization of a Schottky Diode on an AlGaAs/GaAs HEMT Structure for On-Chip RF Power Detection. *Superlattices and Microstructures*. 47: 274-287.
- [64] B. S. Nair, S. R. Deepa. (2009). Basic Electronics Includes Solved Problems & MCQS. I. K. International Publishing House Pvt. Ltd.
- [65] J. O. McSpadden, L. Fan, K. Chang. (1998). Design and Experiments of a High Conversion-Efficiency 5.8-GHz Rectenna. *IEEE Transactions on Microwave Theory and Techniques*. 46: 2053-2060.
- [66] E. Ozbay, D.M. Bloom, D.H. Chow, and J.N. Schulman, "1.7-ps, microwave, integrated-circuit-compatible InAs/AlSb resonant tunneling diodes," *IEEE Electron Device Letters*, Vol. 14, No. 8, pp. 400-402, Aug. 1993.
- [67] L. Esaki, "New phenomenon in narrow germanium p-n junctions," *Phys. Rev.*, vol. 109, pp. 603-604, 1958.
- [68] R. F. Trambaruo, "Esaki diode amplifiers at 7, 11 and 26 kMc/s," *Proc. I. R. E.*, vol. 48, pp. 20-22, 1960.
- [69] C. A. Burrus, "Millimeter wave Esaki diode oscillators," *Proc. I. R. E.*, vol. 48, pp. 20-24, 1960.
- [70] G. B. Smith, "Tunnel diode generates rectangular pulses," *Electronics*, vol. 33, pp. 124-128, 1960.

- [71] R. A. Kaenel, "High speed analog to digital converters utilizing tunnel diodes," I. R. E. Trans. Electronic Comput., vol. EC-10, pp. 273, 1961.
- [72] A. Seabaugh, X. Deng, T. Blake, B. Brar, T. Broekaert, R. Lake, F. Morris, and G. Frazier, "Transistors and tunnel diodes for analog/mixed-signal circuits and embedded memory," Int. Electron Dev. Mtg. Technical Digest, pp. 429-432, 1998.
- [73] T. P. E. Broekaert, B. Brar, J. P. A. v. d. Wagt, A. C. Seabaugh, F. J. Morris, T. S. Moise, E. A. Beam, and G. A. Frazier, "A monolithic 4-bit 2-Gsps resonant tunneling analog-to-digital converter," IEEE J. Solid State Circ., vol. 33, pp. 1342-1349, 1998.
- [74] H. J. D. L. Santos, K. K. Chui, D. H. Chow, and H. L. Dunlap, "An efficient HBT/RTD oscillator for wireless applications," IEEE Micro. Wireless Comp. Lett., vol. 11, pp. 193-195, 2001.
- [75] Q. Liu and A. Seabaugh, "Design approach using tunnel diodes for lowering power in differential comparators," IEEE Trans. of Circuits and Systems II: Analog and Digital Signal Processing, vol. 52, pp. 572-575, 2005.
- [76] C. A. Burrus, "Germanium and silicon high-frequency Esaki diodes," Proc. I. R. E., vol. 50, pp. 1689-1692, 1962.
- [77] A. Seabaugh, B. Brar, T. Broekaert, F. Morris, and P. v. d. Wagt, "Resonant tunneling mixed-signal circuit technology," Solid State Electronics, vol. 43, pp. 1355-1365, 1999.
- [78] M. Reddy, "Schottky-collector Resonant Tunnel Diodes for Sub-Millimeter-Wave Applications," http://www.ece.ucsb.edu/Faculty/rodwell/Downloads/the_ses/madhu_the_sis.pdf 1997.

- [79] T. Wei and S. Stapleton, "Equivalent circuit and capacitance of double barrier resonant tunneling diode, " in J. app. Phys. Vol. 73, Vol. 12, pp. 829-834, Jan. 1993.
- [80] U. A. Bakshi and A. P. Godes, Analog and Digital Electronics. India: Shaniwar path, 2009.
- [81] T. L. Floyd, Electronic devices. 7th ed. Newyork: prentice Hall, 2005.
- [82] M. G. Case, "Nonlinear Transmission Lines for Picosecond Pulse, Impulse and Millimeter-Wave Harmonic Generation," University of California, USA,1993,IEEE, vol. 35, Feb 2005.
- [83] M. Remoissenet," Waves Called Solitons," ch. 3: Solitons in Nonlinear Transmission Lines, pp. 37–64, 1999.
- [84] M. Case," Nonlinear Transmission Lines for Picosecond Pulse, Impulse and Millimeter-Wave Harmonic Generation" PhD thesis, University of California, Santa Barbara, 1993.
- [85] T. Tsuboi, "Formation process of solitons in a nonlinear transmission line: Experimental study," Physical Review A, vol. 41, pp. 4534–4537, April 1990.
- [86] J. Breitbarth, Design and Characterization of Low Phase Noise Microwave Circuits. PhD thesis, University of Colorado, 2006.
- [87] D. Salameh and D. Linton, "MicrostripGaAs Nonlinear Transmission-Line (NLTL) Harmonic and Pulse Generators," IEEE Transactions on Microwave Theory and Techniques, vol. 47, pp. 1118–1121, July 1999.
- [68] J.M. Duchamp, P. Ferrari, M. Fernandez, A. Jrad, X. Mélique, J. Tao, S. Arscott, D. Lippens, and R. G. Harrison, "Comparison of Fully Distributed and Periodically Loaded Nonlinear Transmission Lines," IEEE Transactions on Microwave Theory and Techniques, vol. 51, pp. 1105–1116, April 2003.

- [89] R. Hirota and K. Suzuki, "Studies on lattice solitons by using electrical networks," *J. Phys. Soc. Jpn.*, Vol. 28, pp. 1366-1367, 1970.
- [90] M. Rodwell, S. T. Allen, R. Y. Yu, M. G. Case, U. Bhattacharya, M. Reddy, E. Carman, M. Kamegawa, Y. Konishi, J. Pustl, and R. Pallela, "Active and nonlinear wave propagation devices in ultrafast electronics and optoelectronics," *Proc. IEEE*, Vol. 82, 1037-1059, 1994.
- [91] <http://tempest.das.ucdavis.edu/mmwave/NLTL/NLTL.html>.
- [92] M. G. Case, "Nonlinear transmission lines for picosecond pulse, impulse and millimeter-wave harmonic generation" Ph.D Dissertation, Department of Electrical and Computer Engineering, University of California, Santa Barbara, California, U.S.A., 1993.
- [93] J. S. Russell, "Report on waves," in *Rep. 14th Meeting of the British Association for the Advancement of Science*, pp. 311–90, Sep. 1844.
- [94] P. G. Drazin and R. S. Johnson, *Solitons*. Cambridge, U.K.: Cambridge Univ. Press, 1989.
- [95] M. J. Ablowitz and H. Segur, "Solitons and the Inverse Scattering Transform. Philadelphia," PA: Society for Industrial and Applied Mathematics, 1981.
- [96] J. R. Taylor, *Optical Solitons—Theory and Experiment*. Cambridge, U.K.: Cambridge Univ. Press, 1992.
- [97] R. K. Bullough and P. J. Caudrey, *Solitons*. Berlin: Springer- Verlag, 1980.
- [98] E. Infeld and G. Rowlands, *Nonlinear Waves, Solitons and Chaos*. Cambridge, U.K.: Cambridge Univ. Press, 1990.

- [99] P. J. Olver and D. H. Sattinger, *Solitons in Physics, Mathematics, and Nonlinear Optics*. New York: Springer-Verlag, 1990.
- [100] M. Remoissenet, *Waves Called Solitons: Concepts and Experiments*. Berlin, Germany: Springer-Verlag, 1994.
- [101] M. G. Case, "Nonlinear Transmission Lines for Picosecond Pulse, Impulse and Millimeter-Wave Harmonic Generation," Ph.D. dissertation, Univ. of California, Santa Barbara, 1993.
- [102] M. J. W. Rodwell, M. Kamegawa, R. Yu, M. Case, E. Carman, and K. Giboney, "GaAs nonlinear transmission lines for picosecond pulse generation and millimeter-wave sampling," *IEEE Trans. Microwave Theory Tech.*, vol. 39, no. 7, pp. 1194–1204, Jul. 1991.
- [103] R. A. Scholtz, "Signal selection for the indoor wireless impulse radio channel," in *Proc. IEEE Vehicular Technology Conf.*, May 1997.
- [104] T.C. Kofane, B. Michaux, and M. Remoissenet, "THEORETICAL AND EXPERIMENTAL STUDIES OF DIATOMIC LATTICE SOLITONS USING AN ELECTRICAL TRANSMISSION-LINE," *J. Phys. C: Solid State Phys.*, Vol. 21, No. 8, pp. 1395-1412, Mar. 1988.
- [105] P. Marqui'e, J.M. Bilbault, and M. Remoissenet, "Observation of nonlinear localized modes in an electrical lattice," *Phys. Rev.*, Vol. 51, No. 6, pp. 6127-6133, Jun 1995.
- [106] H. Nagashima and Y. Amagishi, "Experiment on Solitons in the Dissipative Toda Lattice Using Nonlinear Transmission Line," *J. Phys. Soc. Japan*, Vol. 47, pp. 2021-2027, July 1979.
- [107] M.S. Ody, A.K. Common, and M.Y. Sobhy, "Transmission of Solitary Pulse in Dissipative Nonlinear Transmission Lines," *Eur. J. Appl. Math.* Vol. 10, pp. 265-269, 1999.

- [108] E. Kengne, B.A. Malomed, S.T. Chui, and W.M. Liu, "Solitary. Signals In Electrical Nonlinear Transmission Line," J. Math. Phys. Vol. 48, No. 1, pp. 013508- 013513 , 2007.
- [109] M. Harwood et al., "A 12.5Gb/s serdes in 65nm CMOS using a baud-rate ADC with digital receiver equalization and clock recovery," IEEE International Solid-State Circuits Conference (ISSCC) Digest of Technical Papers, pp. 436-437, February 2007.
- [110] D. J. Foley and M. P. Flynn, "A low-power 8-PAM serial transceiver in 0.5 μ m digital CMOS," IEEE Journal of Solid-State Circuits, vol. 37, pp. 310-316, March 2002.
- [111] C. K. Yang, V. Stojanovic, S. Mojtahedi, M. Horowitz, and W. Ellersick, "A serial-link transceiver based on 8-G samples/s A/D and D/A converters in 0.25 μ m CMOS," IEEE Journal of Solid-State Circuits, vol. 36, pp. 293–301, Nov. 2001.
- [112] R. Thirugnanam, D. S. Ha, S. S. Choi, "Design of a 4-bit 1.4G Samples/s low power folding ADC for DS-CDMA UWB," IEEE International Conference on Ultra-Wideband (ICU), pp. 536 – 541, Sep. 2005.
- [113] T. Yamamoto, S.-I. Gotoh, T. Takahashi, K. Irie, K. Ohshima, and N. Mimura, "A mixed-signal 0.18- μ m CMOS SoC for DVD systems with 432-M Sample/s PRML readchannel and 16-Mb embedded DRAM," IEEE Journal of Solid-State Circuits, vol. 36, pp. 1785–1794, November 2001.
- [114] K. Poulton, R. Neff, A. Muto, A. W. L. Burstein, and M. Heshami, "A 4 G Sample/s 8b ADC in 0.35 μ m CMOS," IEEE International Solid-State Circuits Conference (ISSCC) Digest of Technical Papers, pp. 166-167, February 2002.

- [115] K. Poulton et al., "A 20Gs/s 8b ADC with a 1Mb memory in 0.18 μ m CMOS," IEEE International Solid-State Circuits Conference (ISSCC) Digest of Technical Papers, pp. 318-319, February 2003.
- [116] L. Y. Nathawad, R. Urata, B. A. Wooley, and D.A.B. Miller, "A 20GHz bandwidth, 4b photoconductive-sampling time-interleaved CMOS ADC," IEEE International Solid-State Circuits Conference (ISSCC) Digest of Technical Papers, pp. 320-321, Feb. 2003.